SANDIA REPORT

SAND95-1904 • UC-814
Unlimited Release
Printed September 1997

Yucca Mountain Site Characterization Project

Thermal Expansion of the Paintbrush Tuff Recovered from Borehole USW SD-12 at Pressures 30 MPa: Data Report

R. J. Martin, J. S. Noel, P. J. Boyd, M. Riggins, R. H. Price

Prepared by
Sandia National Laboratories
Albuquerque, New Mexico 87185 and Livermore, California 94550

Sandia is a multiprogram laboratory operated by Sandia Corporation, a Lockheed Martin Company, for the United States Department of Energy under Contract DE-AC04-94AL85000.

Sandia National Laboratories

SF2900Q(8-81)

"Prepared by Yucca Mountain Site Characterization Project (YMSCP) participants as part of the Civilian Radioactive Waste Management Program (CRWM). The YMSCP is managed by the Yucca Mountain Project Office of the U.S. Department of Energy, DOE Field Office, Nevada (DOE/NV). YMSCP work is sponsored by the Office of Geologic Repositories (OGR) of the DOE Office of Civilian Radioactive Waste Management (OCRWM)."

Issued by Sandia National Laboratories, operated for the United States Department of Energy by Sandia Corporation.

Available to DOE and DOE contractors from
Office of Scientific and Technical Information
P.O. Box 62
Oak Ridge, TN 37831

Prices available from (615) 576-8401, FTS 626-8401

Available to the public from
National Technical Information Service
U.S. Department of Commerce
5285 Port Royal Rd
Springfield, VA 22161

NTIS price codes
Printed copy: A06
Microfiche copy: A01

SAND95-1904
Unlimited Release
Printed September 1997

Distribution
Category UC-814

Thermal Expansion of the Paintbrush Tuff Recovered from Borehole USW SD-12 at Pressures 30 MPa: Data Report

R.J. Martin, J. S. Noel, P. J. Boyd
New England Research, Inc.
White River Junction, Vermont 05001

M. Riggins, R. H. Price
YMP Performance Assessment Applications Department
Sandia National Laboratories
P.O. Box 5800
Albuquerque, New Mexico 87185-1325

ABSTRACT

Experimental results are presented for twenty-four (24) thermal expansion experiments performed on five (5) welded specimens of the Paintbrush tuff recovered from borehole USW SD-12 at Yucca Mountain, Nevada. The thermal expansion experiments were performed at constant confining pressures between 1 and 30 MPa. On three specimens, the highest confining pressure measurements were performed first to inhibit thermally induced damage which might occur at lower confining pressures. At each confining pressure two complete thermal cycles were performed. The specimens were heated (to a nominal temperature of 250 °C) and cooled at the nominal rate of 0.319°C per minute. The change in specimen length as a function of temperature was measured with two LVDTs mounted on endcaps secured to the specimen.

The strain increases with increasing temperature and the strain vs temperature curves are concave upward. On cooling, there is hysteresis at the higher temperatures at all confining pressures. The first heating/cooling cycle is anomalous; hysteresis is pronounced, and a permanent shortening of the specimen is observed at the termination of the cycle. The magnitude of the effect was similar for all five specimens regardless of whether the first cycle was carried out at the highest or lowest confining pressure. For subsequent cycles at all confining pressures, no permanent strain develops, and the strain versus temperature curves are very similar. The mean coefficients of thermal expansion (α) range from 7.9 to 10.8^{-6} °C^{-1} at temperatures below 100 °C, to 14.2 to 20.6 x 10^{-6} °C^{-1} at temperatures approaching 250 °C. The effect of confining pressure on thermal expansion is small. For temperatures above 175 °C, the mean coefficients of thermal expansion decreases by 10-12 % as the pressure increases from 1 to 30 MPa.

This report was prepared for the Yucca Mountain Site Characterization Project. The scientific investigation discussed in this report is covered under the description of work for WBS number 1.2.3.2.7.1.2, QA Grading Report #1.2.3.2.7.1.2, Revision 00. The planning documents that guided this work activity are Site Characterization Plan Section 8.3.1.15,1.2; Study Plan SP-8.3.1.15,1.2; and Work Agreement WA-00187, Revision 00. The information and data documented in this report were collected under a fully qualified QA Program and may be used in the licensing process. The data contained in this report have been submitted on Technical Data Information Forms (TDIFs) #305514 and #305453 under Data Tracking Numbers SNL01B02019501.001 and SNL04011895001.001, respectively.

CONTENTS

List of Figures

List of Tables

1.0 INTRODUCTION

An integral part of the licensing procedure for the potential nuclear waste repository at Yucca Mountain, Nevada involves the prediction of *in situ* characteristics of the tuff for the emplacement of containers containing radioactive waste. The data used to model the thermal and mechanical behavior of the repository rock and surrounding lithologies require a detailed knowledge of the thermal expansion of the tuff. In particular, the lithophysae poor Topopah Spring welded unit (TSw2), the potential repository horizon must be characterized. In this study a suite of experiments was performed on cores recovered from the USW SD-12 borehole drilled at Yucca Mountain. USW SD-12 was drilled to a depth of 1453.3 feet through five thermal/mechanical units of the Paintbrush tuff. The thermal/mechanical stratigraphy was defined by Ortiz et al. (1985) to group rock horizons of similar properties for the purpose of simplifying modeling efforts. The relationship between the geologic stratigraphy and the thermal/mechanical stratigraphy is presented in Figure 1. The tuff samples at Yucca Mountain have a wide range of welding characteristics (usually reflected in sample porosity), and a smaller range of mineralogy and petrology characteristics. Generally, the samples are silicic, ash-flow tuffs that exhibit large variability in their thermal and mechanical properties (see Price and Bauer, 1985).

2.0 EXPERIMENTAL PROCEDURE

Twenty-four thermal expansion experiments were performed on five specimens prepared from core recovered from borehole USW SD-12. The specimens were from thermal/mechanical unit TSw2, a welded tuff designated as the potential repository horizon. The specimen were prepared from vertical cores by subcoring parallel to the axis. Each specimen was a ground, right circular cylinder. The nominal dimensions of each specimen are 50.8 mm in diameter and 101.6 mm in length. The length and diameter have a tolerance of $\pm$ 0.125 mm. The ends of the specimens were parallel to within 0.025 mm. Room dry bulk densities were measured on each of the specimens prior to testing (specimens were not oven dried prior to testing). In addition, average grain density was determined with the water

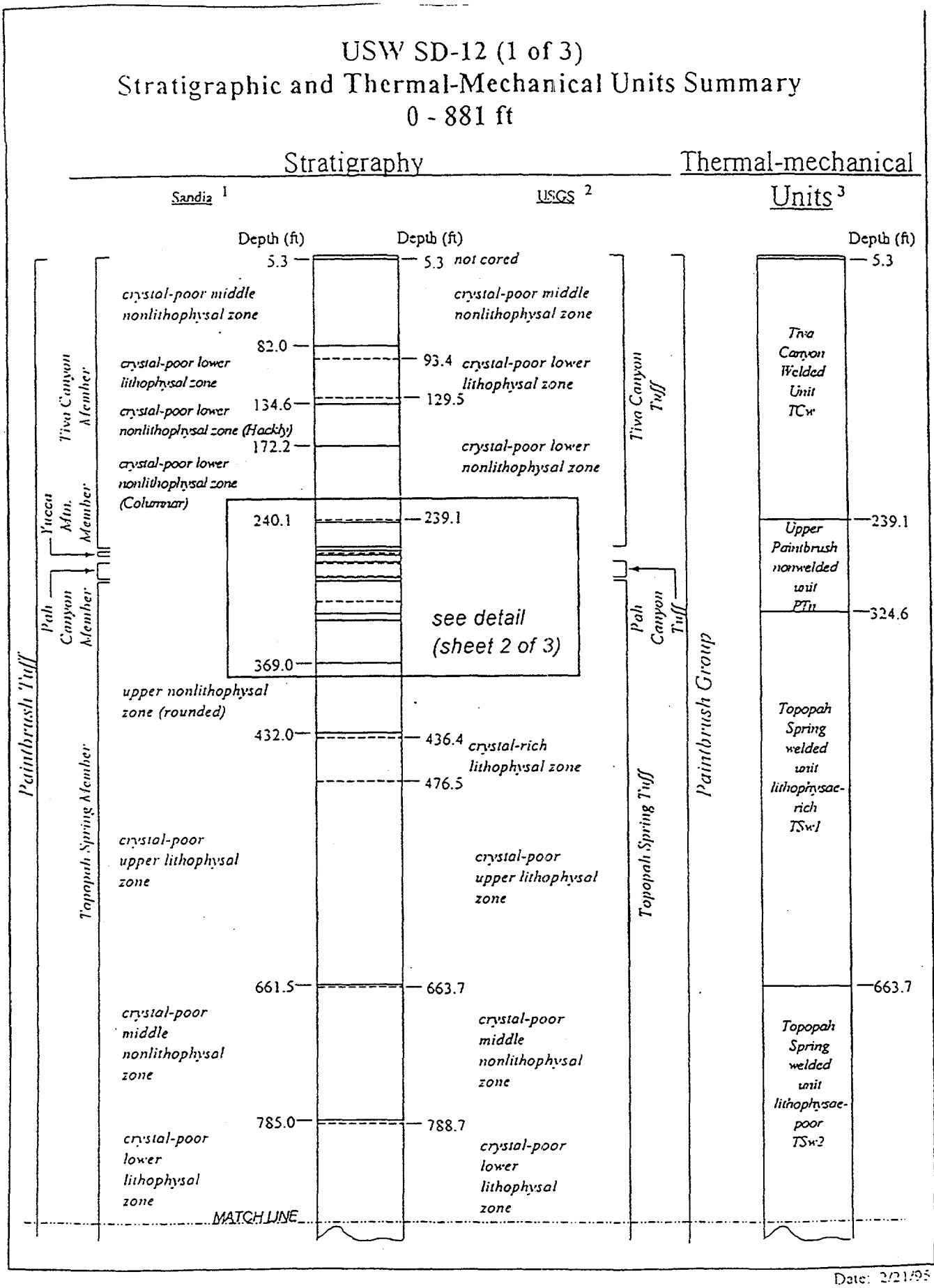

Figure 1: The correlation between the stratigraphic and thermal/mechanical units for borehole USW SD-12 at Yucca Mountain, Nevada (stratigraphy by Buesh et al: USGS Open File **Report 94-469, 1996).**

USW SD-12 Stratigraphy (2 of 3)
Stratigraphic and Thermal-Mechanical Units Summary
Detail 239.1 - 369.0 ft

Stratigraphy

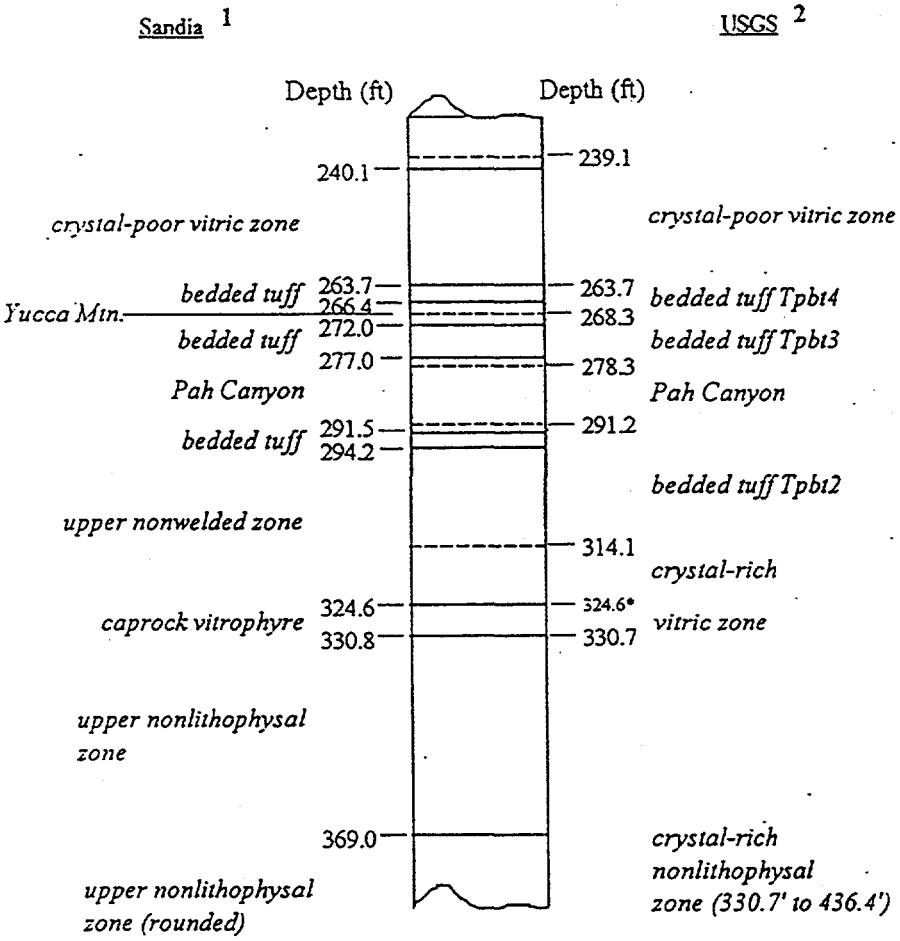

*Break between welded and moderately welded subzones at 324.6'.

Date: 2/21/95

USW SD-12 (3 of 3)
Stratigraphic and Thermal-Mechanical Units Summary
881 - 1435.3 ft

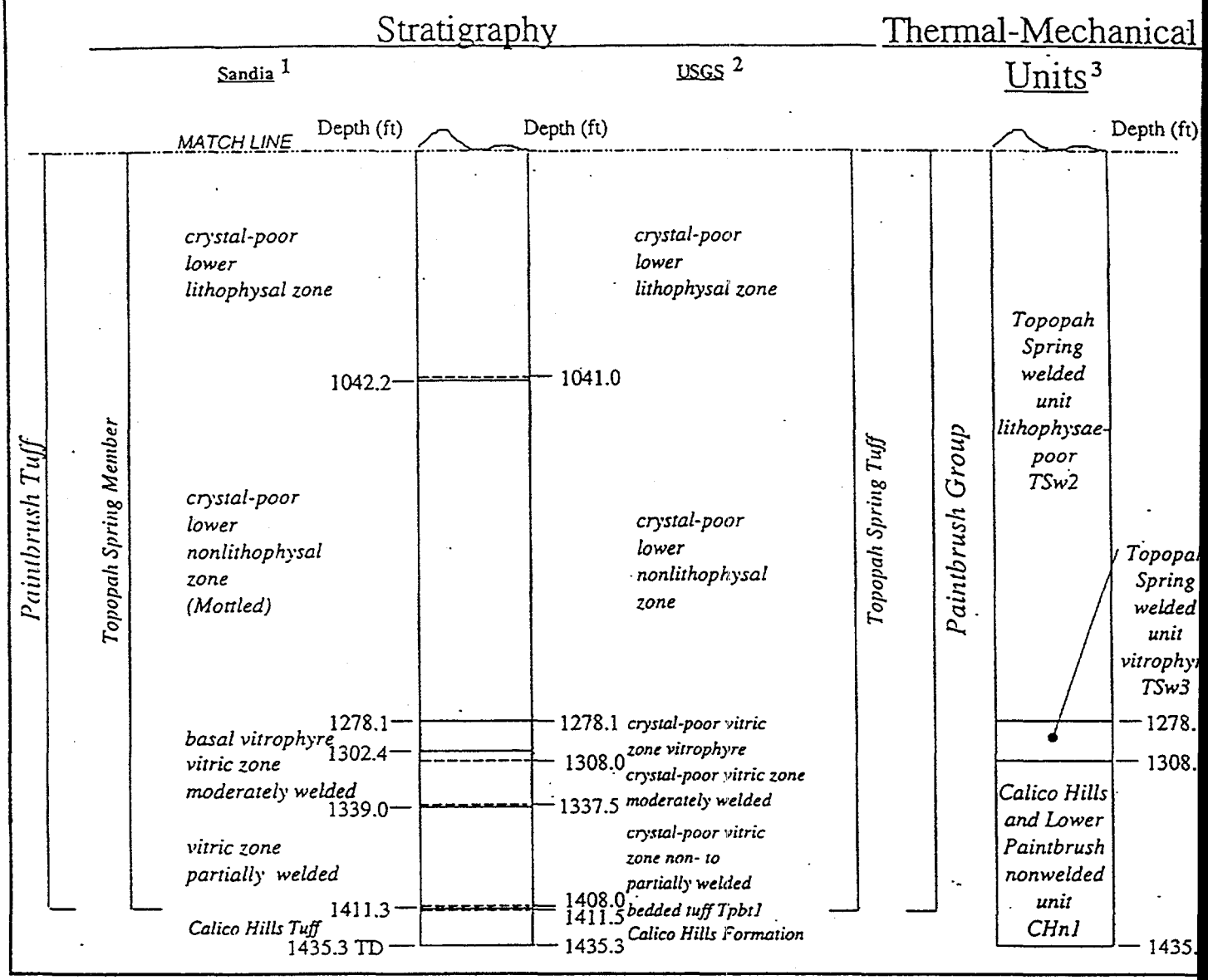

Date: 3/1/9

1 Lithologic log of Borehole USW SD-12. Dale Engstrom, unpublished data.

2 U.S.Geological Survey - Graphical Lithologic Log of the Paintbrush Group in Borehole USW SD-12, J.K. Geslin and J.R. Wunderlich, DTN: GS940908314211.045

3 Thermal-mechical units as defined by Buesch, et al., USGS Open File Report 94-469, "Proposed statigraphic nomenclature and macroscopic identification of lithostratigraphic units of the Praintbrush Group exposed at Yucca Mountain, Nevada."

pycnometry technique using pieces remaining from the subcoring attendant to the preparation of the test specimens (see Boyd et al., 1994; Martin et al., 1995). The composition and total porosity of each specimen was very similar. The porosities ranged from 7.3 to 10.3%.

The selection of specimens for thermal expansion measurements were based on the relative percentages of the silica phases in each specimen. Unconfined thermal expansion tests on TSw2 tuff exhibit increases in the coefficient of thermal expansion between 150 and 200 °C. Phase transitions in tridymite occur between 117 and 163 °C and in cristobolite near 272 °C with an attendant volume change. It is possible that the phase changes will produce the variations in the coefficient of thermal expansion, especially at temperatures near the transition temperatures. Therefore specimens were selected that exhibited a range in the relative percentages of quartz, cristobolite, and tridymite to determine if there is any effect of the relative concentration of each polymorph on the thermal expansion of the welded tuff. Table 1 presents the relative percentages of quartz, cristobolite, and tridymite in each specimen (TDIF #305435, 1996). The percentages shown are the relative concentrations of each of the phases normalized to the total content of all three polymorphs. The total concentration of SiO_2 in the specimens is approximately 30 %. In addition, Table 1 also gives the lithostratographic unit for each of the test specimens.

Table 1

Relative Percentages of SiO_2 Polymorphs in the Thermal Expansion Specimens

Specimen Depth, ft	Lithostratographic Unit	Porosity %	Quartz %	Cristobolite %	Tridymite %
687.8	Tptpmn	8.7	16	84	0
742.9	Tptpmn	10.6	19	75	16
776.4	Tptpmn	8.0	19	81	0
883.5	Tptpll	8.9	71	29	0
1204.8	Tptpln	7.6	49	51	0

2.1 Sample Preparation

All specimens prepared for the thermal expansion experiments were ground, right circular

cylinders with the nominal dimensions listed above. The dimensions of the specimens were checked and verified according to the Sandia National Laboratories (SNL) Technical Procedure (TP) 51 entitled "Preparing Cylindrical Samples, Including Inspection of Dimensional and Shape Tolerances."

The prepared specimens were labeled and stored in containers until the measurement sequence was initiated.

The general measurement sequence for each specimen is given below:

Dimensions measurement

Specimen description

Bulk density measurement in an room dry condition

Compressional and shear wave velocities in the room dry condition

Thermal expansion testing at confining pressures of 1, 5, 10, 20, and 30 MPa, over a nominal temperature range of 25 to 250 °C

Compressional and shear wave velocities for the "post test" condition

Bulk density measurement in a "post test" condition

Description of the post test condition of the specimens

2.2 Compressional and Shear Wave Velocity Measurements

Compressional and shear wave velocities were measured on right circular cylinders of TSw2 tuff with a nominal length to diameter ratio of 2:1. The velocities were measured in a benchtop apparatus before and after each suite of thermal expansion measurements. The velocity measurements were conducted at ambient temperature and pressure.

Changes in compressional and shear wave velocity data may reflect damage to the specimen. Previous studies have shown that thermal cycling of low porosity crystalline rocks damages the specimens (Martin et al., 1996). The damage is reflected by a decrease in the compressional and shear wave velocities measured after the thermal expansion experiments.

A self-contained ultrasonic measuring system is used to perform the velocity measurements. A tuff specimen is placed between a matched set of ultrasonic transducers. One transducer serves as the

source; the second as the receiver (Figure 2). The travel time through the rock is divided by the sample length to compute the velocity. The travel time includes the travel time through the rock as well as the titanium end pieces. A series of calibrations are performed to determine the travel time through the titanium end pieces. These values are subtracted from the total travel time to obtain the travel time through the rock.

Each ultrasonic transducer contains one compressional and one or two polarized shear wave elements. For the measurements parallel to the core axis one compressional and two orthogonally polarized shear waves are propagated.

The transducers are constructed using piezoelectric crystals with a resonant frequency of 1 MHz. The multicomponent piezoelectric crystals are bonded to a titanium substrate. Titanium has been selected because it has a good acoustical impedance match both to the rock and to the piezoelectrical crystals. The source crystal is excited with a fast rise time pulse generator. The crystal produces a broad band ultrasonic pulse propagated through the adjacent titanium substrate, the rock, the titanium at the opposite end of the core, and into the receiver crystal. The signals are amplified, and high pass filtered above 0.3 MHz. The time series displayed on the oscilloscope is then digitized and transferred to a computer for subsequent analysis including picking the first arrival of the compressional and shear wave energy to compute the compressional and shear wave velocities. The accuracy of the travel time is $\pm$ 0.02 microseconds.

2.3 Thermal Expansion Measurements on Specimens of TSw2

The thermal expansion experiments were performed on TSw2 tuff at constant confining pressures of 1, 5, 10, 20, and 30 MPa, over a nominal temperature range of 25 to 250 °C. The test specimen is jacketed and secured to Invar 36 alloy endcaps. The endcaps support the cores and the barrels for two Linear Variable Displacement Transducers (LVDT) positioned on a diametral plane through the specimen. The LVDTs are positioned at one end of the pressure vessel away from the furnace. The cores and barrels of the LVDTs are mounted in fused quartz tubing. After adjusting the LVDTs, the sample assembly is inserted into a pressure vessel. The confining pressure is increased and thermal cycling initiated. The change in length of the sample is measured as a function of

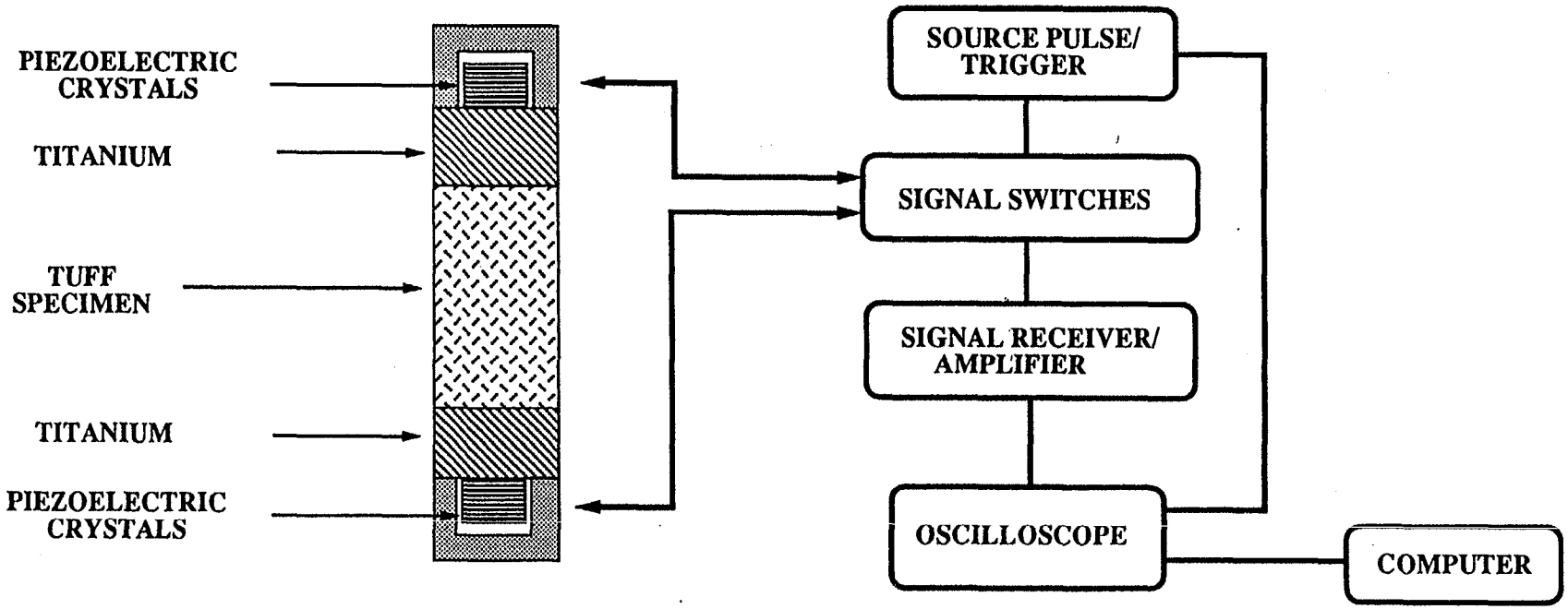

Figure 2: Schematic diagram of the geometry used to measure compressional and shear wave velocities in tuff. The diagram shows the setup for the measurement of velocities parallel to the core axis.

temperature. The sample is heated and cooled at a nominal rate of 0.319 °C per minute. The test procedure adheres to the requirements of ASTM D 4535-85 "Standard Test Method for the Measurement of Thermal Expansion of Rock Using a Dilatometer", with the following exceptions:

1. A single standardization cycle was performed at each confining pressure and a verification of the system performance is obtained by measuring the thermal expansion on a known standard to within 5%.
2. The 95% confidence limits for the data are not calculated because there are insufficient data. These two variations have no effect on the accuracy of the data.

2.3.1 Test Apparatus

Thermal expansion experiments were conducted in the test apparatus described below. The key features of the system include independent controls for confining pressure, pore pressure, and temperature. The measurements performed in this study were conducted in a drained condition. The measurements were performed in a pressure vessel that accommodates test specimens up to 50.8 mm in diameter and 120 mm in length, at confining pressures to 35 MPa, pore pressures to 35 MPa, and temperatures to 250 °C.

A schematic diagram of the test apparatus is shown in Figure 3. A long bore pressure vessel is divided into a hot and a cool region. The temperature in the hot zone is controlled with an external furnace consisting of three band heaters surrounded by insulation and protected with a stainless steel shroud. The cool end of the pressure vessel houses the LVDTs sensing the displacement of the rock core during thermal expansion. The lower end of the vessel is encased in a cooling water jacket.

The pressure vessel is constructed of 4140 tool steel, hardened to R_C 35. The threaded closures of the vessel are fabricated from hardened 17-4 stainless steel. The bore diameter of the vessel is 92.1 mm; the overall length of the vessel is 457 mm.

The confining and pores pressures are controlled with two independent servo-hydraulic intensifiers. Each of the servo intensifiers maintains the pressure constant to within ± 0.15 MPa. Fluctuations in pressure are due to long term drift in the servo valve, pressure transducer, and electronics. The confining pressure is generated and controlled with a servo-hydraulic intensifier with an intensification ratio of 2.4:1. The feedback for the servo-controller is a Sensotec Model Z/743

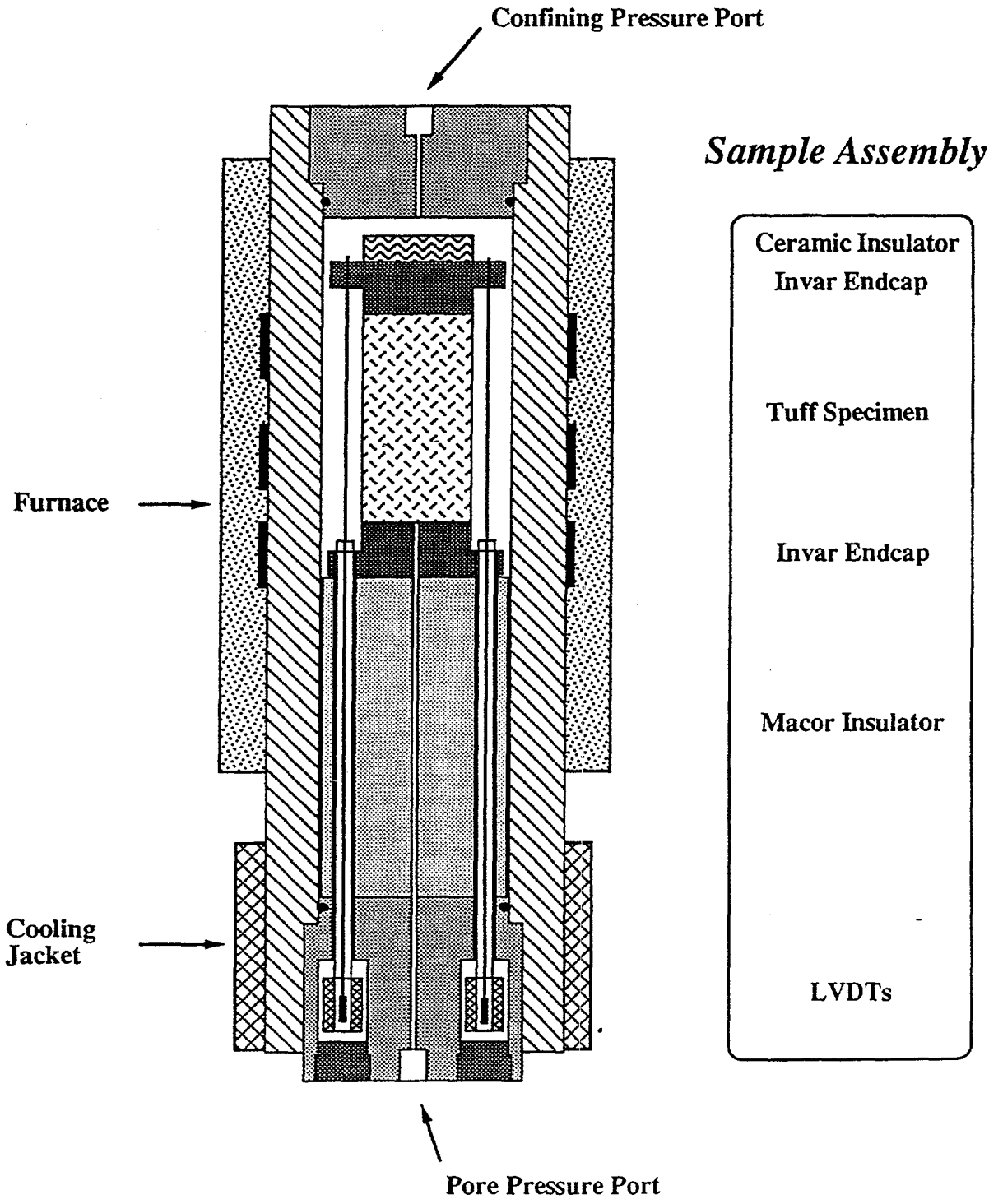

Figure 3: Schematic of the pressure vessel, sample assembly, and LVDT position for the test apparatus used to perform the thermal expansion measurements.

pressure transducer. The accuracy of the transducer is ± 0.5 %. The pressure rating of the transducer is 35 MPa.

Specimens may be tested in either a drained or undrained condition. For this series of tests, the specimens were drained. This condition was selected because it closely represented the anticipated *in situ* condition during the heating of the rock mass when the waste canisters are in place. For the drained condition, the access port in the base plug supporting the sample assembly is vented to the atmosphere. In some instances it may be desirable to test saturated specimens at elevated pore fluid pressure. The pore pressure is generated and maintained with an independent servo-hydraulic intensifier. Fluid is injected into the base of the sample; in most cases water is used as a pore fluid. The output volume of the pore pressure intensifier is 5.5 cm^3. The intensification ratio of the intensifier is 16:1. The feedback for the servo-controller is provided with a Sensotec Model Z/743 pressure transducer.

The temperature of the test specimen is controlled with an external furnace. The furnace consists of three band heaters positioned at the upper end of the pressure vessel as shown in Figure 3. The band heaters are adjusted to produce a temperature profile constant to within ± 1 °C over the test specimen at temperatures to 250 °C (Details are presented below in the System Calibration Section). The feedback for the temperature controller is a type J thermocouple mounted on the outside of the vessel near the band heaters. The outside of the vessel is insulated with a 40 mm thick, high density fiber insulation. A stainless steel safety shroud protects the furnace assembly. The power to the band heaters is regulated with a Watlow Series 982 temperature controller. The controller is adjusted according to the manufacturer's procedure. The programmable controller is set to provide reproducible cycles. A thermal cycle consists of heating from ambient to 250 °C, and cooling to ambient conditions. A two hour delay is imposed between the first and second cycle to allow the system to equilibrate with room temperature. The nominal heating and cooling rate for the experiments is 0.319 °C per minute.

The sample assembly consists of a jacketed tuff specimen secured between two Invar endcaps. The specimen is wrapped with two layers of 0.13 mm thick dead soft, annealed copper. The copper extends approximately 12 mm beyond each end of the specimen. The specimen is then jacketed with heat shrink teflon and secured to the endcaps using two wraps of wire.

The jacketed specimen is placed on to the base plug of the pressure vessel. The base plug of the vessel contains inlet ports for confining pressure, pore pressure, four thermocouples and high pressure feedthrus for electrical devises. A Macor insulator is secured to the base plug. The Macor has an outside diameter 1 mm less than the bore of the pressure vessel and a length of 152.4 mm. The insulator provides a thermal barrier between the tuff specimen, subjected to the high temperatures, and the LVDT cores and barrels measuring the displacement of the specimen in the low temperature portion of the vessel. Pore pressure access ports, as well as holes for thermocouples and LVDTs, are drilled through the insulating piece. The test specimen is inserted into the insulator and secured with a small nipple fabricated into the lower endcap. Three thermocouples extend through the insulator and are positioned at the base, midpoint, and top of the test specimen.

Two LVDTs are used to monitor the change in length of the specimen as a function of temperature. Since LVDTs will not survive temperatures to 250 °C the displacement at each end of the specimen is transferred into a cooler region of the pressure vessel. First, the barrels of the LVDTs are mounted on large diameter fused quartz tubes secured to the lower end cap of the test specimen. The fused quartz tubes extend into the base plug of the pressure vessel. A second pair of fused quartz tubes, with a much smaller diameter, support the cores for the LVDTs. These tubes are attached to the upper end cap. Each tube is adjusted so that the core is centered in the barrel of the LVDT. All fused quartz tubes are secured to the end caps with spring loaded set screws. The output of each LVDT is adjusted prior to inserting the specimen into the pressure vessel.

During each experiment the outputs from seven devices are continuously monitored. The transducers include four thermocouples (three positioned in proximity to the specimen and one in the base plug sensing the temperature of the LVDTs), the confining pressure transducer, and the two LVDTs monitoring the change in length of the test specimen. The outputs from these transducers are conditioned using a Validyne MC 170 signal conditioning module. The conditioned outputs are recorded with the data acquisition system.

2.3.2 System Calibrations

System calibration consists of three procedures designed to ensure suitable operation of the

entire test apparatus:

1) Verify that the temperature along the length of the specimen does not deviate by more than ± 1 °C;

2) Separate the contribution of the test system components to the total displacement from the displacement of tuff;

3) Perform a system check with a known standard to ensure that the measurements of thermal expansion are accurate and that the entire system performs according to specifications.

2.3.2.1 Temperature Gradient in Tuff Specimens

The system is adjusted to achieve a constant temperature gradient throughout the tuff specimen at all temperatures. To observe the temperature distribution a dummy specimen of tuff with an axial hole is jacketed in the same manner as the tuff to be tested for thermal expansion. Detailed thermal profiles through the dummy test specimen subjected to a confining pressure of 30 MPa were performed at 250 °C and 125 °C. The apparatus is tuned to the specific sample geometry used in these experiments. The procedure includes adjusting the position of the band heaters, as well as varying the flow rate through the cooling coils at the base of the pressure vessel. By trial and error, an acceptable variation of ± 1 °C through the test specimen is achieved. It was determined that the optimum flow rate through the lower cooling jacket was 0.07 ± 0.01 gallons per minute. To ensure reproducibility, a flow meter, in series with a needle valve, is placed on the inlet of the cooling jacket. The flow rate is checked periodically throughout the experiment.

The results of the tuning procedure are shown in Figure 4. First, the specimen was pressurized to 30 MPa, heated to 250 °C, and the profile through the test specimen measured. The water flow rate through the cooling jacket was 0.05 gal min^{-1}. These data are presented with open squares. Next, the temperature was reduced to 125 °C, the flow rate increased to 0.07 gal min^{-1}, and the specimen profiled once again. These data are shown in diamonds. Finally, the temperature was increased to 250 °C and the specimen profiled. These data are shown with open circles. The LVDTs are located approximately 250 mm below the base of the test specimen. The temperature in this section of the pressure vessel ranges from 25 to 65 °C.

The temperatures measured with the three thermocouples located outside the test specimen agreed within ± 1 degree with the temperatures measured along the axis of the test specimen. Therefore, not only is the thermal gradient parallel to the axis small, but there also is little radial variation in temperature.

2.3.2.2 Correction for Displacement of the Test System

Since the fused quartz support rods for the LVDT cores and barrels are attached to the end caps positioned at each end of the specimen, the displacement measured with the LVDTs at the base of the pressure vessel includes the displacement of the tuff specimen as well as that of the end caps, the fused quartz rods, the connections, etc. To separate the system displacements from that of the specimen, a series of calibrations were performed using fused quartz as a test specimen. The fused quartz has the same nominal dimensions as the tuff specimens. It was jacketed and secured to the end caps as described above and inserted in the pressure vessel and the confining pressure increased to 30 MPa. The specimen was then thermally cycled over the range of 25 to 250 °C. The displacement of the two LVDTs was recorded as a function of temperature. The raw data are shown in Figure 5. The displacement was calculated using the room temperature and pressure calibrations for the LVDTs. The displacement as a function of temperature is not linear. The slope of the curve is concave upward. The nonlinearity is due to the nonlinear thermal expansion of the Invar end caps.

To obtain the system effect at 30 MPa, the thermal expansion of the fused quartz specimen is subtracted from the total displacement. Figure 6 shows the average (of the two LVDTs) displacement as a function of temperature. For reference, the calculated displacement for the fused quartz is shown. These data were computed using a coefficient thermal expansion for fused quartz of 5.5×10^{-7} °C^{-1} (reference: Product Manual, GE Fused Quartz Products). The difference between the two curves is the correction. The resulting system correction is shown in Figure 7. The curve was fit with a third order polynomial. This allows us to compute sample displacement as a function of temperature at 30 MPa.

Additional calibrations were performed at confining pressures of 1, 5, 10, and 20 MPa. The correction factors at each confining pressure are different. The magnitude of the correction increases a small amount with decreasing confining pressure.

Topopah Spring Member Tuff, TSw2

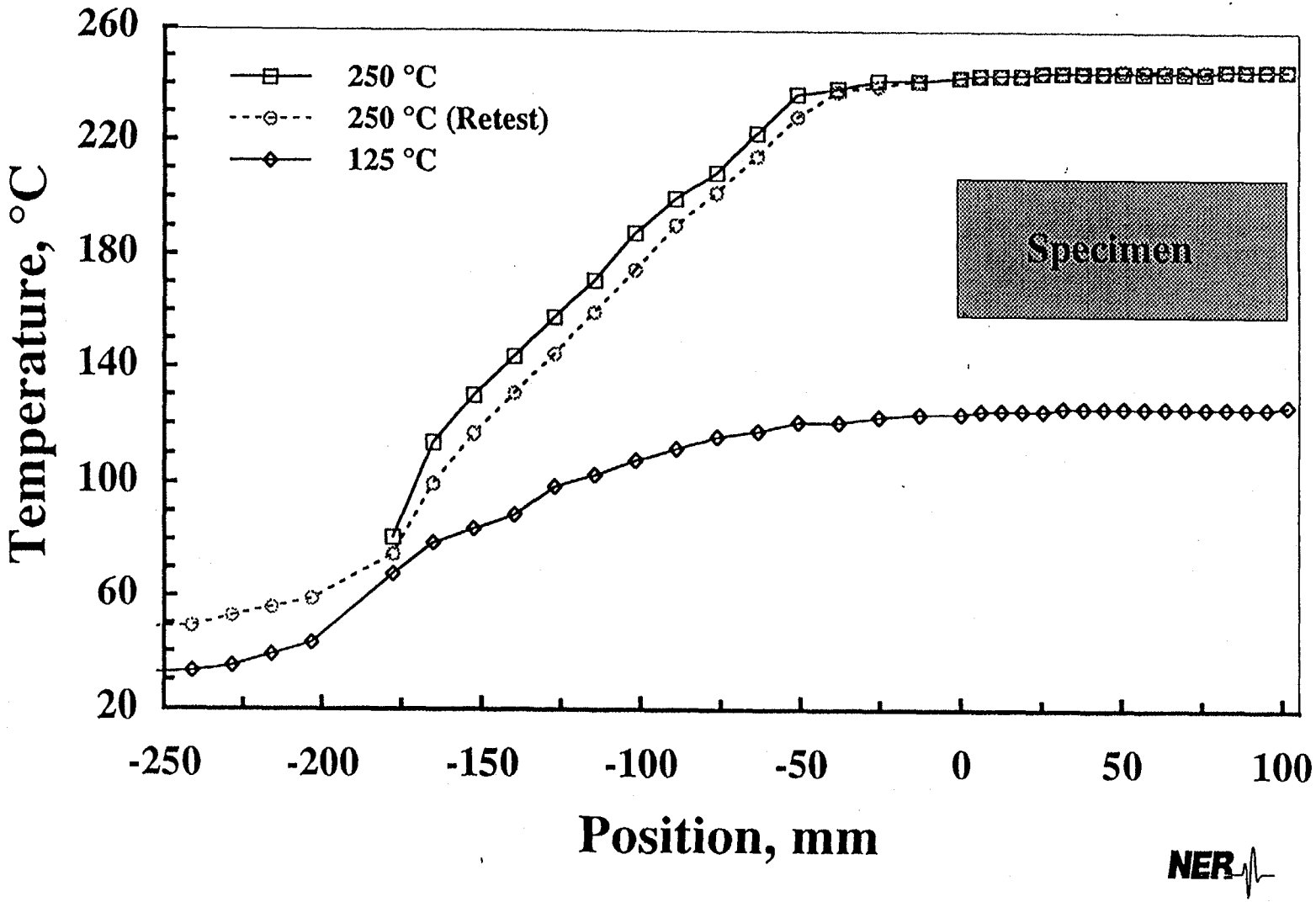

Figure 4: Temperature is plotted as a function of position through the sample assembly. The test specimen, in the upper partition of the vessel, shows a temperature variation of ± 1°C through the sample.

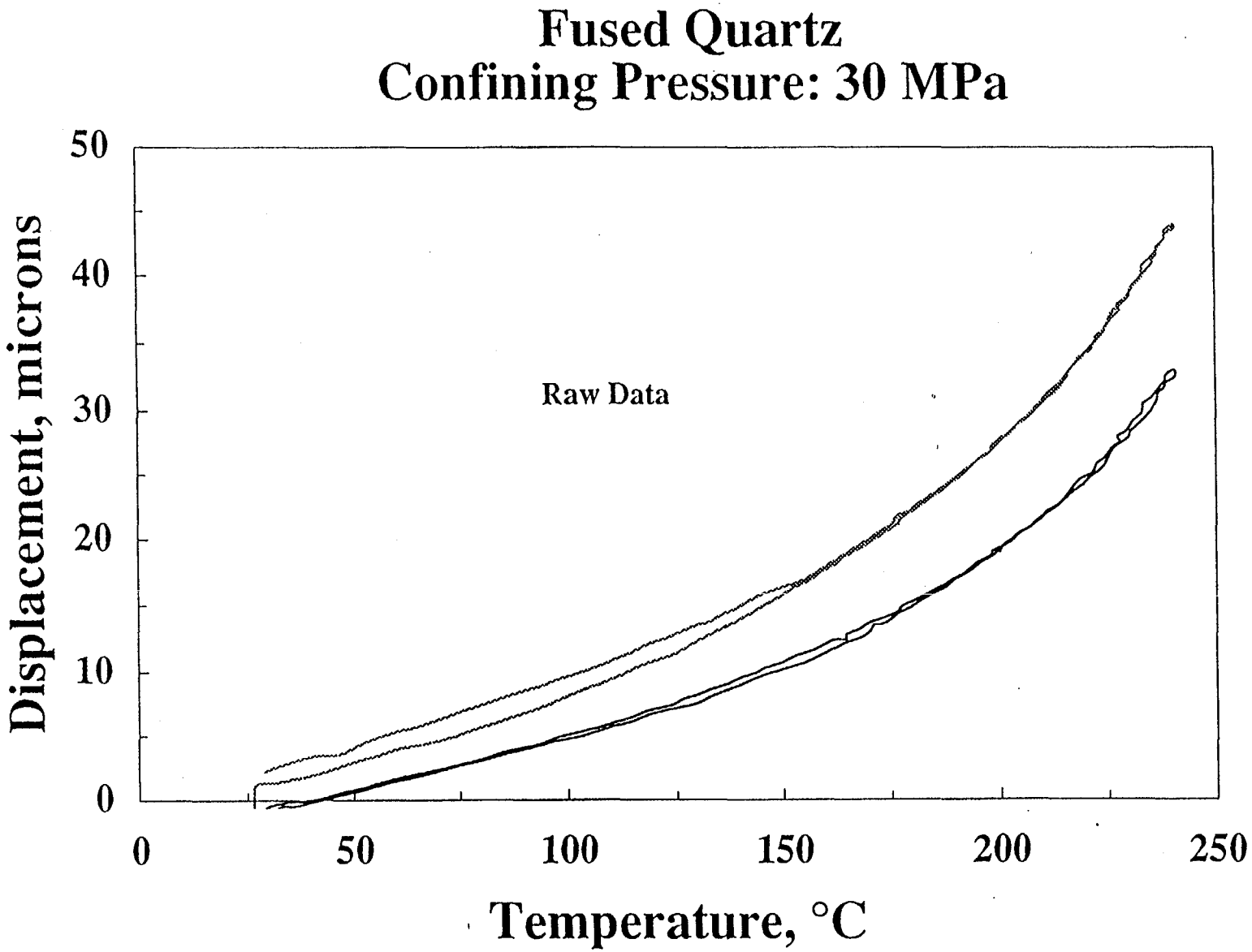

Figure 5: Displacement is plotted as a function of temperature for the two LVDTs measuring the displacement on a fused quartz specimen at a confining pressure of 30 MPa.

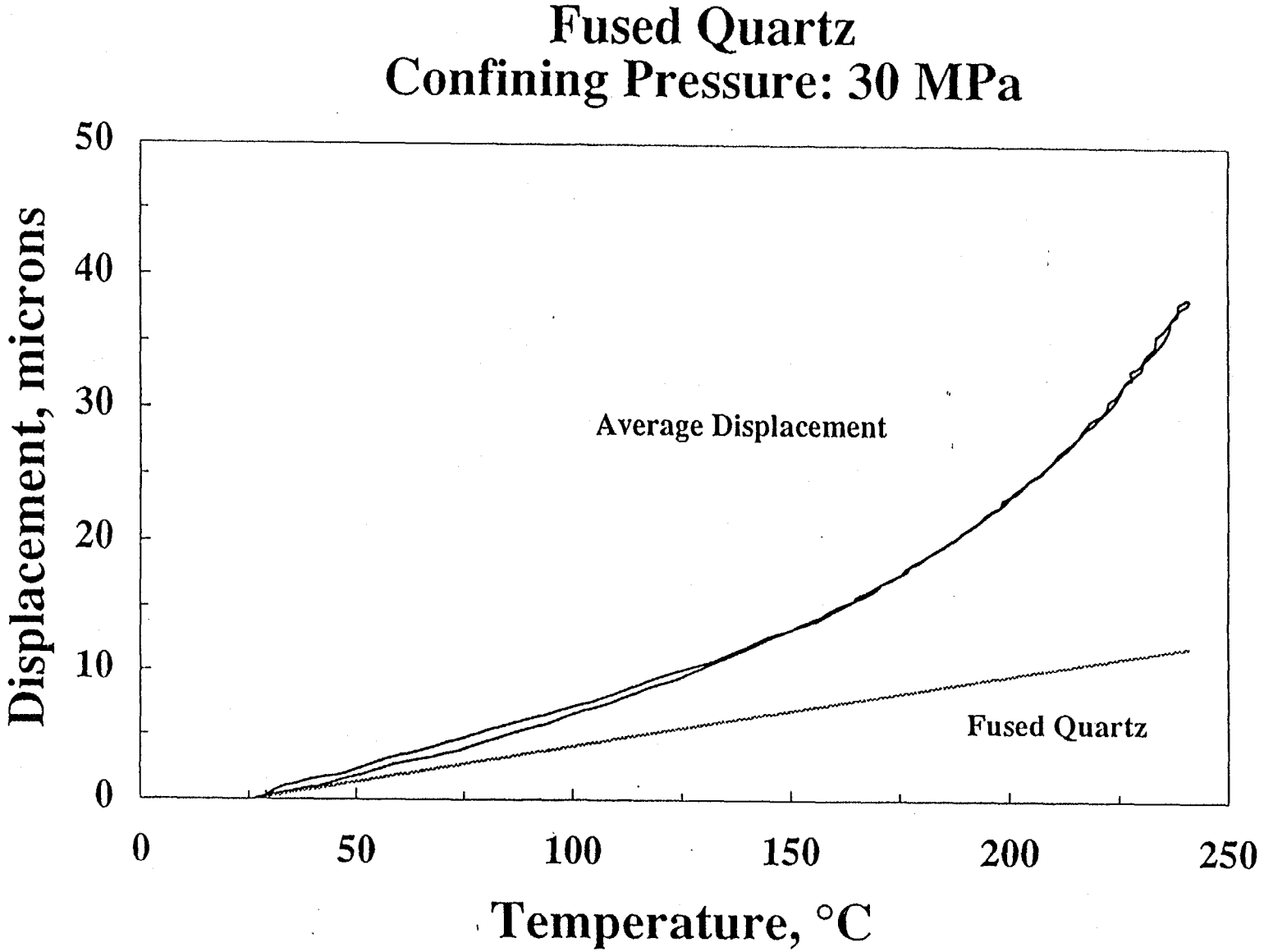

Figure 6: The average displacement is plotted as a function of temperature for a thermal cycle on fused quartz at a confining pressure of 30 MPa. The calculated displacement attributable to fused quartz is plotted for a reference.

As an integral part of the calibration process the temperature in proximity to the LVDTs was monitored. The data are shown in Figure 8. The temperature at the LVDTs is not constant throughout the experiment. It increases to near 65 °C during the heating cycle. The thermal history of the tuff specimens are compared to those of the fused quartz. If the temperature response at the LVDTs differs from that obtained in the calibration using fused quartz, the strain calculation from the displacement data may be in error. In the upper portion of the plot, the temperatures at the base, midpoint, and top of the specimen are shown. The data overlay each other in most instances.

2.3.3 Experimental Procedure for Thermal Expansion Experiments at Elevated Confining Pressure

Thermal expansion experiments were performed on a series of welded tuff specimens at constant confining pressures. The specimen was thermally cycled over the nominal range of 25 to 250 °C.

The following section includes the step-by-step procedures used to conduct the experiments.

1. Machine each test specimen according to SNL TP-51. Measure ultrasonic velocities of each specimen after the machining process is complete.

2. List all transducers used in each experiment. The information includes the serial number of the device, signal conditioning amplifier number, the computer channel on which the output is recorded, and the scaling factor of the amplified output.

3. Visually inspect the specimen and note any surface irregularities and imperfections.

4. Jacket the specimen with two layers of 0.13 mm thick fully annealed copper wrapped around the specimen and extending 12 mm beyond each end of the specimen. Invar end caps are positioned at the ends of the test specimen. The entire specimen assembly is then jacketed with teflon heat shrink tubing and secured with two wraps of wire at each end.

5. Position the specimen assembly on the base plug of the pressure vessel.

6. Insert the fused quartz tubes supporting the LVDT barrels through the base plug of the pressure vessel and secure them to the lower Invar endcap of the test specimen.

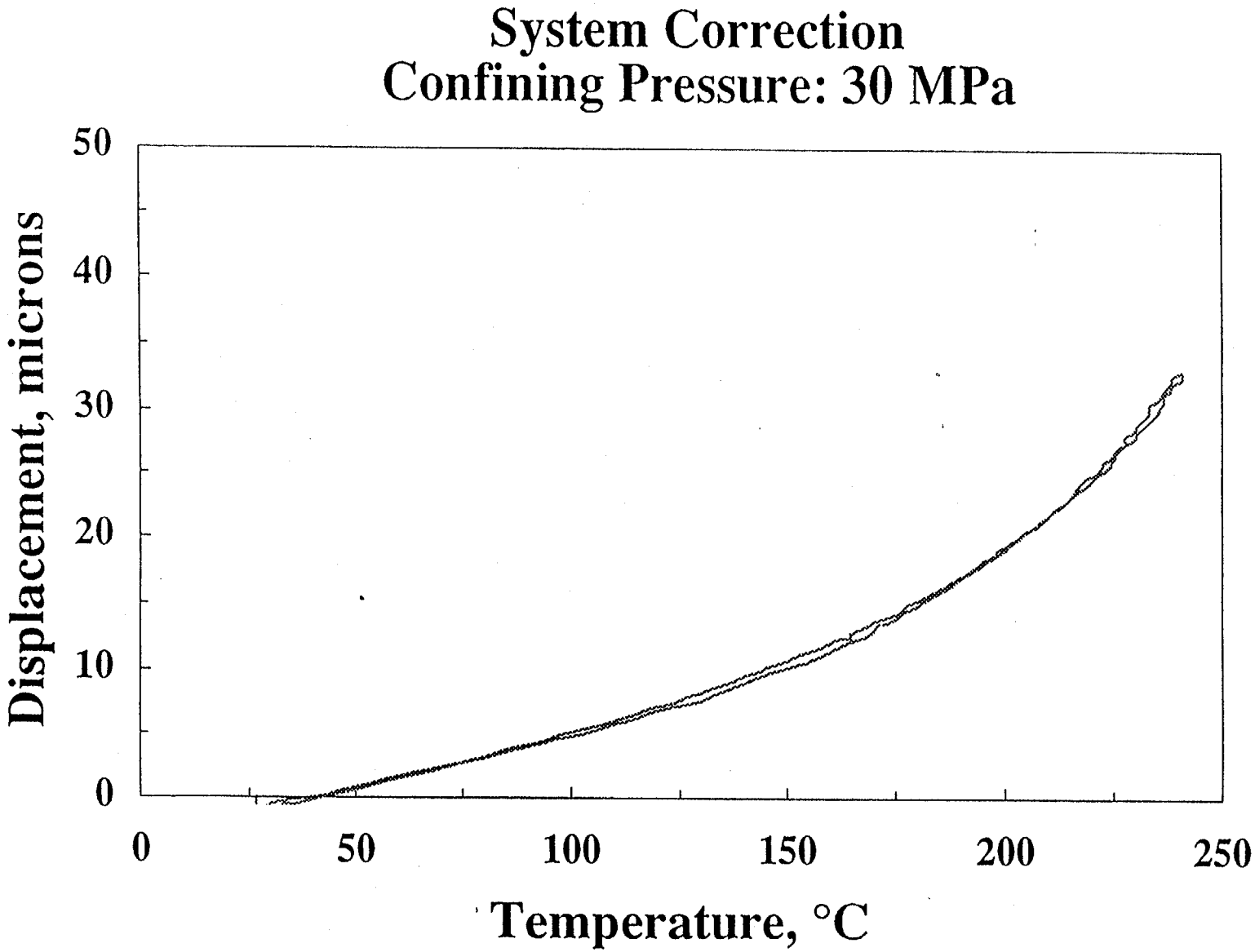

NER

Figure 7: The displacement attributable to the system and end caps in the sample assembly is plotted as a function of temperature. This is the correction that will be applied to all data collected at a confining pressure of 30 MPa.

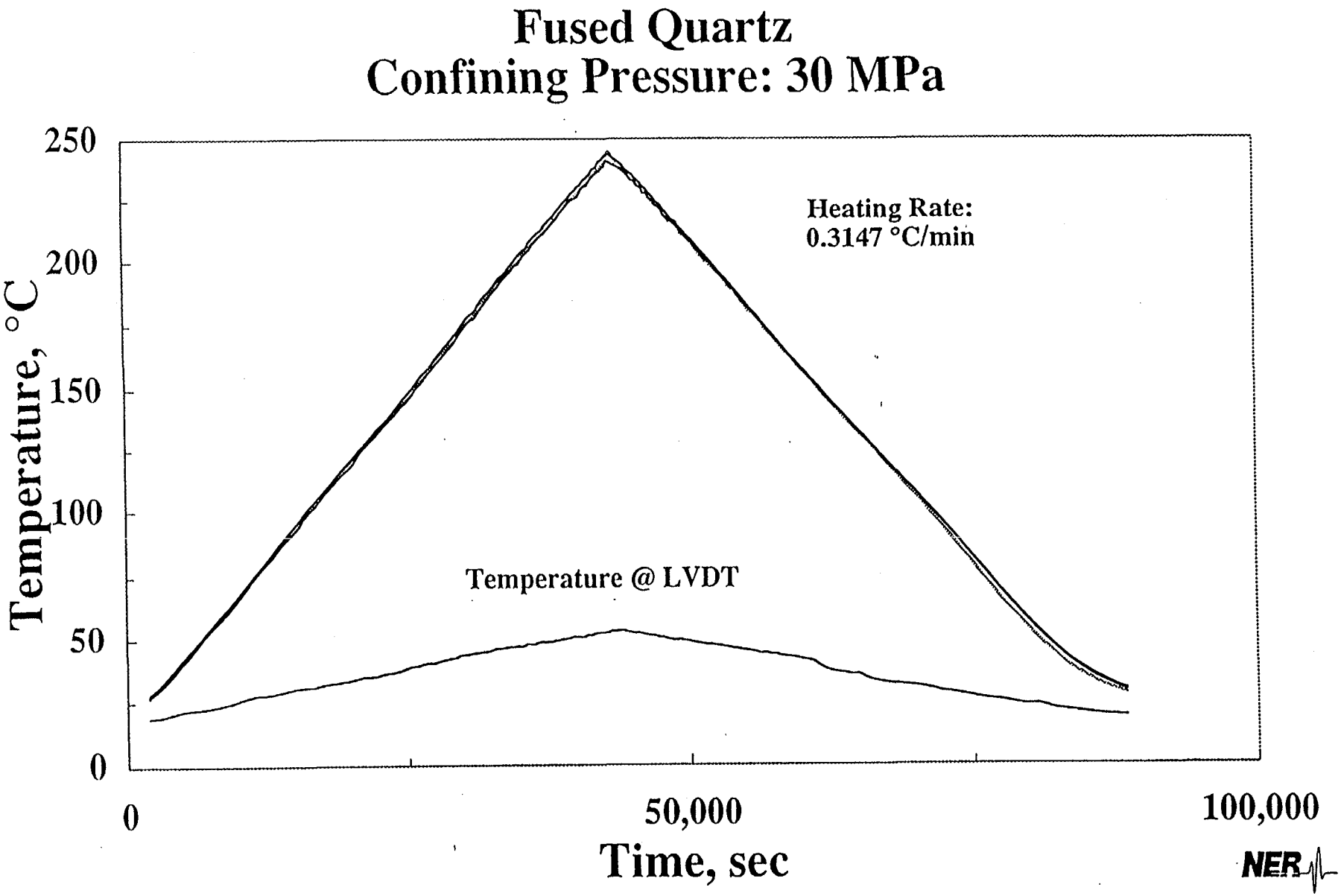

Figure 8: The temperature is plotted as a function of time for four positions in the pressure vessel. The top curves represent data collected at the base, midpoint, and top of the fused

7. Insert the fused quartz tube supporting the LVDT cores into the LVDT barrels and secure them to the Invar cap at the top of the test specimen.

8. Adjust the LVDTs so that their initial output is approximately nine (9) volts. (Note: The output of the LVDT will decrease with increasing temperature.)

9. Position the three thermocouples outside the test specimen at the top, midpoint, and base of the tuff specimen.

10. Insert the specimen assembly into the pressure vessel.

11. Plug the access ports at the base of each LVDT in the base plug of the pressure vessel.

12. Ensure that the output voltage for the LVDTs has not changed.

13. Increase the confining pressure to the specified value.

14. Initiate data acquisition.

15. Begin thermal cycling. The thermal cycling consists of two cycles at a nominal rate of 0.319 °C per minute over the range of 25 to 250 °C. A two hour delay is programmed between the first and second cycles.

16. Monitor the output of all of the devices to ensure that the system is performing satisfactorily.

17. Terminate the data acquisition at the completion of two heating/cooling cycles.

18. Change the confining pressure to its next value in the sequence and repeat the thermal cycling procedure (steps 14 to 17) for each specified pressure.

19. Remove the specimen from the pressure vessel at the completion of the thermal cycles for all designated pressures and examine any features related to the deformation of the specimen. Record the observations in the scientific notebook. Reweigh the specimen.

20. Measure the compressional and shear wave velocities in the post-test condition.

21. Reduce the data. The following information is determined: the axial strain (ε_a) (which is the change in length of the specimen, divided by its original length), temperature at the top, midpoint, and base of the specimen and at the LVDTs, and confining pressure.

The coefficient of thermal expansion (α_p) at constant pressure is given by:

$$\alpha_p = \left(\frac{\partial \varepsilon_a}{\partial T}\right)_p$$

where ε_a is the strain and T is the temperature at the midpoint of the specimen. For this study, the mean coefficient of thermal expansion calculated over 25 °C intervals is reported. A least squares fit to the data is used to compute the coefficients. The temperature intervals are: 25-50, 51-75, 76-100, 101-125, 126-150, 151-200, 201-225, 226-250 °C.

2.3.4 System Checks

To verify that the test system, including the data acquisition, is performing correctly a series of system checks are periodically performed on a specimen of AISI 446 stainless steel. AISI 446 stainless steel has coefficient of thermal expansion of $10.5 \pm 1.0 \times 10^{-6}$ °C^{-1} over a nominal range of 25 to 250 °C which is close to the anticipated values for tuff. The test specimen with the same dimensions as the tuff specimens, is tested over a nominal temperature range of 25 to 250 °C. One of the five confining pressures used in the experiments on tuff is selected and a single thermal cycle is performed using the test procedure outlined above. The system check is considered successful if the thermal expansion is reproduced to within ± 5% over selected temperature intervals. This procedure is used instead of performing three cycles with the fused quartz standard as recommended by ASTM to verify repeatability in the system.

Satisfactory performance of the system is essential for the accuracy of the test measurements on tuff. In light of this, a system check was performed prior to initiating the measurements on tuff and after testing three specimens. The results of the system checks are described in Appendix III.

3.0 RESULTS

Twenty-four thermal expansion measurements were conducted as a function of confining pressure on five specimens of Topopah Spring Member tuff (TSw2) recovered from borehole USW SD-12 from depths of 687.8, 742.9, 776.4, 883.5 and 1204.8 feet. Each specimen was tested at confining pressures between 1 and 30 MPa over a nominal temperature range of 25 to 250 °C. On three specimens, the higher confining pressure thermal cycles were performed first to inhibit thermal effects that may occur at lower confining pressures. Measurements on SD-12-883.5 and SD-12-1204.8 were conducted from the lowest to the highest confining pressure. Two thermal cycles were performed at each confining pressure. After the first thermal cycle at 10 MPa on SD-12-883.5, several drops of oil were observed at the base of the pressure vessel. This may indicate a jacket leak. The specimen was removed and examined. The jacket did not leak. The specimen was rejacketed and the test sequence resumed. Two complete thermal cycles at 10 MPa were performed. Consequently on this specimen, three thermal cycles were performed at a confining pressure of 10 MPa.

The thermal expansion as a function of temperature was similar for all specimens. During the first thermal loading cycle (at both 1 and 30 MPa), the strain as a function of temperature curve was concave upward. Upon unloading there was a hysteresis. More strain was observed during cooling than heating. The specimen was shorter after the first thermal cycle by an amount of approximately 0.025 mm. The magnitude of the effect was the same whether or not the initial thermal cycle was at 1 or 30 MPa. For the second thermal cycle, the strain versus temperature curve was also concave upward, however, there was no permanent change in specimen length at the termination of the cycle. The hysteresis during cooling was small but evident at temperatures greater than 175 °C. Subsequent experiments at the other confining pressures were nearly identical to those observed for the second thermal loading cycle at the initial pressure. These characteristics were the same for all specimens tested. The data for these experiments are presented in Appendix II.

The mean coefficient of thermal expansion, α, for the first two thermal cycles on specimen SD-12-687.8 conducted at a confining pressure of 30 MPa are shown in Figures 9 and 10. The data for the first loading cycle is shown in Figure 9. The mean coefficient of thermal expansion was

computed over 25 °C intervals by taking the least squares fit to the strain versus temperature data. The coefficient is plotted at the mid point of the interval. Open circles indicate heating and the diamonds indicate cooling. The mean coefficients of thermal expansion at temperatures below 175 °C increases from 8.75 to 10.48 x 10^{-6} $°C^{-1}$. For temperatures above 175 °C, the thermal expansion increases rapidly. Mean coefficients of thermal expansion in excess of 16.4 x 10^{-6} $°C^{-1}$ are observed between 225 and 250 °C. Upon cooling there is a pronounced hysteresis; over each temperature interval the coefficient of thermal expansion is greater during cooling than upon initial heating.

The mean coefficients of thermal expansion for the second cycle are shown in Figure 10. The values are very similar to those observed during cooling for the first cycle. The values for heating and cooling at temperatures between 25 and 175 °C show very little scatter. The scatter is slightly larger between 175 and 250 °C.

The mean coefficients of thermal expansion were computed over 25 °C increments for all the tuff specimens tested. The results are shown in Tables 2, 3, 4, 5, and 6. The data in each table are arranged in the order that the tests were performed; for some specimens the highest pressure cycles were conducted first whereas on other specimens the lowest pressure cycles were run first. The greatest uncertainty involves the data between 226 and 250 °C during the cooling cycles. In all specimens, hysteresis is observed when cooling is initiated at the peak temperature. Calculations of the mean coefficients of thermal expansion for cooling do not include data within 3 °C of the peak temperature for the cycle.

The effect of confining pressure on thermal expansion is small. One effect of pressure on the specimens studied is shown in Figures 11, 12, 13, 14, and 15. The mean coefficients of thermal expansion computed for cooling cycles over temperature ranges 76-100 and 201-225 °C are plotted as a function of confining pressure . At temperatures between 76 and 100 °C, the coefficients increase several percent as the confining pressure increases from 1 to 30 MPa. In contrast, the coefficient decreases by up to 12% over the same pressure interval for temperatures between 201 and 225 °C.

At the termination of each experiment, the specimen was removed from the pressure vessel and weighed. The specimens lost mass due to thermal cycling. The loss is attributable to water driven out of the specimen due to heating. During the first thermal cycle on each specimen, steam and water were

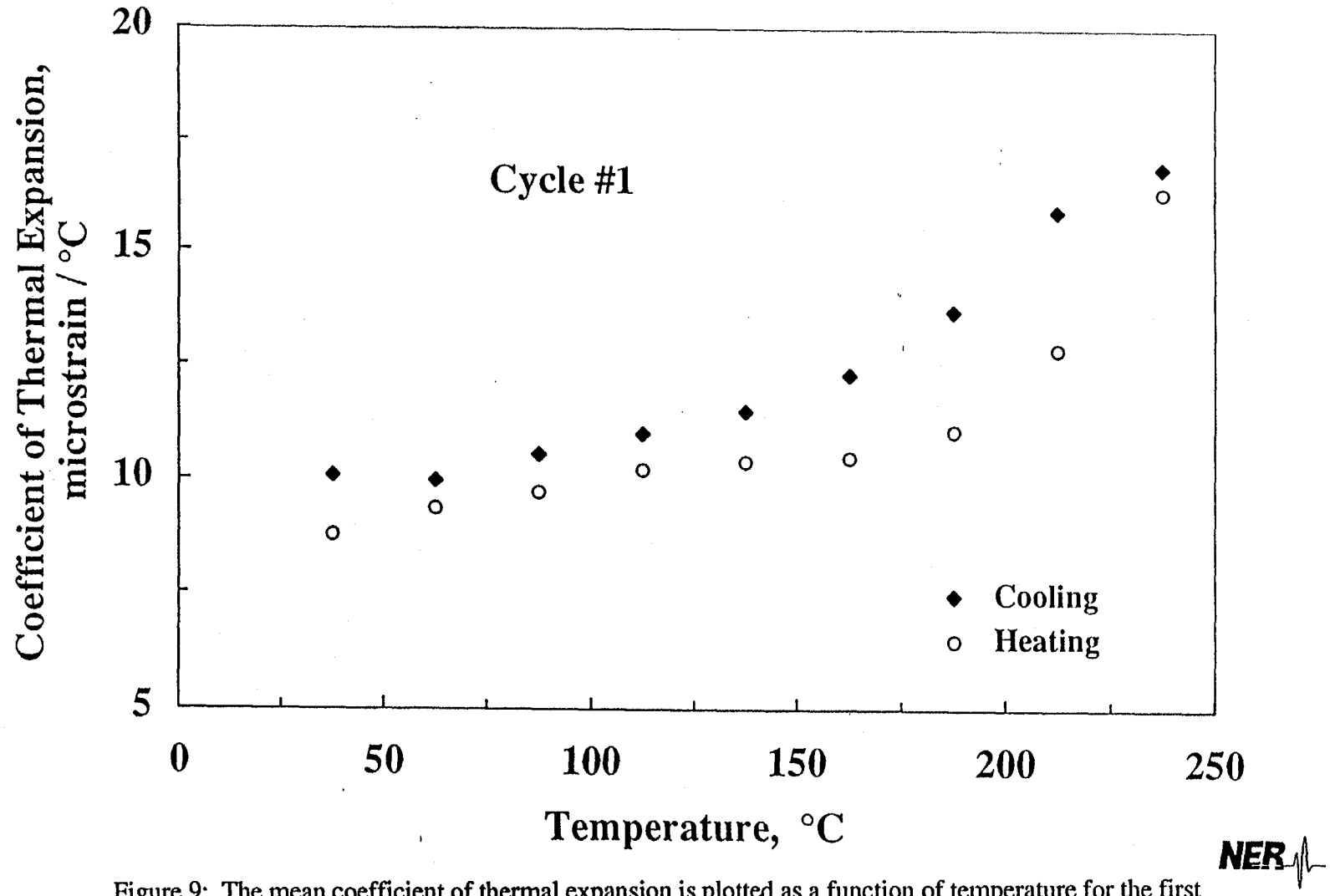

Figure 9: The mean coefficient of thermal expansion is plotted as a function of temperature for the first thermal cycle on specimen SD 12-687.8 at a confining pressure of 30 MPa. The coefficient of linear thermal expansion is computed over 25 °C intervals. The data are plotted at the mid point of the range.

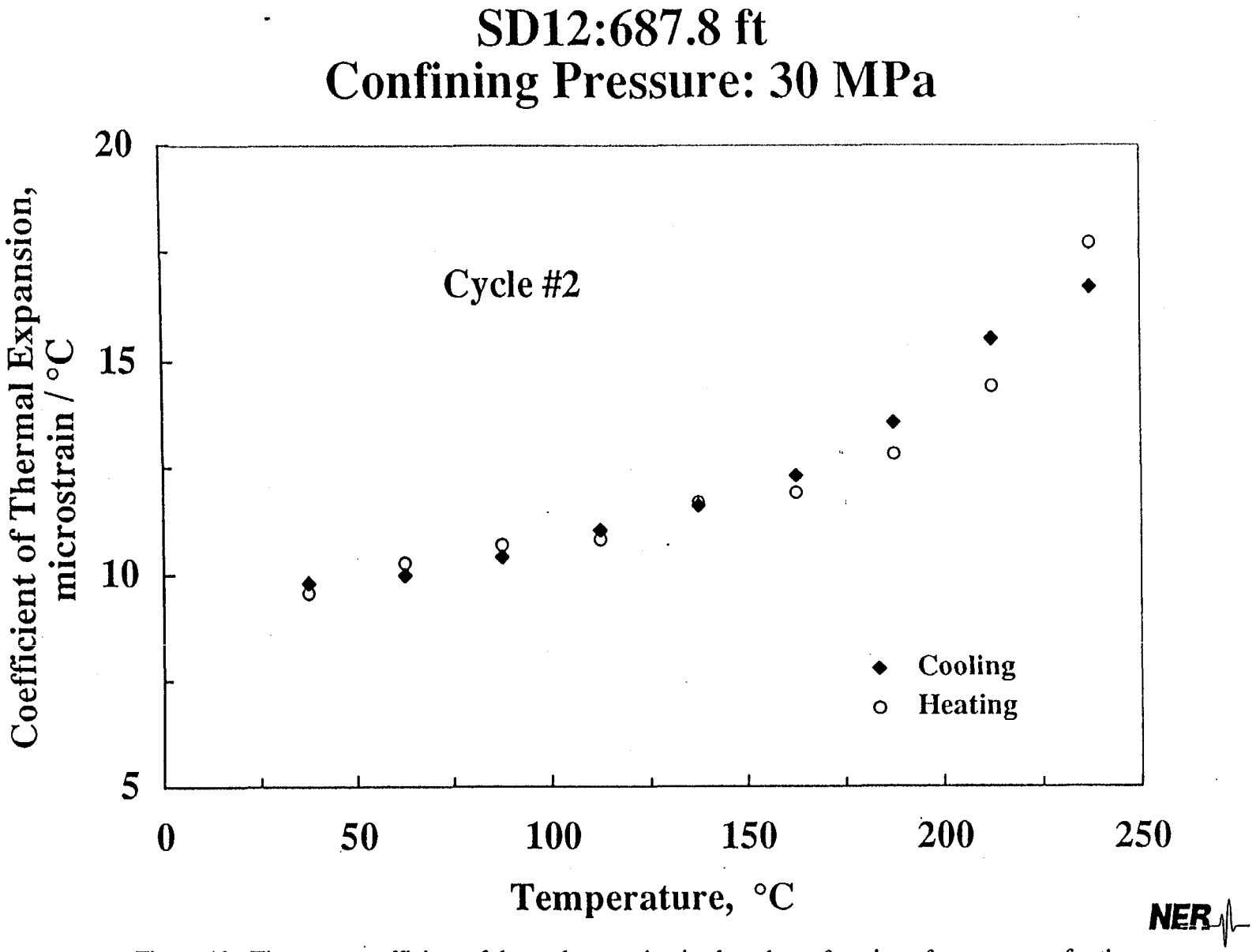

Figure 10: The mean coefficient of thermal expansion is plotted as a function of temperature for the second thermal cycle on specimen SD 12-687.8 at a confining pressure of 30 MPa. The coefficient of linear thermal expansion is computed over 25 °C intervals. The data are plotted at the mid point of the range.

Table 2

Mean Coefficient of Thermal Expansion, microstrain/°C

Borehole: SD-12; Depth: 687.8 feet

Confining Pressure: 30 MPa

	Cycle 1		Cycle 2	
Temperature, °C	*Heating*	*Cooling*	*Heating*	*Cooling*
25-50	8.75	10.06	9.58	9.80
51-75	9.34	9.95	10.28	10.00
76-100	9.71	10.54	10.70	10.41
101-125	10.21	10.99	10.82	11.02
126-150	10.39	11.48	11.69	11.59
151-175	10.48	12.28	11.91	12.31
176-200	11.08	13.67	12.84	13.58
201-225	12.86	15.91	14.48	15.51
226-250	16.35	16.90	17.70	16.67

Confining Pressure: 20 MPa

	Cycle 1		Cycle 2	
Temperature, °C	*Heating*	*Cooling*	*Heating*	*Cooling*
25-50	9.33	9.96	9.86	9.95
51-75	10.16	10.00	10.22	10.10
76-100	10.68	10.38	10.75	10.86
101-125	11.21	11.16	11.21	11.08
126-150	11.24	11.69	11.59	11.63
151-175	11.80	12.24	11.71	12.33
176-200	12.85	14.13	13.01	13.76
201-225	14.28	15.07	14.71	14.86
226-250	17.95	16.85	19.05	16.35

Confining Pressure: 10 MPa

	Cycle 1		Cycle 2	
Temperature, °C	*Heating*	*Cooling*	*Heating*	*Cooling*
25-50	10.10	9.95	10.25	10.20
51-75	10.23	10.30	10.43	10.12
76-100	10.56	10.35	10.62	10.29
101-125	10.78	11.06	10.65	11.07
126-150	10.84	11.74	10.70	11.51
151-175	11.69	12.20	12.30	12.09
176-200	12.94	14.43	12.85	14.35
201-225	14.82	15.66	15.50	15.06
226-250	19.03	17.24	18.15	16.36

Confining Pressure: 5 MPa

	Cycle 1		Cycle 2	
Temperature, °C	*Heating*	*Cooling*	*Heating*	*Cooling*
25-50	9.45	9.20	9.18	9.21
51-75	9.60	9.55	10.09	9.46
76-100	10.21	9.85	10.19	10.07
101-125	10.75	10.86	10.65	10.75
126-150	11.29	11.59	11.08	11.48
151-175	11.66	12.22	11.79	12.48
176-200	13.50	13.46	13.58	14.20
201-225	16.18	16.51	15.26	15.93
226-250	18.18	17.57	18.77	17.63

Table 3

Mean Coefficient of Thermal Expansion, microstrain/°C

Borehole: SD-12; Depth: 742.9 feet

Confining Pressure: 30 MPa

	Cycle 1		Cycle 2	
Temperature, °C	*Heating*	*Cooling*	*Heating*	*Cooling*
25-50	9.18	10.02	9.48	9.66
51-75	9.70	9.94	10.35	9.90
76-100	9.78	10.27	10.74	10.30
101-125	10.09	11.06	10.84	10.91
126-150	10.17	11.44	11.27	11.41
151-175	10.19	11.99	11.44	11.96
176-200	10.21	12.77	12.32	13.51
201-225	12.37	14.76	14.92	13.96
226-250	16.87	17.31	16.07	15.48

Confining Pressure: 20 MPa

	Cycle 1		Cycle 2	
Temperature, °C	*Heating*	*Cooling*	*Heating*	*Cooling*
25-50	9.56	9.53	9.31	9.54
51-75	10.28	9.85	10.32	9.89
76-100	10.60	10.26	10.80	10.29
101-125	10.65	11.11	10.88	11.05
126-150	11.10	11.52	11.23	11.47
151-175	11.77	12.05	11.72	12.03
176-200	12.64	13.42	12.53	13.27
201-225	14.18	14.52	14.12	14.25
226-250	16.53	15.22	17.36	15.55

Confining Pressure: 10 MPa

	Cycle 1		Cycle 2	
Temperature, °C	*Heating*	*Cooling*	*Heating*	*Cooling*
25-50	9.96	10.07	9.96	10.08
51-75	10.38	10.21	10.32	10.02
76-100	10.70	10.32	10.66	10.32
101-125	10.80	10.93	10.78	10.94
126-150	10.98	11.36	10.96	11.28
151-175	11.53	11.94	11.67	11.98
176-200	13.03	13.81	13.08	13.61
201-225	14.95	15.18	14.82	15.36
226-250	18.49	16.29	17.36	16.24

Confining Pressure: 5 MPa

	Cycle 1		Cycle 2	
Temperature, °C	*Heating*	*Cooling*	*Heating*	*Cooling*
25-50	8.91	9.11	9.12	9.23
51-75	9.81	9.55	9.74	9.44
76-100	10.23	9.98	10.30	9.98
101-125	10.39	10.80	10.42	10.60
126-150	10.95	11.49	10.70	11.41
151-175	11.76	12.33	11.59	12.13
176-200	12.94	14.05	12.57	14.07
201-225	14.66	15.85	14.55	15.07
226-250	18.10	16.52	17.99	16.12

Table 3 (Continued)

Mean Coefficient of Thermal Expansion, microstrain/°C

Borehole: SD-12; Depth: 742.9 feet

Confining Pressure: 1.0 MPa

	Cycle 1		Cycle 2	
Temperature, °C	*Heating*	*Cooling*	*Heating*	*Cooling*
25-50	8.79	9.95	8.95	8.89
51-75	9.60	9.49	9.70	9.54
76-100	10.10	10.10	10.12	9.95
101-125	10.46	10.77	10.25	10.71
126-150	10.88	11.40	11.07	11.39
151-175	11.90	12.48	11.59	12.30
176-200	12.93	14.08	12.41	14.08
201-225	14.95	15.71	14.86	15.71
226-250	18.94	16.42	18.28	16.66

Table 4

Mean Coefficient of Thermal Expansion, microstrain/°C

Borehole: SD-12; Depth: 776.4 feet

Confining Pressure: 30 MPa

	Cycle 1		Cycle 2	
Temperature, °C	*Heating*	*Cooling*	*Heating*	*Cooling*
25-50	8.91	9.87	9.47	9.93
51-75	9.55	10.14	10.19	10.16
76-100	9.74	10.6	10.76	10.57
101-125	10.18	11.12	10.98	11.15
126-150	10.28	11.67	11.38	11.75
151-175	10.85	12.55	11.82	12.34
176-200	11.23	13.52	12.44	13.4
201-225	13.21	15.08	14.14	14.98
226-250	17.34	16.37	17.58	15.52

Confining Pressure: 20 MPa

	Cycle 1		Cycle 2	
Temperature, °C	*Heating*	*Cooling*	*Heating*	*Cooling*
25-50	8.69	9.76	9.23	9.84
51-75	10.23	10.14	10.21	10.30
76-100	10.87	10.46	10.84	10.49
101-125	11.09	11.30	11.06	11.06
126-150	11.55	11.60	11.44	11.58
151-175	11.81	12.74	11.72	12.38
176-200	12.90	13.52	12.90	13.49
201-225	14.57	15.33	14.55	15.01
226-250	17.68	16.80	17.91	16.24

Confining Pressure: 10 MPa

	Cycle 1		Cycle 2	
Temperature, °C	*Heating*	*Cooling*	*Heating*	*Cooling*
25-50	9.75	10.00	9.64	10.13
51-75	10.54	10.40	10.44	10.43
76-100	10.91	10.78	10.96	10.72
101-125	11.20	11.31	11.23	11.27
126-150	11.43	11.75	11.58	11.75
151-175	11.83	12.60	11.98	12.55
176-200	12.94	13.69	13.13	13.50
201-225	15.21	15.68	14.92	15.71
[illegible]	[illegible]	[illegible]	[illegible]	[illegible]

Confining Pressure: 5 MPa

	Cycle 1		Cycle 2	
Temperature, °C	*Heating*	*Cooling*	*Heating*	*Cooling*
25-50	9.90	8.68	8.70	9.09
51-75	10.02	9.86	9.77	9.69
76-100	10.39	10.24	10.31	10.24
101-125	10.61	10.93	10.54	10.95
126-150	11.01	11.53	11.16	11.53
151-175	11.28	12.31	11.83	12.22
176-200	12.61	13.92	13.08	14.13
201-225	15.46	15.96	15.27	16.12
[illegible]	[illegible]	[illegible]	[illegible]	[illegible]

Table 4 (Continued)

Mean Coefficient of Thermal Expansion, microstrain/°C

Borehole: SD-12; Depth: 776.4 feet

Confining Pressure: 1.0 MPa

	Cycle 1		Cycle 2	
Temperature, °C	*Heating*	*Cooling*	*Heating*	*Cooling*
25-50	7.87	9.27	8.97	9.33
51-75	9.91	9.76	9.75	9.61
76-100	10.52	10.16	10.31	10.17
101-125	10.57	11.03	10.67	10.94
126-150	11.11	11.70	11.24	11.67
151-175	11.82	12.62	11.89	12.48
176-200	13.52	14.22	13.40	14.58
201-225	15.22	17.01	15.62	16.46
226-250	19.40	18.43	19.27	17.76

Table 5

Mean Coefficient of Thermal Expansion, microstrain/°C

Borehole: SD-12; Depth: 883.5 feet

Confining Pressure: 1 MPa

	Cycle 1		Cycle 2	
Temperature, °C	*Heating*	*Cooling*	*Heating*	*Cooling*
25-50	8.86	9.54	8.70	9.20
51-75	9.55	9.76	9.72	9.64
76-100	9.90	10.34	10.25	10.14
101-125	9.79	11.50	10.46	11.04
126-150	9.95	11.87	11.11	11.92
151-175	10.66	13.51	12.01	13.59
176-200	12.88	15.53	14.46	15.41
201-225	15.59	16.44	16.35	16.06
226-250	20.57	16.10	18.89	16.07

Confining Pressure: 5 MPa

	Cycle 1		Cycle 2	
Temperature, °C	*Heating*	*Cooling*	*Heating*	*Cooling*
25-50	8.17	8.93	8.66	9.29
51-75	9.46	9.64	9.72	9.57
76-100	9.91	10.02	10.21	10.00
101-125	10.18	10.81	10.73	10.74
126-150	10.75	11.52	10.81	11.46
151-175	11.61	12.74	11.83	12.79
176-200	13.84	14.99	13.98	14.93
201-225	15.77	15.98	16.24	15.99
226-250	18.32	16.08	18.48	16.41

Confining Pressure: 10 MPa

	Cycle 1		Cycle 2	
Temperature, °C	*Heating*	*Cooling*	*Heating*	*Cooling*
25-50	9.33	9.77		
51-75	10.10	10.10		
76-100	10.36	10.14		
101-125	10.37	10.68		
126-150	10.50	11.31		
151-175	10.37	12.70		
176-200	13.38	14.68		
201-225	15.25	15.78		
226-250	17.99	16.06		

Confining Pressure: 10 MPa

	Cycle 1		Cycle 2	
Temperature, °C	*Heating*	*Cooling*	*Heating*	*Cooling*
25-50	9.82	9.97	9.28	9.89
51-75	10.34	10.04	9.98	9.98
76-100	10.40	10.15	10.25	10.06
101-125	10.29	10.61	10.18	10.56
126-150	10.55	11.37	10.69	11.22
151-175	11.41	12.56	11.26	12.42
176-200	13.30	14.70	13.17	14.63
201-225	15.39	15.80	15.17	15.72
226-250	17.96	15.93	17.62	15.68

Table 5 (Continued)

Mean Coefficient of Thermal Expansion, microstrain/°C

Borehole: SD-12; Depth: 883.5 feet

Confining Pressure: 20 MPa

	Cycle 1		Cycle 2	
Temperature, °C	*Heating*	*Cooling*	*Heating*	*Cooling*
25-50	8.99	9.46	9.25	9.47
51-75	9.88	9.76	10.05	9.74
76-100	10.21	10.05	10.55	10.16
101-125	10.12	10.52	10.23	10.69
126-150	10.39	11.15	10.45	11.32
151-175	11.11	12.13	11.27	12.03
176-200	12.49	13.79	12.84	13.85
201-225	13.82	14.70	14.14	14.54
226-250	16.47	14.85	16.80	14.46

Confining Pressure: 30 MPa

	Cycle 1		Cycle 2	
Temperature, °C	*Heating*	*Cooling*	*Heating*	*Cooling*
25-50	8.12	9.66	9.02	9.58
51-75	9.79	9.75	10.14	9.17
76-100	10.31	10.80	10.45	10.00
101-125	10.11	10.56	10.23	10.43
126-150	10.47	10.94	10.51	10.91
151-175	11.08	11.83	11.05	11.73
176-200	12.47	13.53	12.03	13.33
201-225	13.38	14.34	13.52	14.08
226-250	15.87	15.05	15.81	14.23

Table 6

Mean Coefficient of Thermal Expansion, microstrain/°C

Borehole: SD-12; Depth: 1204.8 feet

Confining Pressure: 1 MPa

	Cycle 1		Cycle 2	
Temperature, °C	*Heating*	*Cooling*	*Heating*	*Cooling*
25-50	8.82	9.33	9.08	9.22
51-75	9.24	9.70	9.96	9.62
76-100	9.93	10.32	10.20	10.28
101-125	9.16	11.20	10.63	11.21
126-150	9.51	12.20	11.49	12.19
151-175	10.86	13.83	12.45	13.83
176-200	12.99	16.38	14.43	16.02
201-225	16.15	17.55	17.13	17.66
226-250	20.37	18.01	19.93	18.71

Confining Pressure: 5 MPa

	Cycle 1		Cycle 2	
Temperature, °C	*Heating*	*Cooling*	*Heating*	*Cooling*
25-50	9.12	9.33	9.26	9.42
51-75	9.61	9.71	9.86	9.94
76-100	10.13	10.30	10.48	10.28
101-125	10.30	10.91	10.62	10.87
126-150	11.14	12.09	11.29	11.84
151-175	12.04	13.34	12.07	13.53
176-200	14.34	15.45	13.75	13.45
201-225	16.24	17.68	16.44	17.28
226-250	19.04	17.37	18.78	16.50

Confining Pressure: 10 MPa

	Cycle 1		Cycle 2	
Temperature, °C	*Heating*	*Cooling*	*Heating*	*Cooling*
25-50	9.47	10.24	10.13	10.06
51-75	9.86	10.32	10.25	10.17
76-100	10.14	10.54	10.81	10.34
101-125	10.22	10.92	10.65	11.12
126-150	11.04	12.04	11.08	11.73
151-175	11.60	13.33	11.89	12.86
176-200	13.66	15.80	13.53	15.31
201-225	16.64	17.27	16.45	17.30
226-250	18.62	17.07	18.68	16.48

Confining Pressure: 30 MPa

	Cycle 1		Cycle 2	
Temperature, °C	*Heating*	*Cooling*	*Heating*	*Cooling*
25-50	9.07	9.86	8.98	9.91
51-75	9.75	9.88	10.08	9.96
76-100	10.40	10.36	10.73	10.37
101-125	10.25	11.01	10.83	11.00
126-150	10.79	11.63	11.14	11.45
151-175	11.56	12.62	11.64	12.56
176-200	12.77	14.05	12.80	13.88
201-225	14.62	15.90	14.82	15.84
226-250	17.77	16.51	17.95	16.31

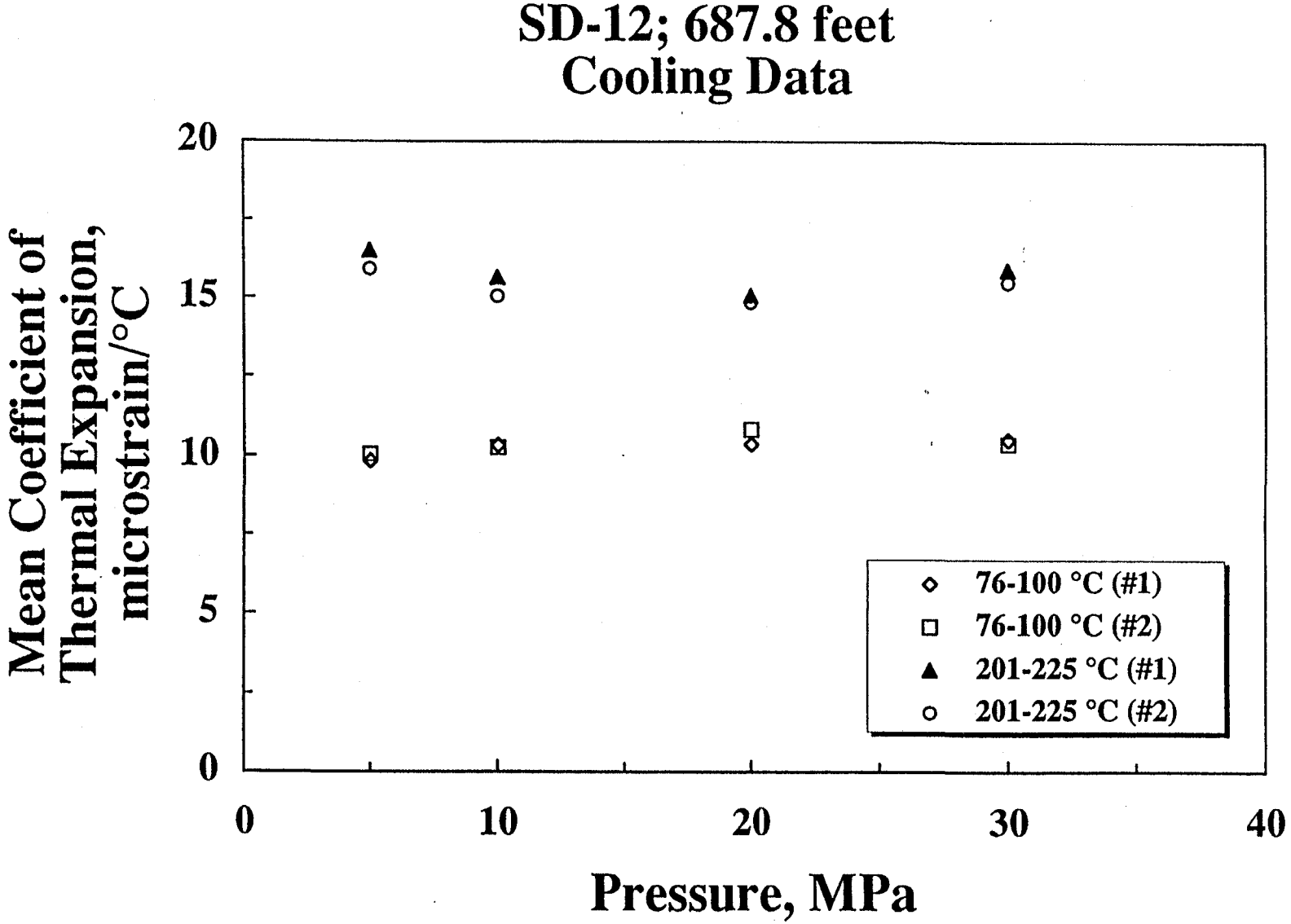

Figure 11: The mean coefficient of thermal expansion is plotted as a function of confining pressure for two temperature intervals: 76 to 100 and 201 to 225 °C. The coefficients were computed from the data collected on the cooling cycles.

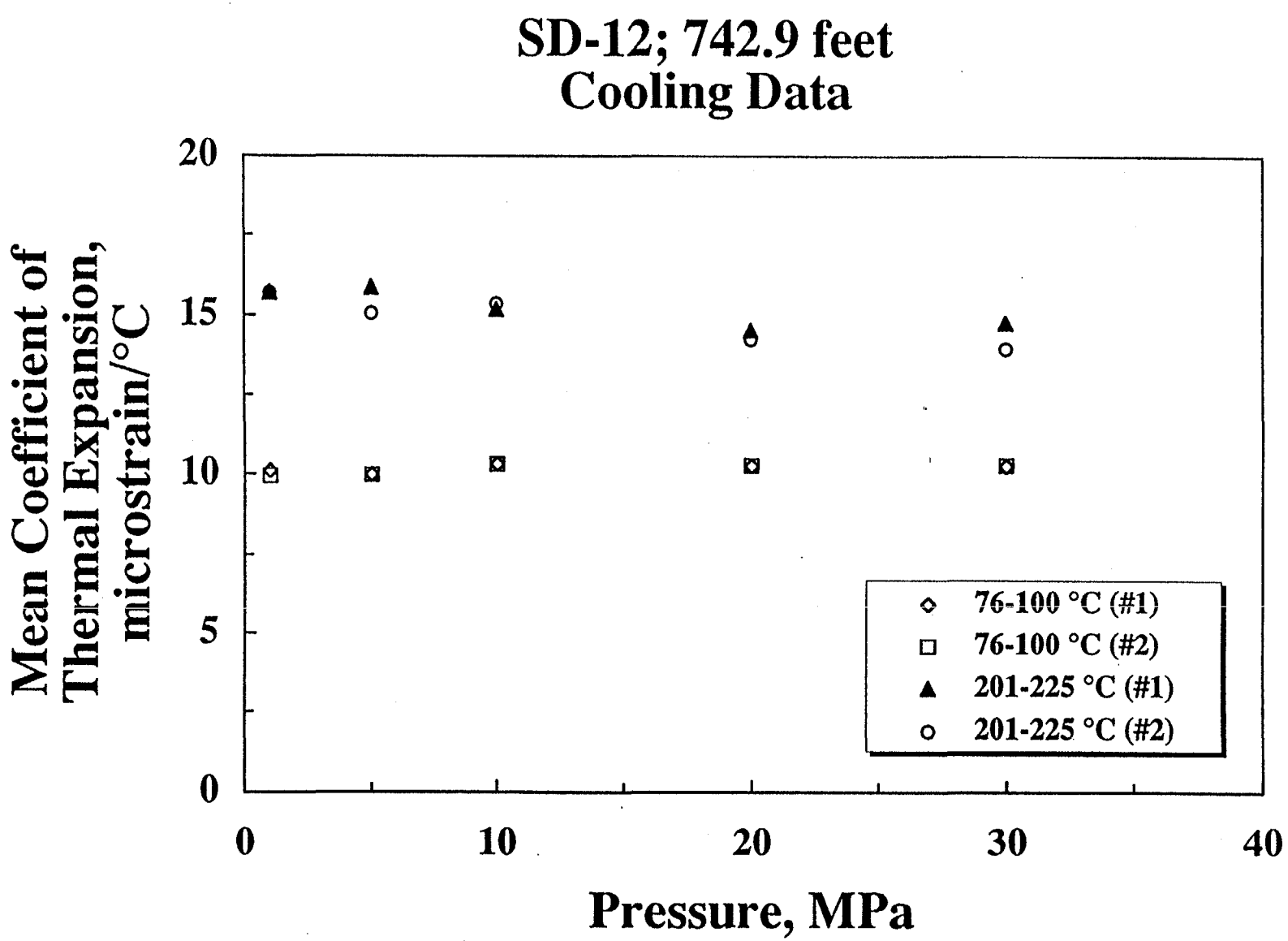

Figure 12: The mean coefficient of thermal expansion is plotted as a function of confining pressure for two temperature intervals: 76 to 100 and 201 to 225 °C. The coefficients were computed from the data collected on the cooling cycle.

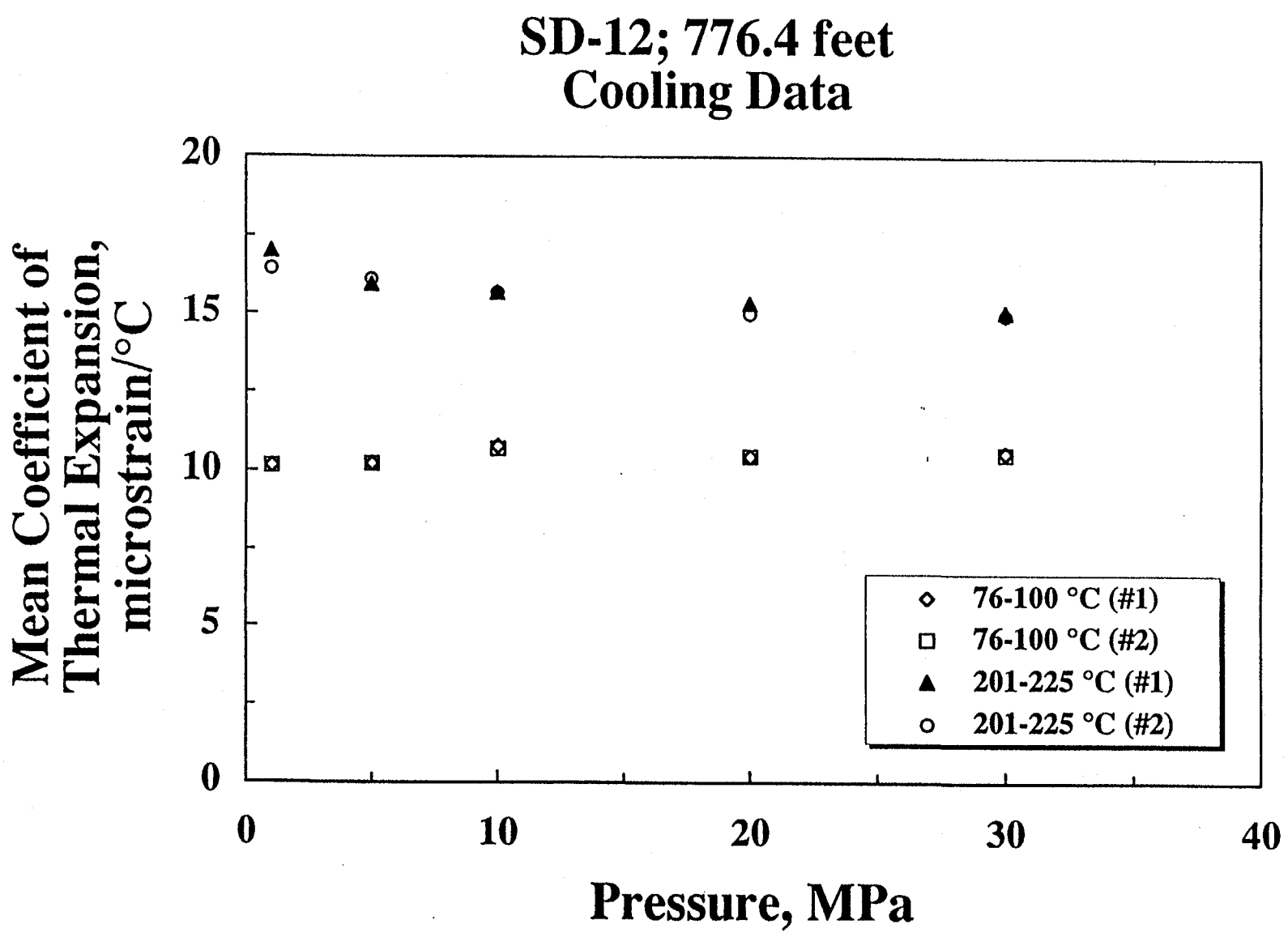

Figure 13: The mean coefficient of thermal expansion is plotted as a function of confining pressure for two temperature intervals: 76 to 100 and 201 to 225 °C. The coefficients were computed from the data collected on the cooling cycles.

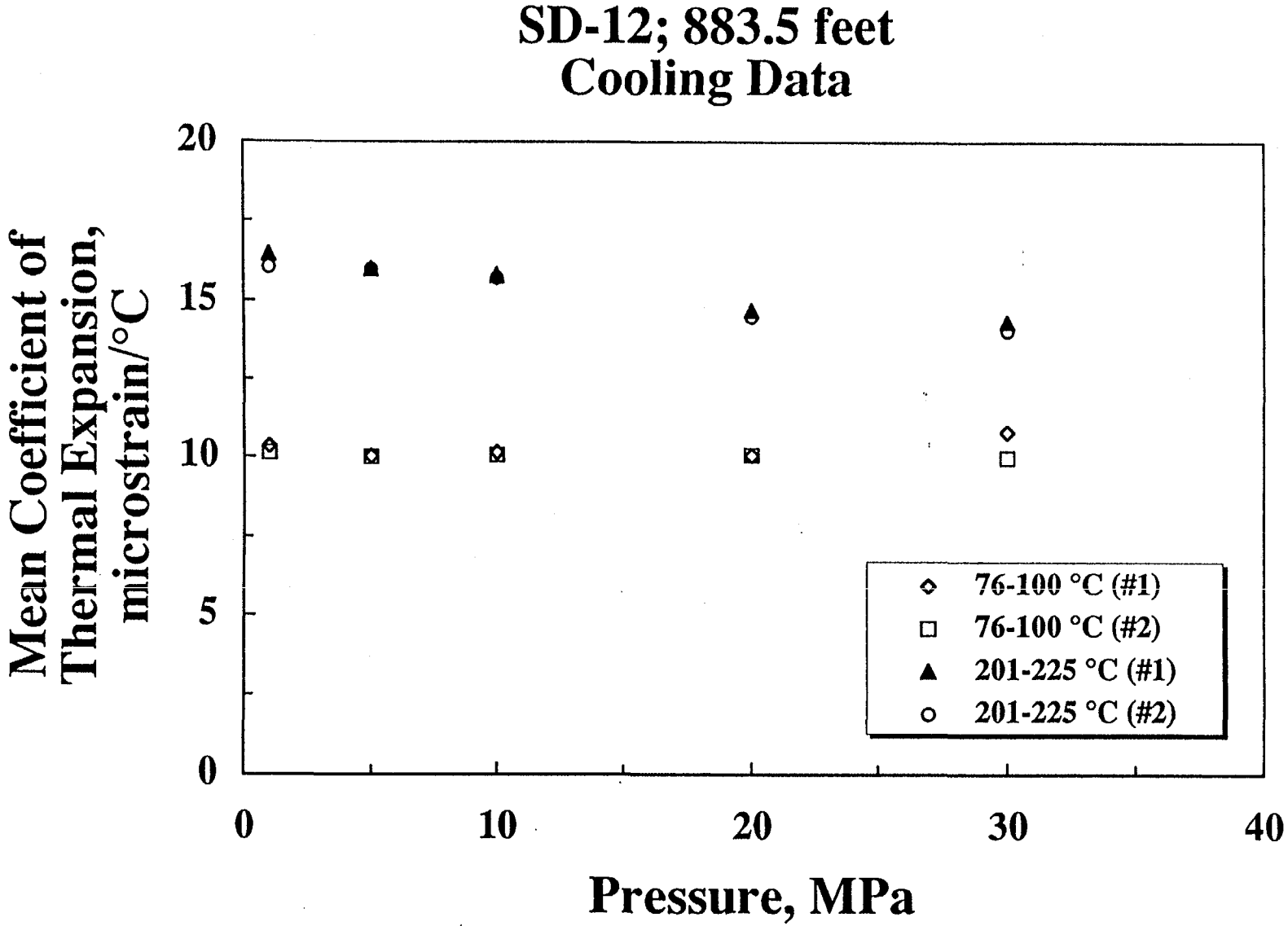

Figure 14: The mean coefficient of thermal expansion is plotted as a function of confining pressure for two temperature intervals: 76 to 100 and 201 to 225 °C. The coefficients were computed from the data collected on the cooling cycles.

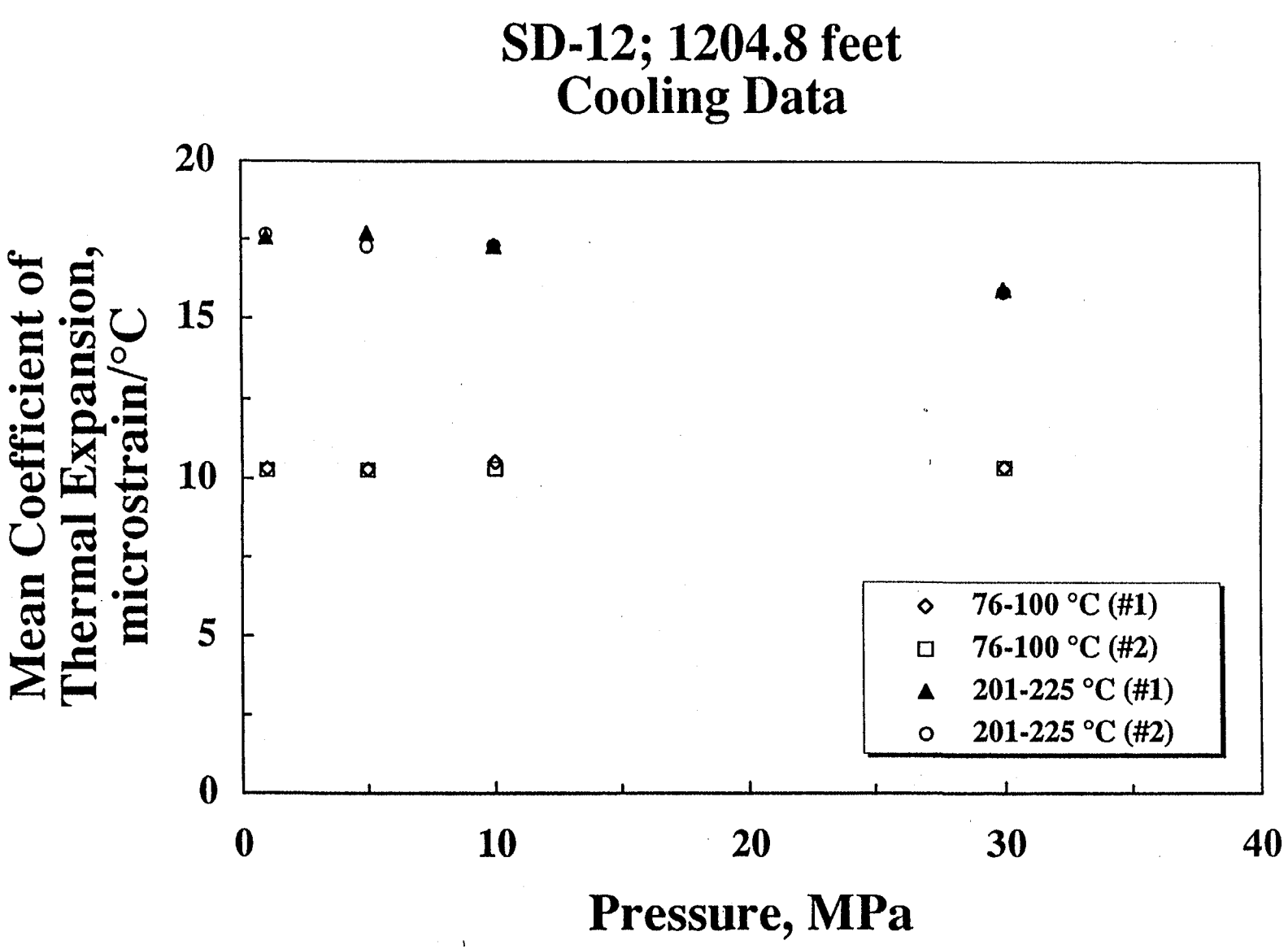

Figure 15: The mean coefficient of thermal expansion is plotted as a function of confining pressure for two temperature intervals: 76 to 100 and 201 to 225 °C. The coefficients were computed from the data collected on the cooling cycles.

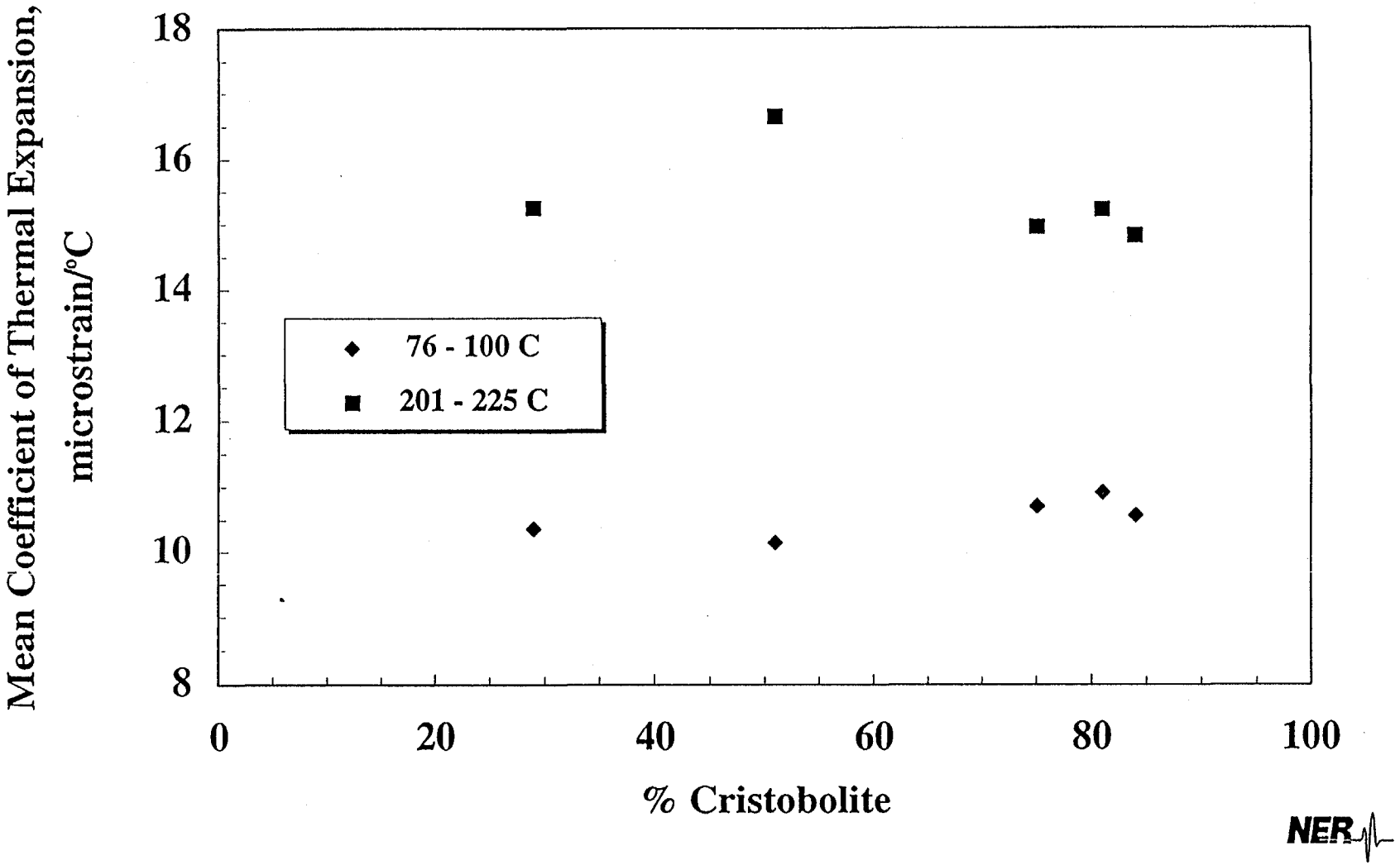

Figure 16: Mean coefficients of thermal expansion at a confining pressure of 10 MPa are plotted as a function of the percentage of cristobolite with respect to the total SiO_2 content.

emitted at the pore pressure port at the base of the specimen assembly.

specimens studied is shown in Figures 11, 12, 13, 14, and 15. The mean coefficients of thermal expansion computed for cooling cycles over temperature ranges 76-100 and 201-225 °C are plotted as a function of confining pressure . At temperatures between 76 and 100 °C, the coefficients increase several percent as the confining pressure increases from 1 to 30 MPa. In contrast, the coefficient decreases by up to 12% over the same pressure interval for temperatures between 201 and 225 °C.

At the termination of each experiment, the specimen was removed from the pressure vessel and weighed. The specimens lost mass due to thermal cycling. The loss is attributable to water driven out of the specimen due to heating. During the first thermal cycle on each specimen, steam and water were emitted at the pore pressure port at the base of the specimen assembly.

Compressional and shear wave velocities were measured prior to and after each experiment. These data are shown in the Tables in Appendix II. The compressional and shear wave velocities after testing were several percent greater than those measured prior to testing. The fact that the compressional and shear wave velocities increased indicate that no damage in the form of microcracks was done to the specimen due to thermal cycling. Furthermore, the data also suggest the possibility that the moisture driven off the specimen may increase the surface energy on pores and microcracks decreasing the effective crack porosity, and increasing the seismic wave velocities. Alternatively, irreversible phase changes may have occurred during the first heating cycle, causing an increase in the velocities.

The effect of cristobolite content on the mean coefficient of thermal expansion is shown in Figure 16. The mean coefficient of thermal expansion at a pressure of 10 MPa is plotted as a function of the percentage of cristobolite with respect to the total SiO_2 content. Data are shown for two temperature intervals: 76 - 100 and 201 - 225 °C. The data exhibit no apparent correlation between the mean coefficient of thermal expansion and the concentration of cristobolite in the welded tuff.

4.0 SUMMARY

Twenty-four thermal expansion measurements were performed on five welded tuff specimens from borehole USW SD-12. All of the specimens were from the potential repository horizon, TSw2.

The measurements were conducted over a nominal temperature range of 25 to 250 °C at confining pressures ranging from 1 to 30 MPa. The data are consistent; all of the strain versus temperature curves are concave upward. There is hysteresis at the initiation of the cooling cycle near a peak temperature of 250 °C. With the exception of the first heating/cooling cycle the strain is recovered at the termination of each cycle. For the first cycle, the hysteresis is pronounced on the cooling cycle; a permanent shortening of the sample is observed at the termination of the first thermal cycle regardless of confining pressure.

The mean coefficients of thermal expansion were calculated at 25 °C intervals for all of the specimens tested. At temperatures below 100 °C the mean coefficient of thermal expansion ranged from 7.7 to 10.8 x 10^{-6} $°C^{-1}$. As temperatures approached 250 °C the thermal expansion increased markedly to values of 14.2 to 20.6 x 10^{-6} $°C^{-1}$. The effect of confining pressure on thermal expansion is small. For temperatures above 175 °C the mean coefficients of thermal expansion decreases by 10 - 12 % as the pressure increases from 1 to 30 MPa.

Variation in the concentrations of quartz, tridymite, and cristobolite in the test specimens have no obvious effect on the strain versus temperature data. The coefficients of thermal expansion are nearly identical for each of the specimens at the same temperature and pressure conditions regardless of the relative concentration of SiO_2 polymorphs.

5.0 REFERENCES

American Society for Testing and Materials, "Standard Test Method for Measurement of Thermal Expansion of Rock Using a Dilatometer", Number: ASTM D 4535, American Society for Testing and Materials, Philadelphia, PA, 1985.

Boyd, P. J., R .J. Martin, III, and R. H. Price, "An Experimental Comparison of Laboratory Techniques in Determining Bulk Properties of Tuffaceous Rocks", SAND92-0119, Sandia National Laboratories, Albuquerque, NM, 1994.

Buesch, D. C., R. W. Spengler, T. C. Moyer, and J. K. Geslin, "Proposed Stratigraphic Nomenclature and Macroscopic Identification of Lithostratigraphic Units of the Paintbrush Group Exposed at Yucca Mountain, Nevada", USGS-OFR-94-469, U.S. Geological Survey, Denver, CO, 1996.

Martin, R. J., III, R. H. Price, P. J. Boyd, and J. S. Noel, "Bulk and Mechanical Properties of the Paintbrush Tuff Recovered from Borehole USW NRG-7/7A: Data Report", SAND94-1996, Sandia National Laboratories, Albuquerque, NM, 1995.

Martin, R. J., III, J. S. Noel, P. J. Boyd, and R. H. Price, "Thermal Expansion as a Function of Confining Pressure for Welded Tuff from Yucca Mountain", In: *Rock Mechanics: Tools and Techniques,* Proceedings of the 2nd North American Rock Mechanics Symposium, NARMS '96, M. Aubertin, F. Hassani, and H. Mitri (eds), A.A. Balkema, Brookfield, VT, 1996.

Ortiz, T. S., R. L. Williams, F. B. Nimick, B. C. Whittet, and D. L. South, "A Three-Dimensional Model of Reference Thermal/Mechanical and Hydrological Stratigraphy at Yucca Mountain, Southern Nevada", SAND84-1076, Sandia National Laboratories, Albuquerque, NM, 1985.

Price, R. H., and S. J. Bauer, "Analysis of the Elastic and Strength Properties of Yucca Mountain Tuff, Nevada", In: *Research and Engineering Applications in Rock Masses*, Proc. 26th U.S. Symposium on Rock Mechanics, E. Ashworth (ed.), A A. Balkema, Boston, MA, Vol. 1, 89-96, 1985.

Sandia National Laboratories, "Preparing Cylindrical Samples, Including Inspection of Dimensional and Shape Tolerances", Technical Procedure 51, 1990.

Technical Data Information Form (TDIF) No. 3305453, Data Tracking Number (DTN) SNL04011895001.001. Preliminary SD-12 XRD Silica Phase Data, May 16, 1996.

APPENDIX I

Information from the Reference Information Base Used in this Report

This report contains no information from the Reference Information Base.

Candidate Information for the Reference Information Base

This report contains no information for the Reference Information Base.

Candidate Information for the Geographic Nodal Information Study and Evaluation System

This report contains no candidate information for the Geographic Nodal Information Study and Evaluation System (GENISES).

APPENDIX II

The thermal expansion data collected as a function of confining pressures on five TSw2 tuff specimens are presented. For each test specimen two thermal cycles were run at four (SD12-687.8) or five confining pressures (SD12-742.9 and SD12-776.4). At each confining pressure the following data are presented: (1) strain versus temperature, and (2) temperature versus time at four positions within the pressure vessel. Three temperatures are measured in proximity to the test specimen and one at the mid point of the LVDTs. The data are presented in the order that they were performed. For two specimens the highest confining pressure test was carried out first. On the remaining specimens, the sequence of tests was from the lowest to the highest confining pressure.

The data for each specimen is preceded by a brief summary giving the following pre-test and post-test data: sample dimensions, mass, and seismic wave velocities.

Yucca Mountain Project
Thermal Expansion
Borehole: SD 12
Depth: 687.8 feet

The specimen was thermally cycled to 247 °C at confining pressures of 30, 20, 10, and 5 MPa. Two thermal cycles were performed at each pressure. The heating rate was 0.328 ± 0.010 °C/min.

	Before Testing	After Testing
Length, mm	101.625	101.625
Diameter, mm	50.749	50.749
Mass, g	473.27	470.27
Porosity, %		8.7
Seismic Velocities Parallel to the Specimen Axis		
P-Wave, km/s	4.492	4.616
S(1)-Wave, km/s	2.823	2.911
S(2)-Wave, km/s	2.829	2.914
Seismic Velocities Normal to the Specimen Axis		
P-Wave, km/s	4.455	4.575
S-Wave, km/s	2.843	2.905

NER

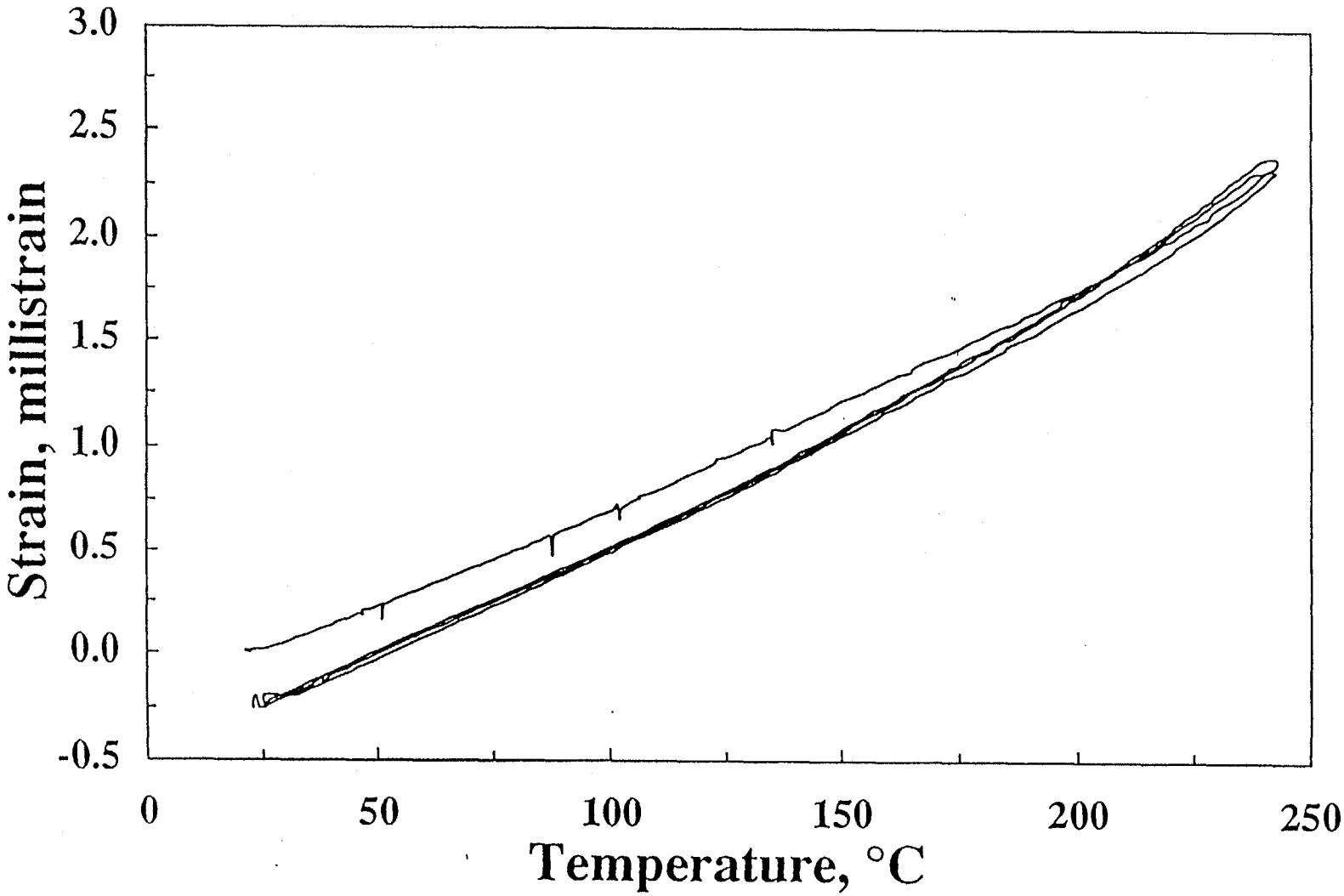

Figure A2-1: Axial strain on the test specimen of TSw2 tuff is plotted as a function of temperature. Two test cycles were performed over a nominal range of 25 to 250 °C. These data were collected at a confining pressure 30 MPa.

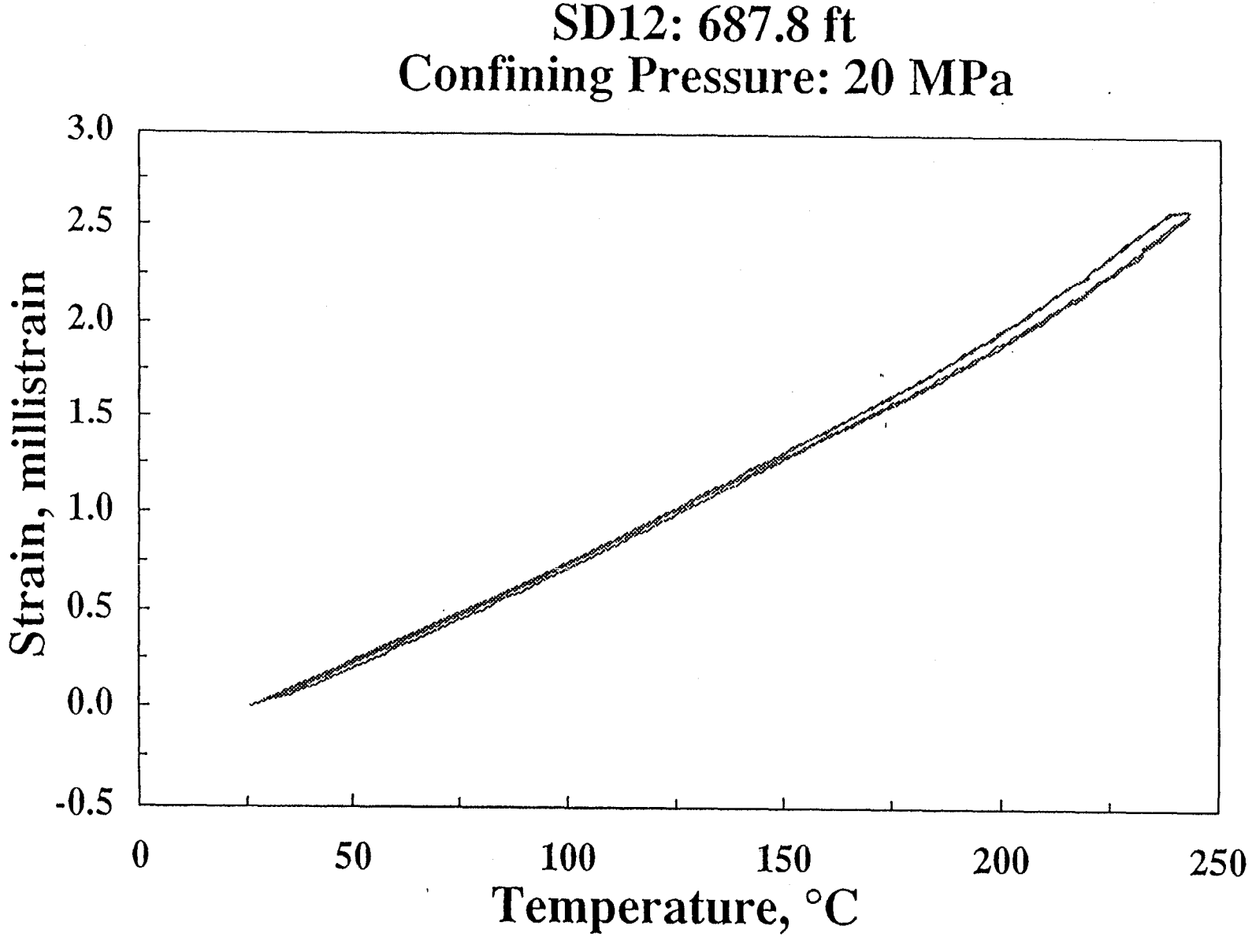

Figure A2-2: Axial strain on the test specimen of TSw2 tuff is plotted as a function of

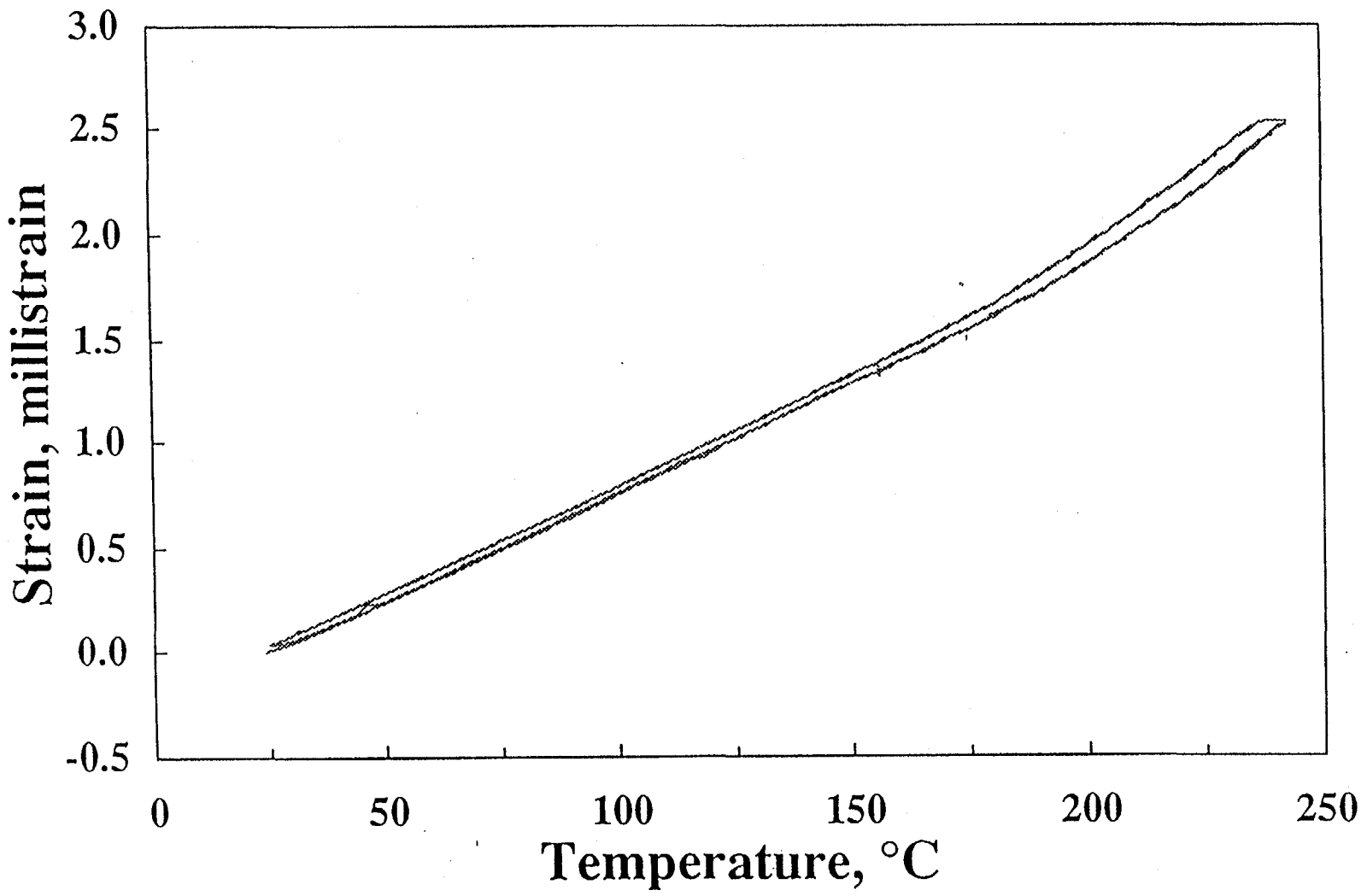

Figure A2-3: Axial strain on the test specimen of TSw2 tuff is plotted as a function of temperature. Two test cycles were performed over a nominal range of 25 to 250 °C. These data were collected at a confining pressure 10 MPa.

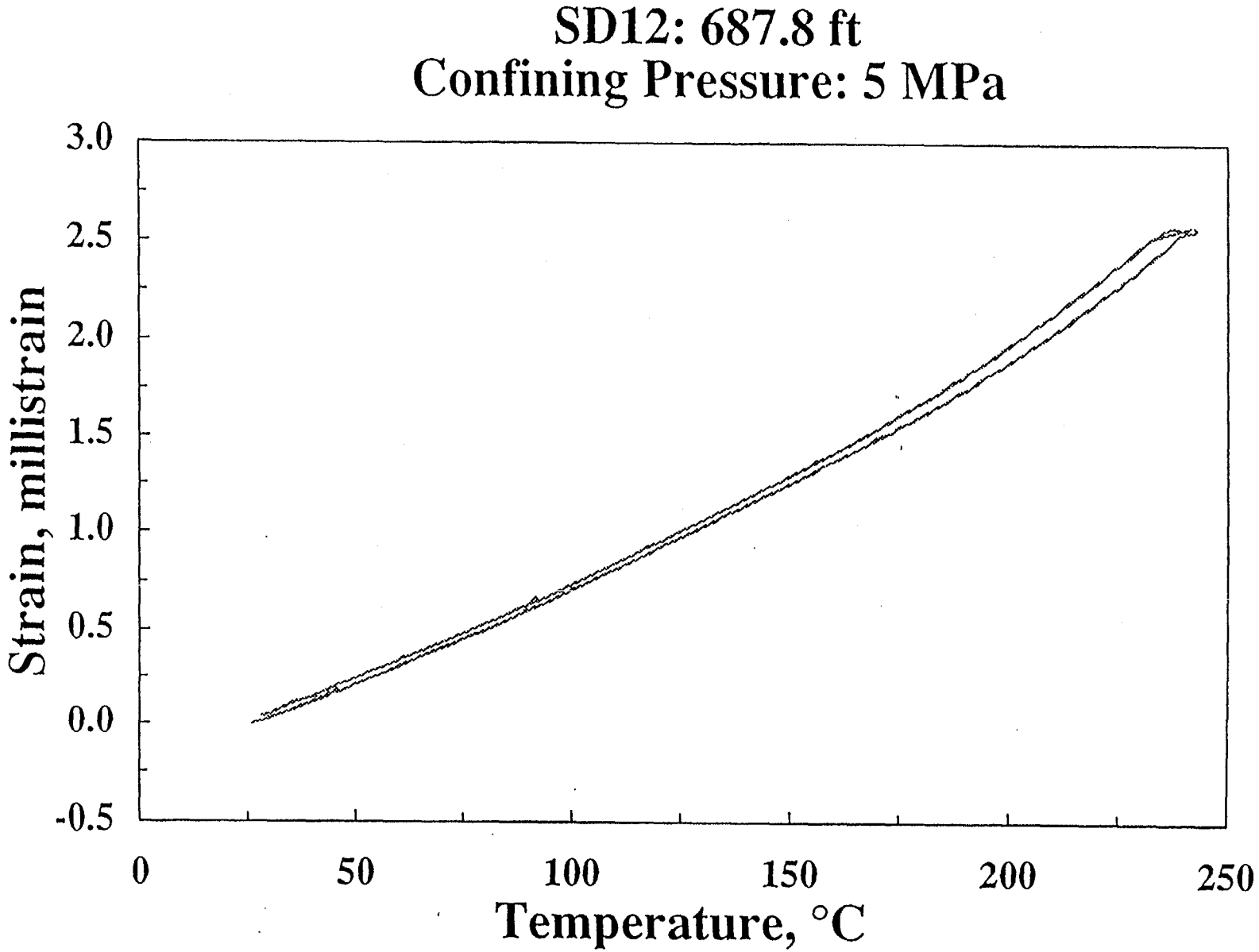

Figure A2-4: Axial strain on the test specimen of TSw2 tuff is plotted as a function of temperature. Two test cycles were performed over a nominal range of 25 to 250 °C. T

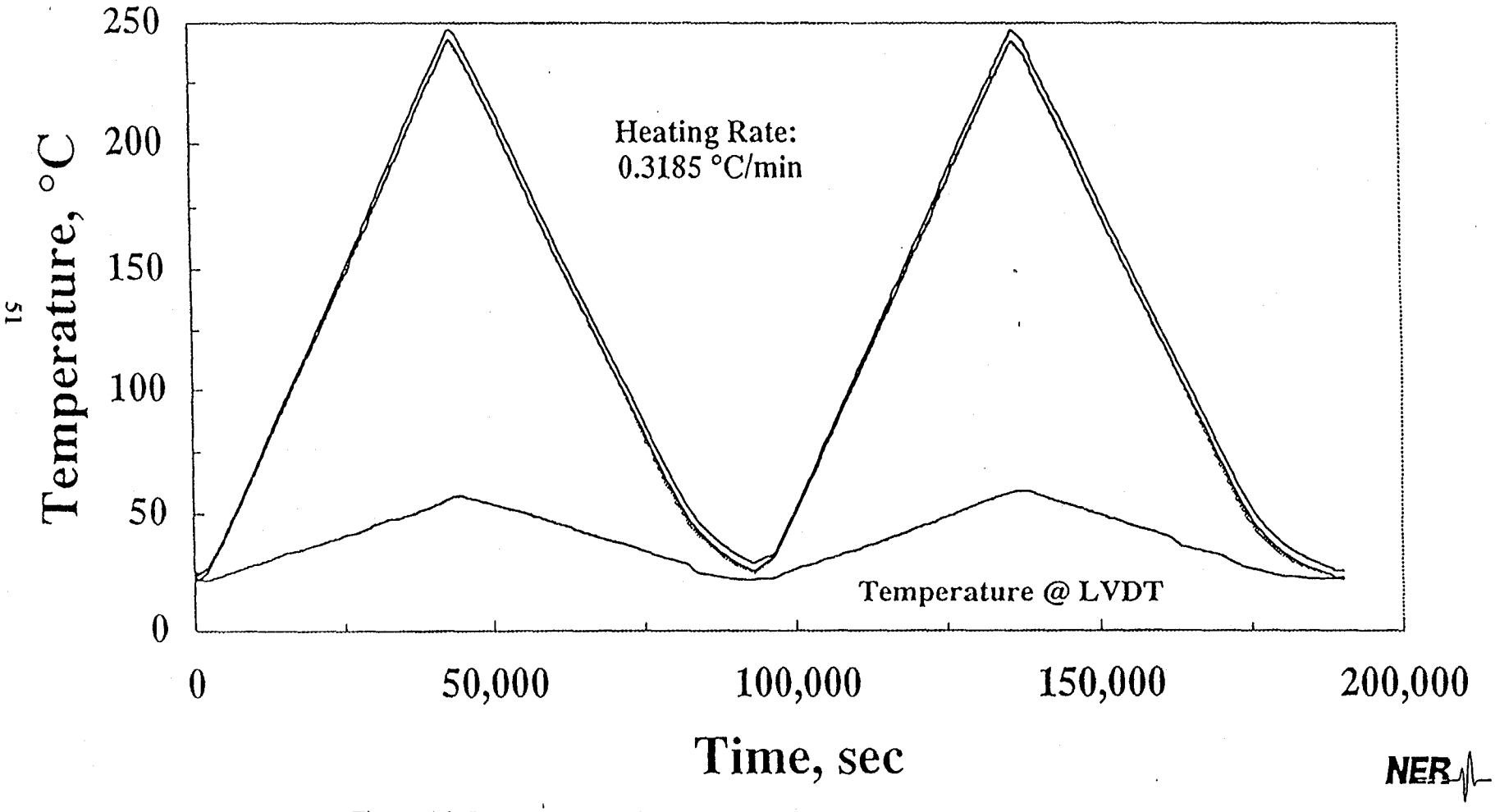

Figure A2-5: Temperature is plotted as a function of time for four locations in the sample assembly. The upper curves represent temperatures at the base, midpoint, and top of the test specimen. The lower curve indicates the temperature at the LVDTs. The experiment was performed at a confining pressure of 30 MPa.

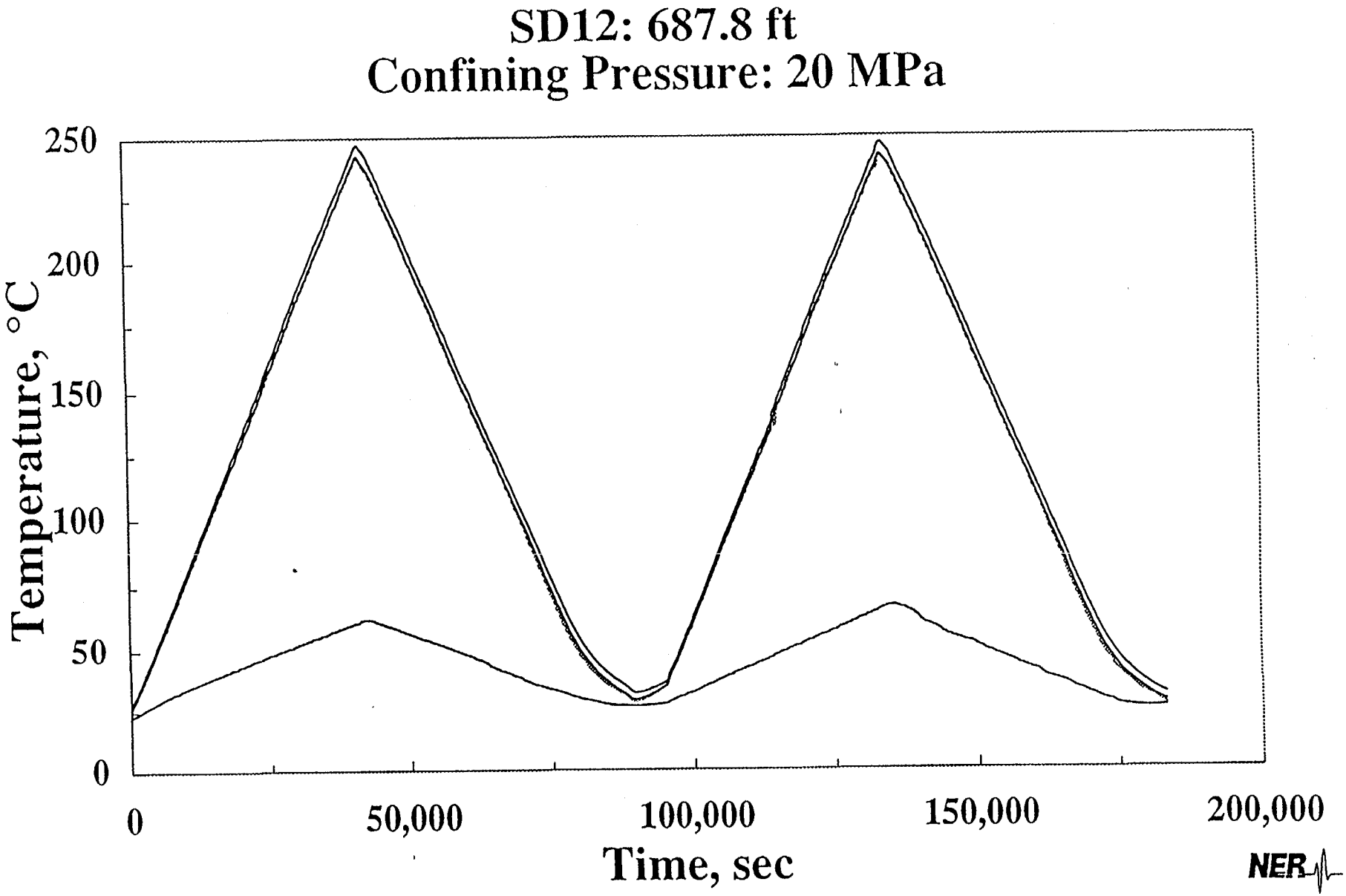

Figure A2-6: Temperature is plotted as a function of time for four locations in the sample assembly. The upper curves represent temperatures at the base, midpoint, and top of the

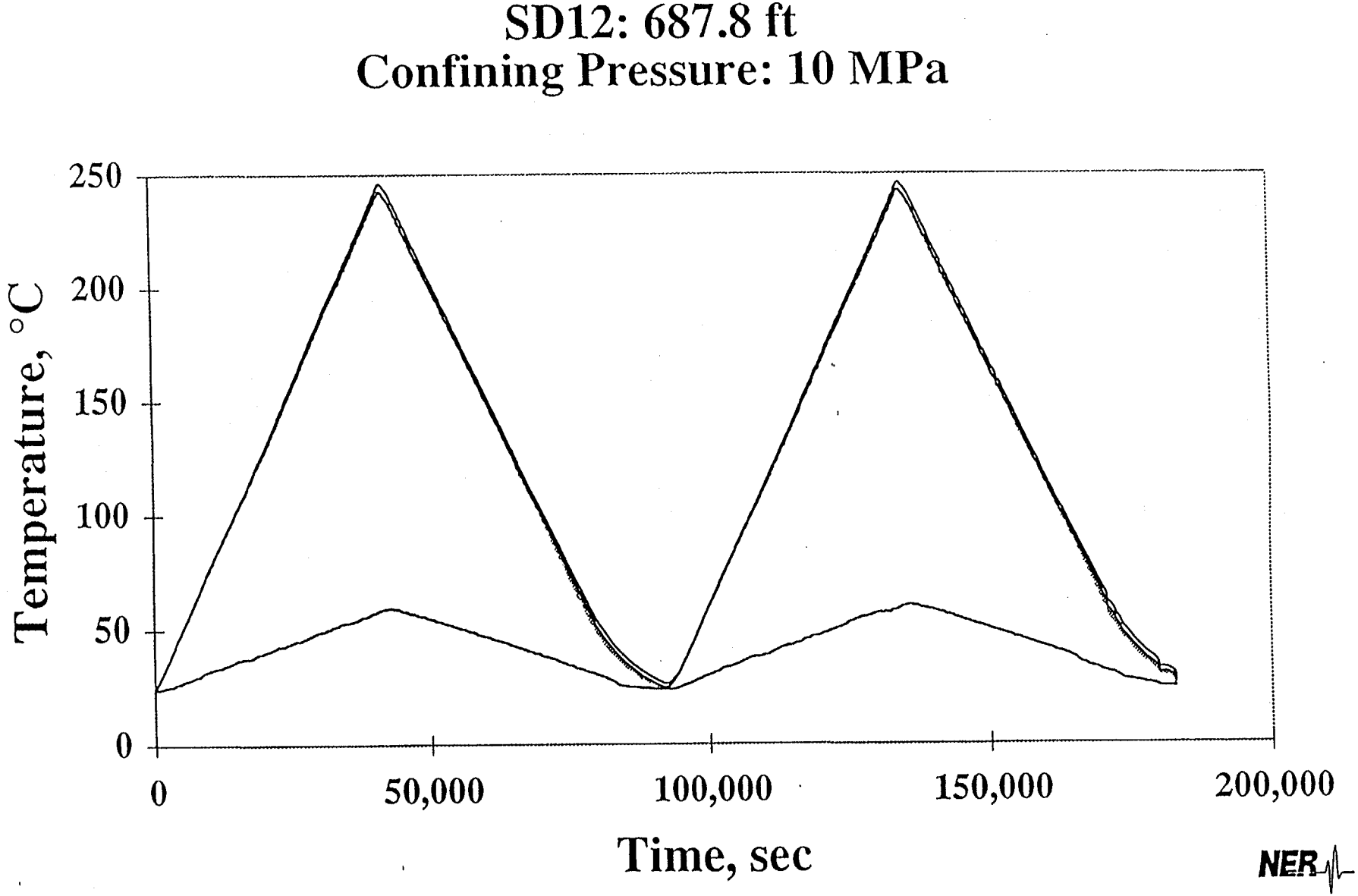

Figure A2-7: Temperature is plotted as a function of time for four locations in the sample assembly. The upper curves represent temperatures at the base, midpoint, and top of the test specimen. The lower curve indicates the temperature at the LVDTs. The experiment was performed at a confining pressure of 10 MPa.

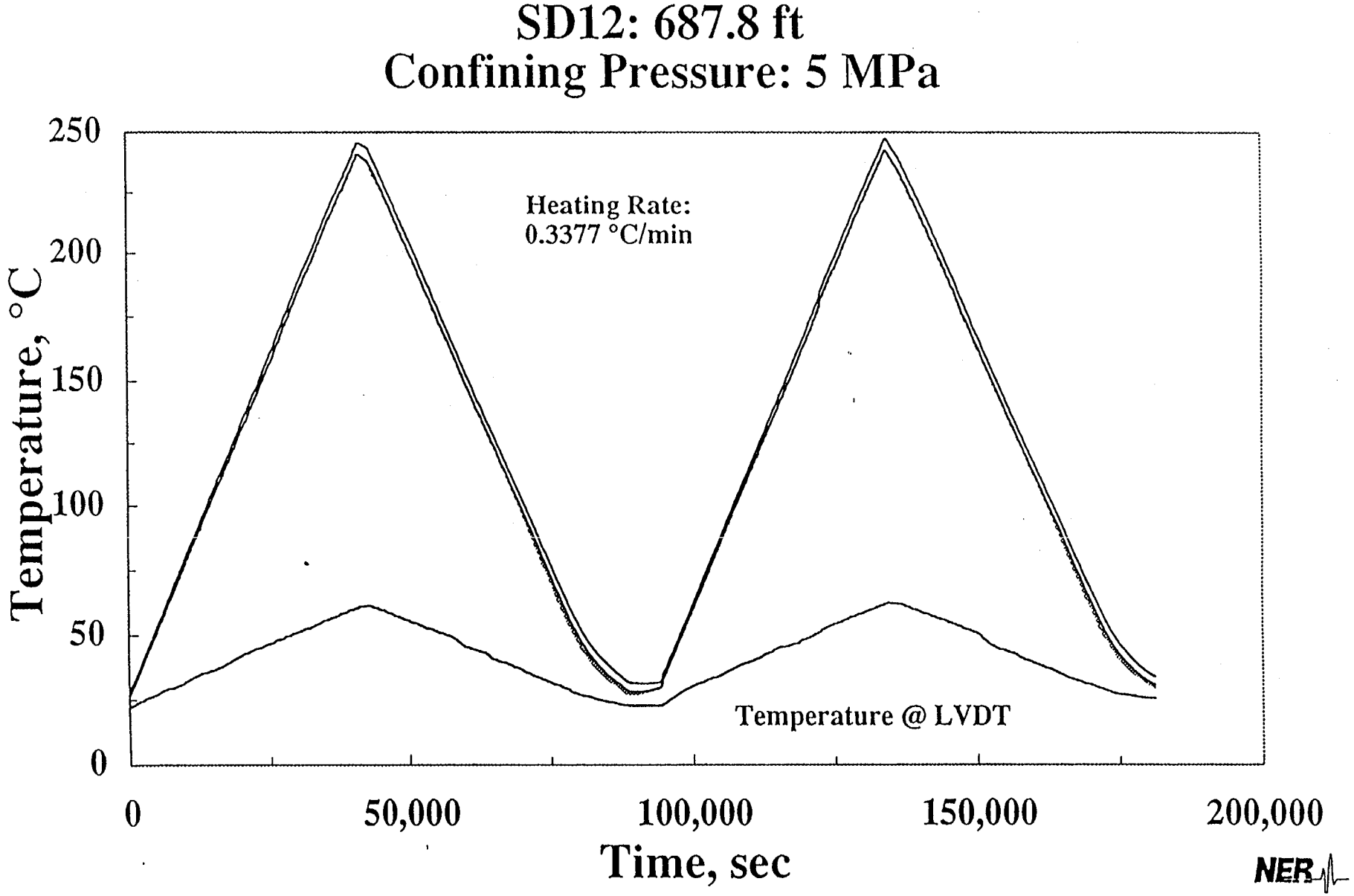

Figure A2-8: Temperature is plotted as a function of time for four locations in the sample assembly. The upper curves represent temperatures at the base, midpoint, and top of the

Yucca Mountain Project
Thermal Expansion
Borehole: SD 12
Depth: 742.9 feet

he specimen was thermally cycled to 247 °C at confining pressures of 30, 20, 10, 5, and 1 MPa. Two thermal cycles were performed at each pressure. The heating rate was 0.317 ± 0.010 °C/min.

	Before Testing	After Testing
ength, mm	101.60	101.58
iameter, mm	50.80	50.75
lass, g	462.27	459.08
orosity, %		10.6
eismic Velocities Parallel to the Specimen Axis		
-Wave, km/s	4.343	4.466
(1)-Wave, km/s	2.742	2.809
(2)-Wave, km/s	2.745	2.805
eismic Velocities Normal to the Specimen Axis		
-Wave, km/s	4.303	N/A
-Wave, km/s	2.746	N/A

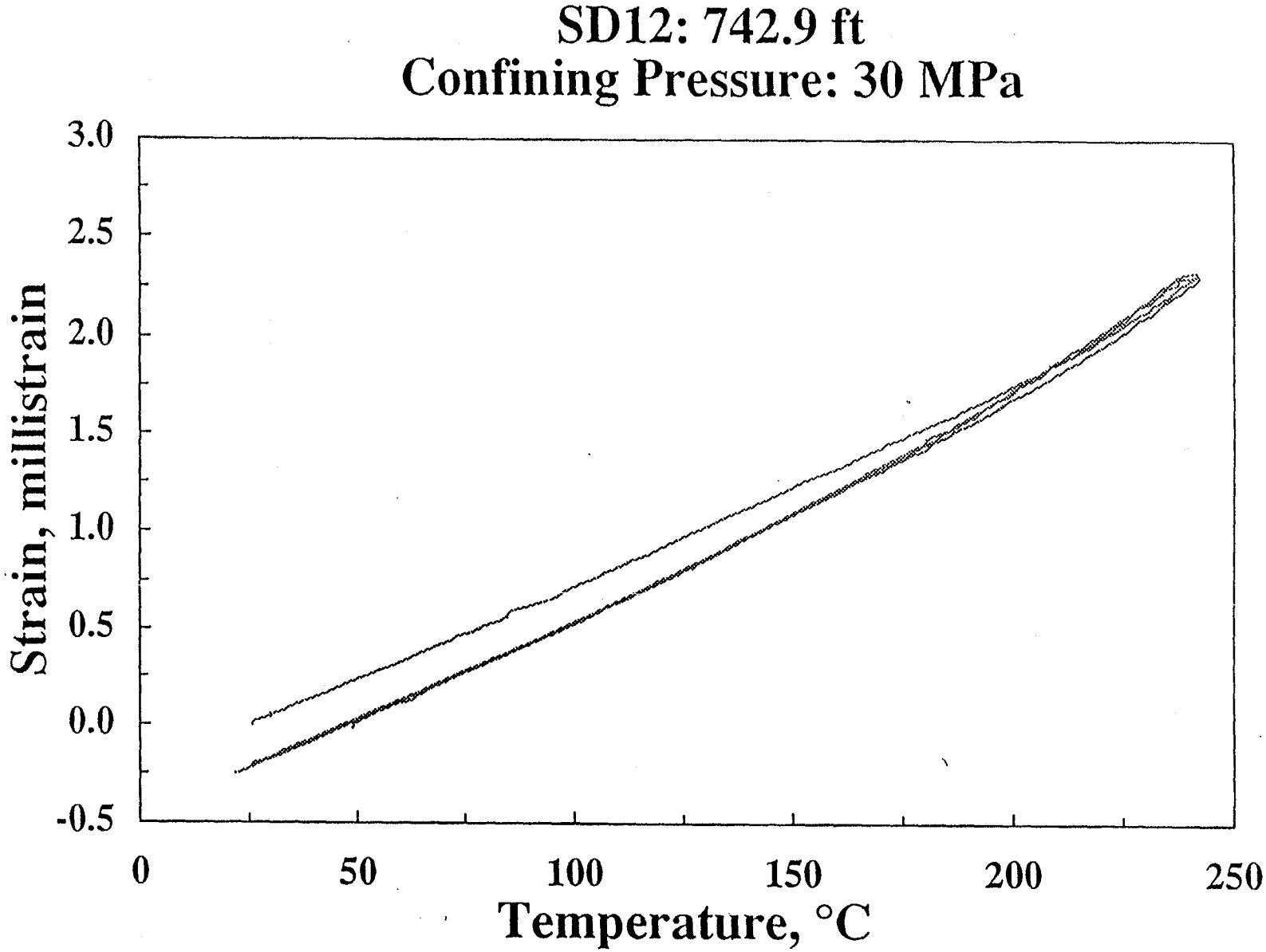

Figure A2-9: Axial strain on the test specimen of TSw2 tuff is plotted as a function of temperature. Two test cycles were performed over a nominal range of 25 to 250 °C. These

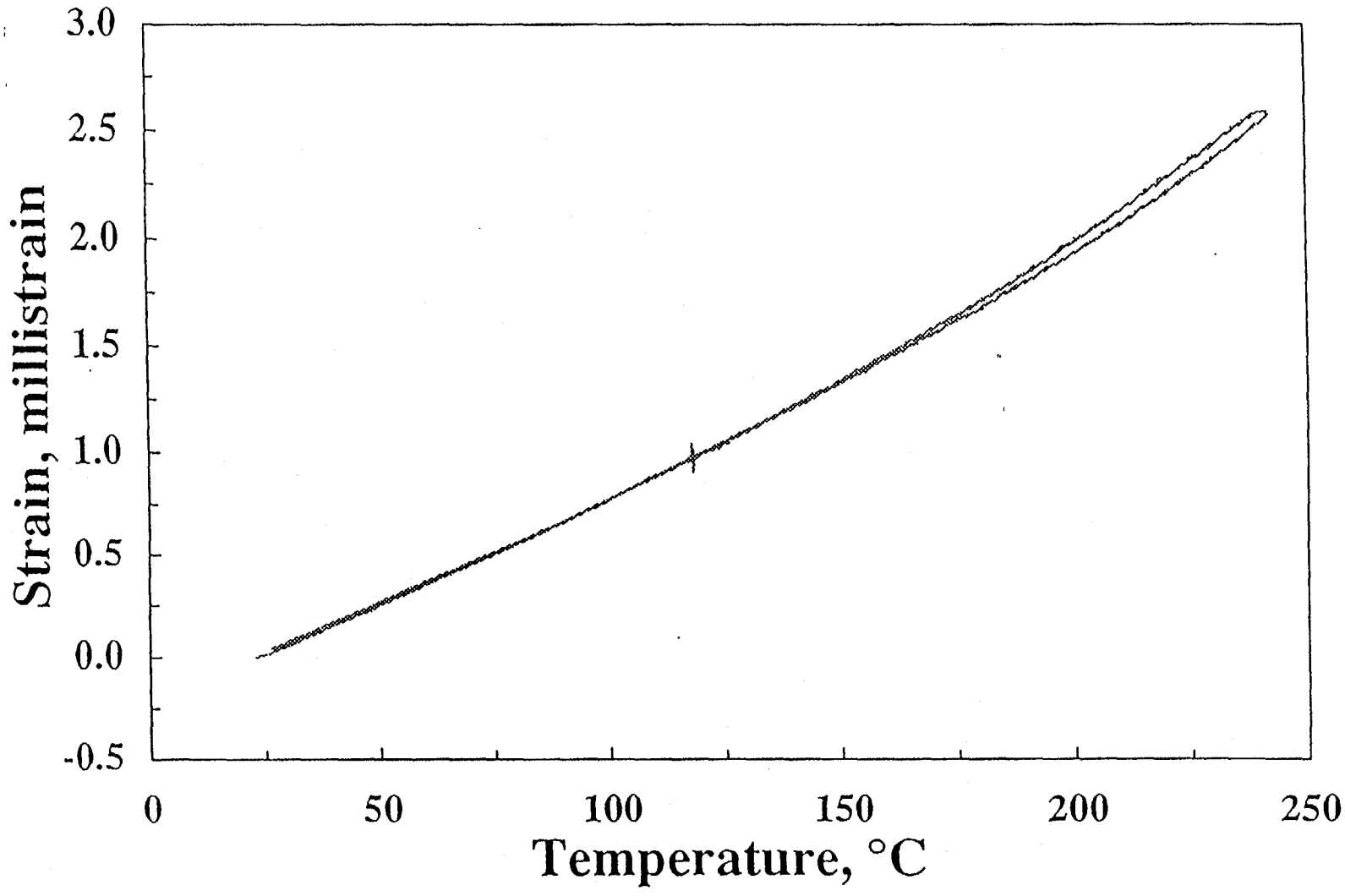

Figure A2-10: Axial strain on the test specimen of TSw2 tuff is plotted as a function of temperature. Two test cycles were performed over a nominal range of 25 to 250 °C. These data were collected at a confining pressure 20 MPa.

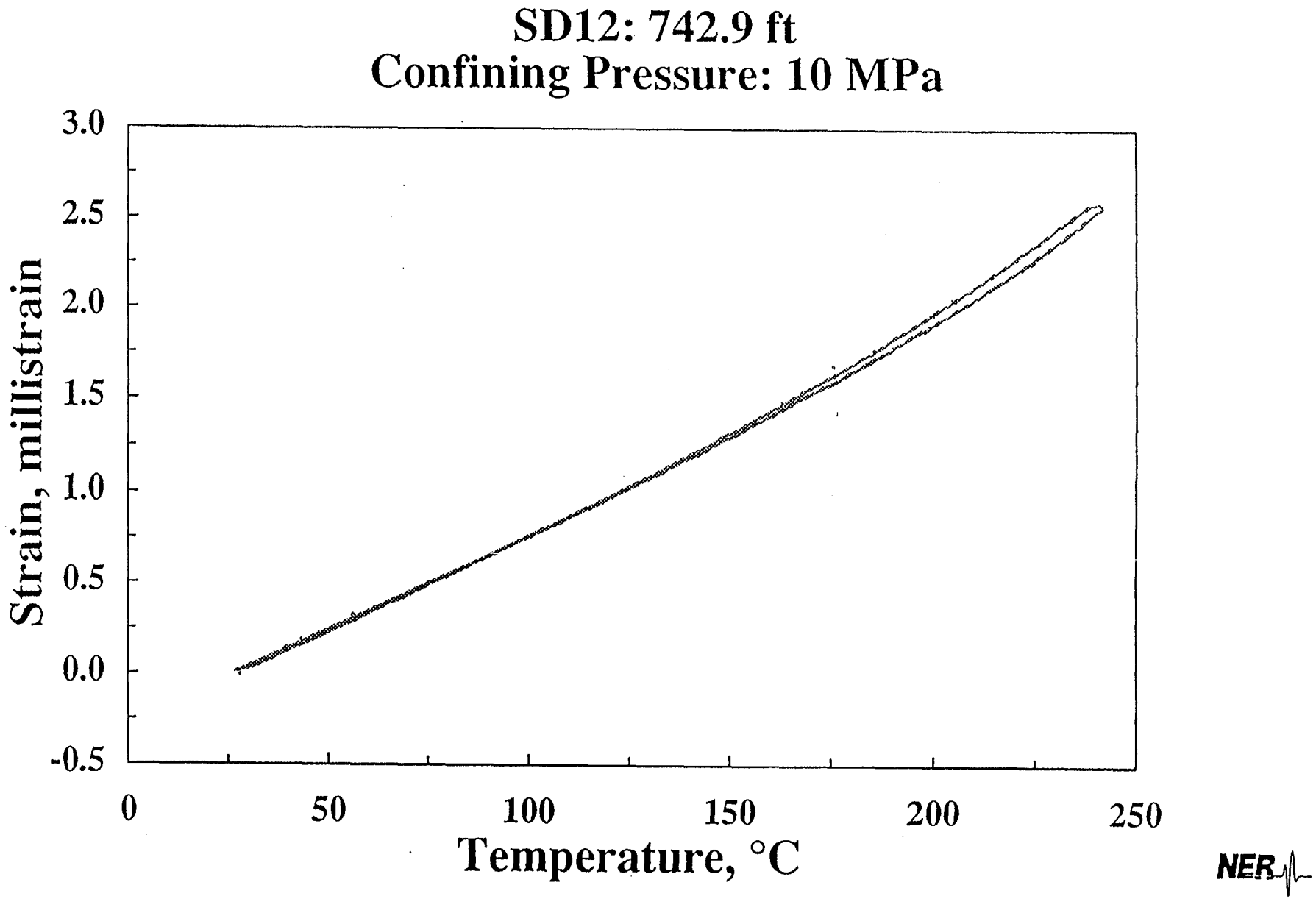

Figure A2-11: Axial strain on the test specimen of TSw2 tuff is plotted as a function of temperature. Two test cycles were performed over a nominal range of 25 to 250 °C. These

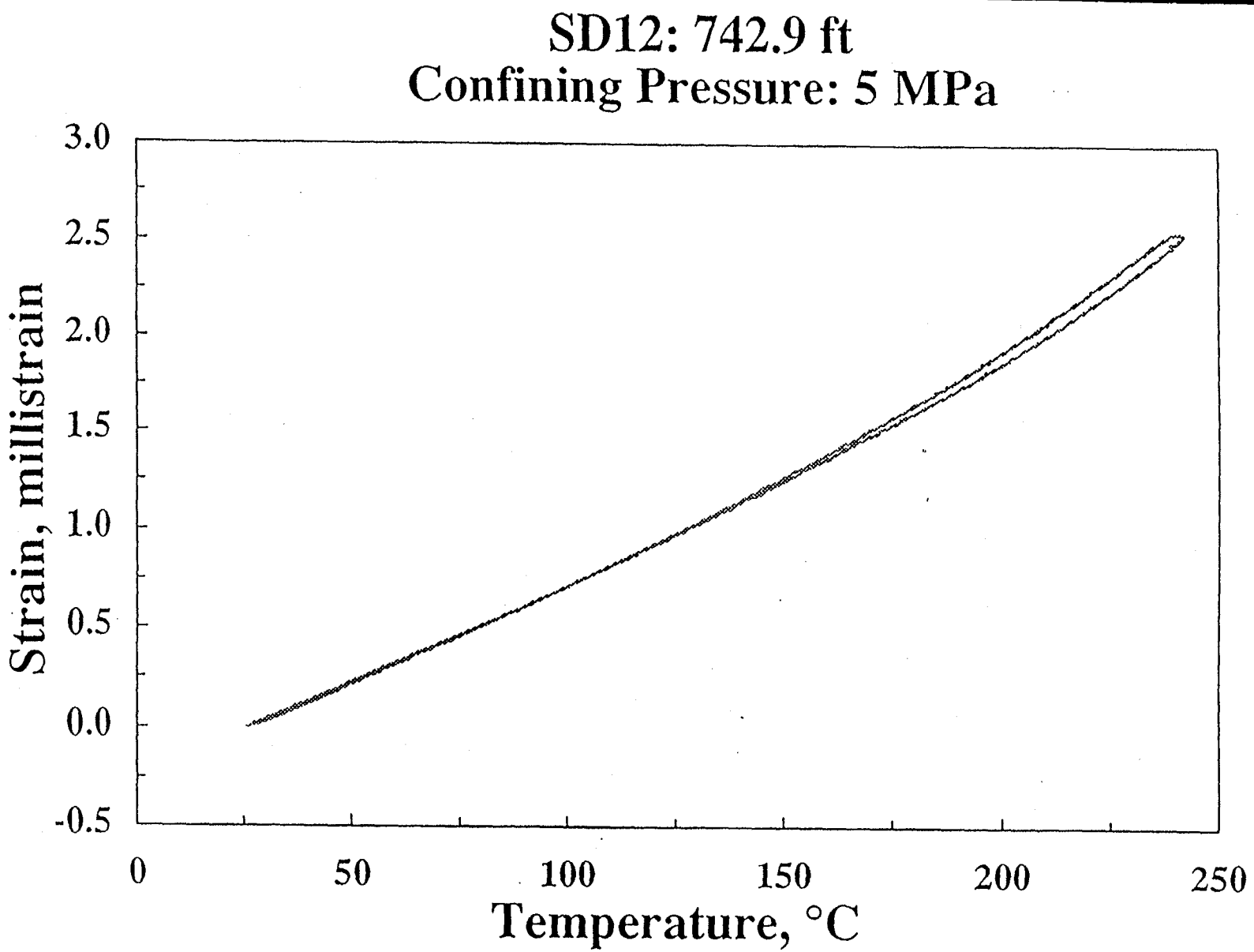

Figure A2-12: Axial strain on the test specimen of TSw2 tuff is plotted as a function of temperature. Two test cycles were performed over a nominal range of 25 to 250 °C. These data were collected at a confining pressure 5 MPa.

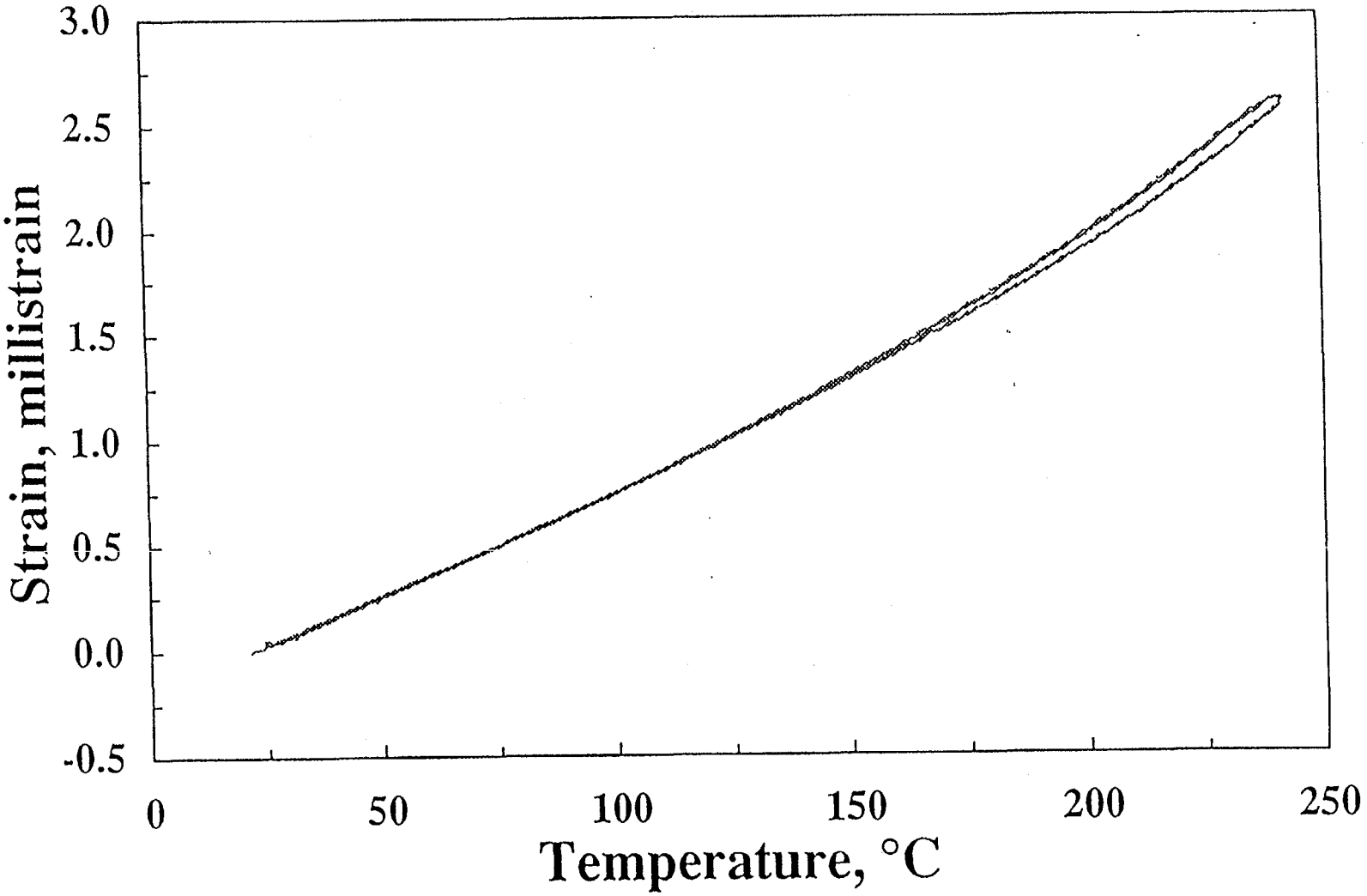

Figure A2-13: Axial strain on the test specimen of TSw2 tuff is plotted as a function of temperature. Two test cycles were performed over a nominal range of 25 to 250 °C. These data were collected at a confining pressure 1.0 MPa.

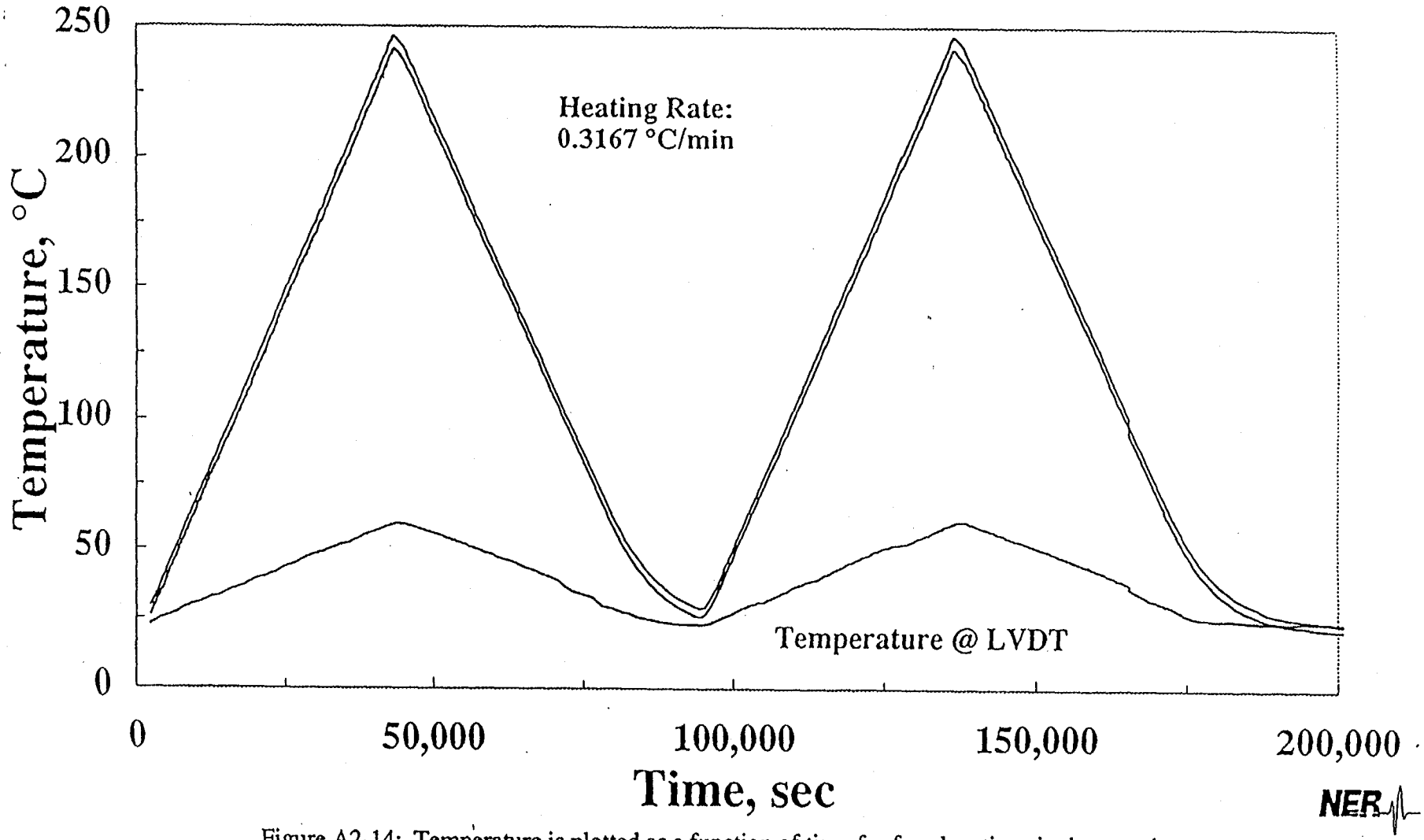

Figure A2-14: Temperature is plotted as a function of time for four locations in the sample assembly. The upper curves represent temperatures at the base, midpoint, and top of the test specimen. The lower curve indicates the temperature at the LVDTs. The experiment was performed at a confining pressure of 30 MPa.

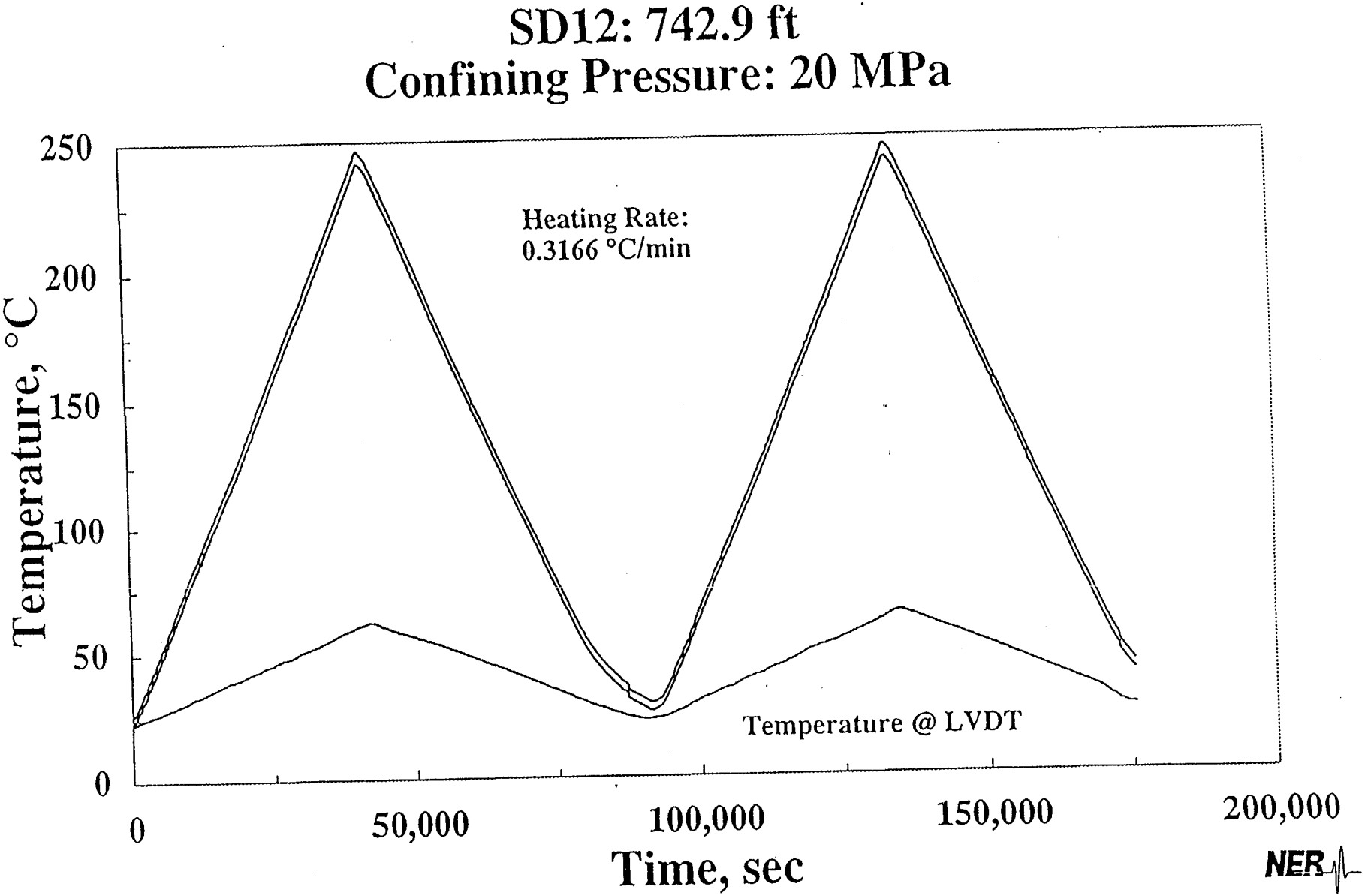

Figure A2-15: Temperature is plotted as a function of time for four locations in the sample assembly. The upper curves represent temperatures at the base, midpoint, and top of the test specimen. The lower curve indicates the temperature at the LVDTs. The experiment

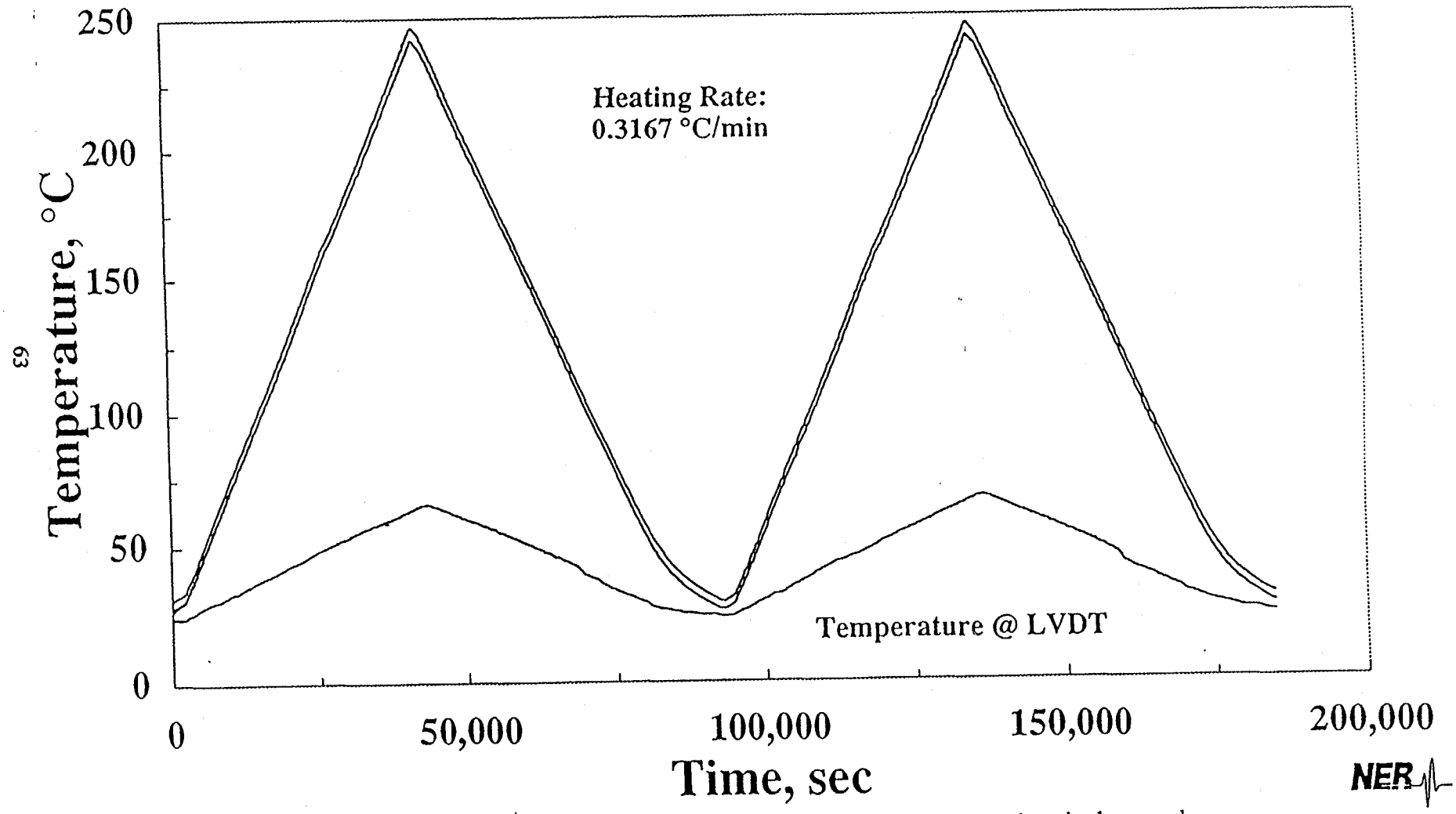

Figure A2-16: Temperature is plotted as a function of time for four locations in the sample assembly. The upper curves represent temperatures at the base, midpoint, and top of the test specimen. The lower curve indicates the temperature at the LVDTs. The experiment was performed at a confining pressure of 10 MPa.

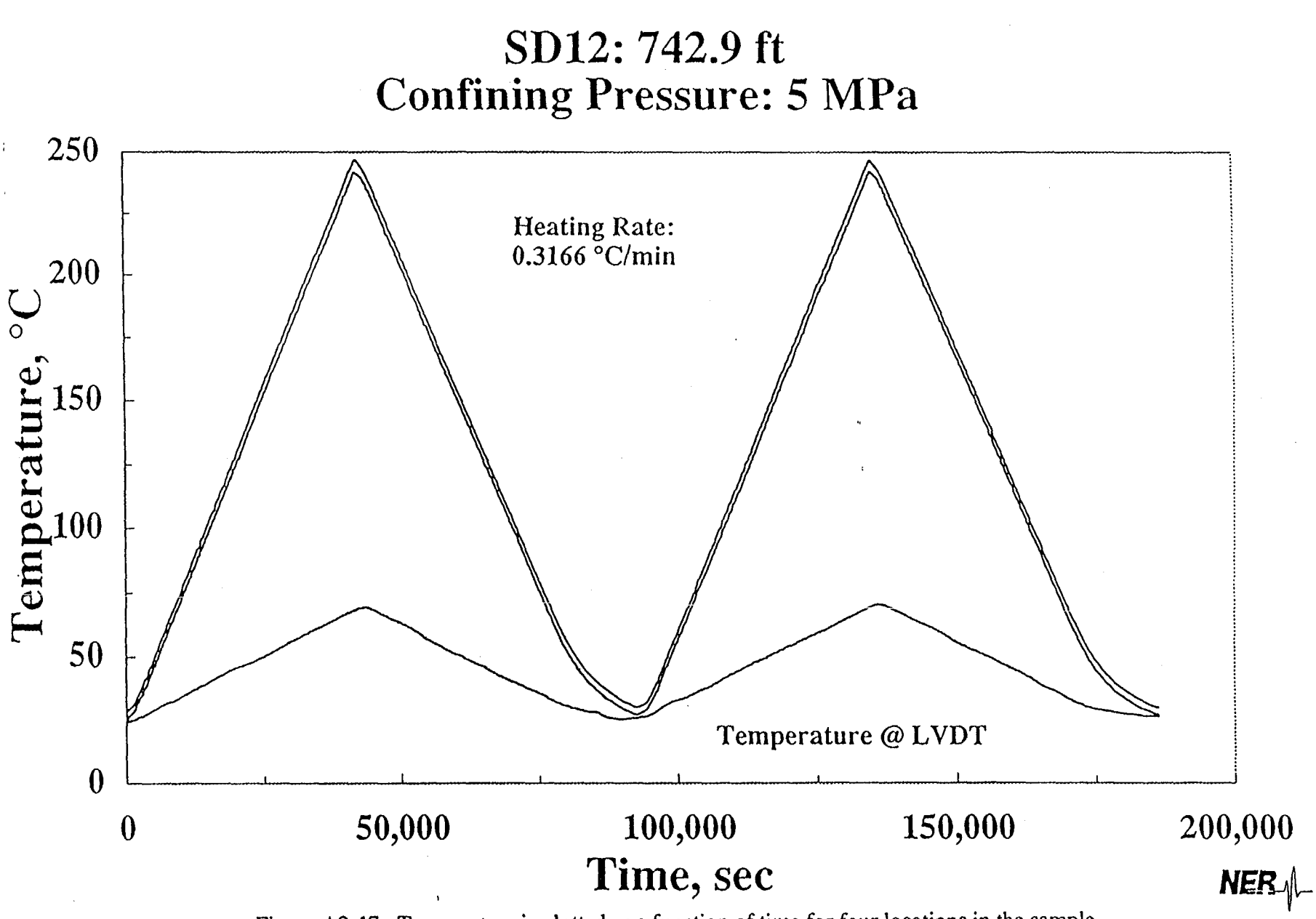

Figure A2-17: Temperature is plotted as a function of time for four locations in the sample assembly. The upper curves represent temperatures at the base, midpoint, and top of the test specimen. The lower curve indicates the temperature at the LVDTs. The experiment

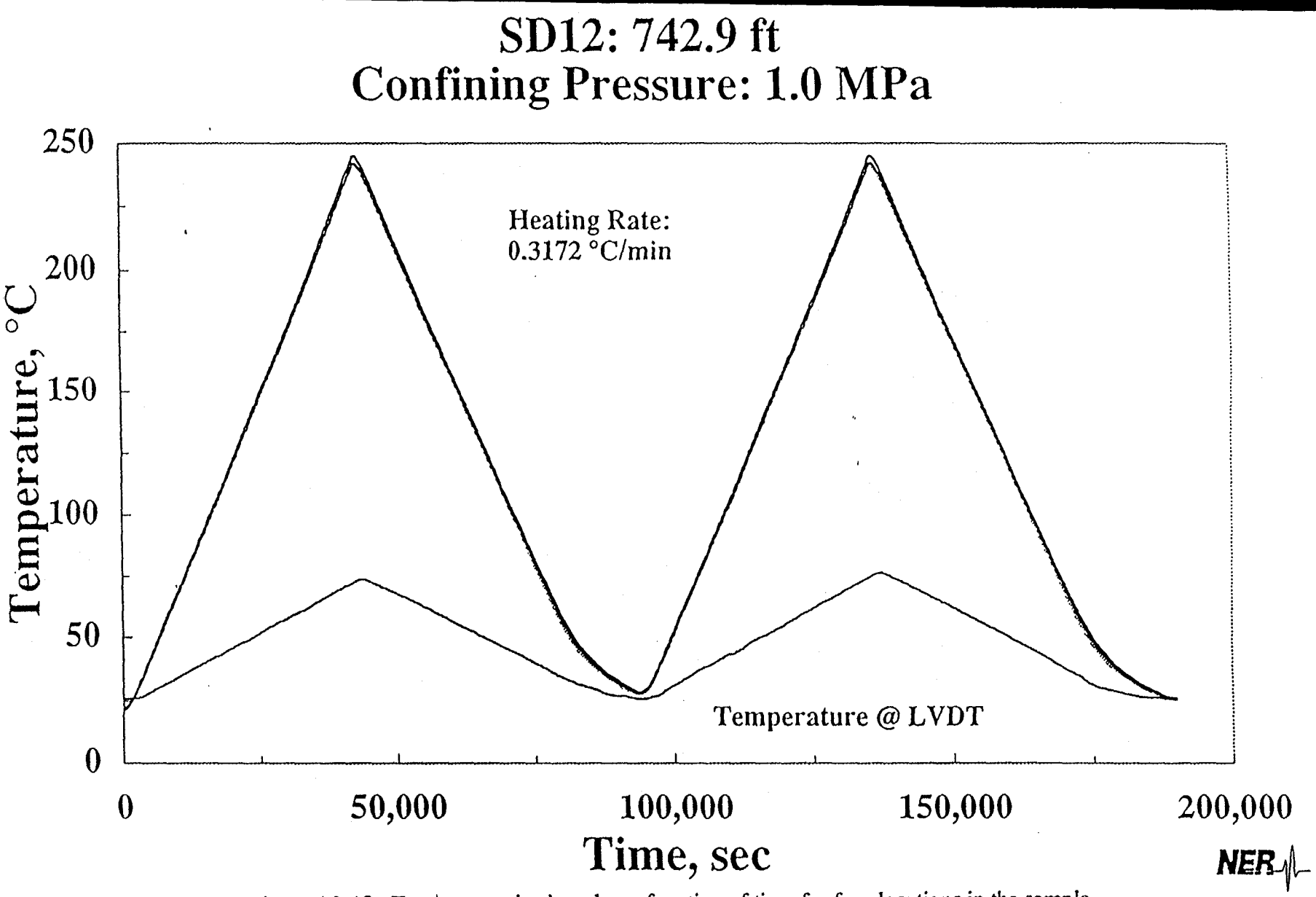

Figure A2-18: Temperature is plotted as a function of time for four locations in the sample assembly. The upper curves represent temperatures at the base, midpoint, and top of the test specimen. The lower curve indicates the temperature at the LVDTs. The experiment was performed at a confining pressure of 1.0 MPa.

Yucca Mountain Project
Thermal Expansion
Borehole: SD 12
Depth: 776.4 feet

The specimen was thermally cycled to 247 °C at confining pressures of 30, 20, 10, 5, and 1 MPa. Two thermal cycles were performed at each pressure. The heating rate was 0.319 ± 0.030 °C/min.

	Before Testing	After Testing
Length, mm	101.60	101.55
Diameter, mm	50.85	50.80
Mass, g	483.47	474.95
Porosity, %		8.0
Seismic Velocities Parallel to the Specimen Axis		
P-Wave, km/s	N/A	4.641
S(1)-Wave, km/s	N/A	2.939
S(2)-Wave, km/s	N/A	2.950
Seismic Velocities Normal to the Specimen Axis		
P-Wave, km/s	N/A	4.619
S-Wave, km/s	N/A	2.949

Compressional and shear wave velocity measurements were not performed before testing.

NER

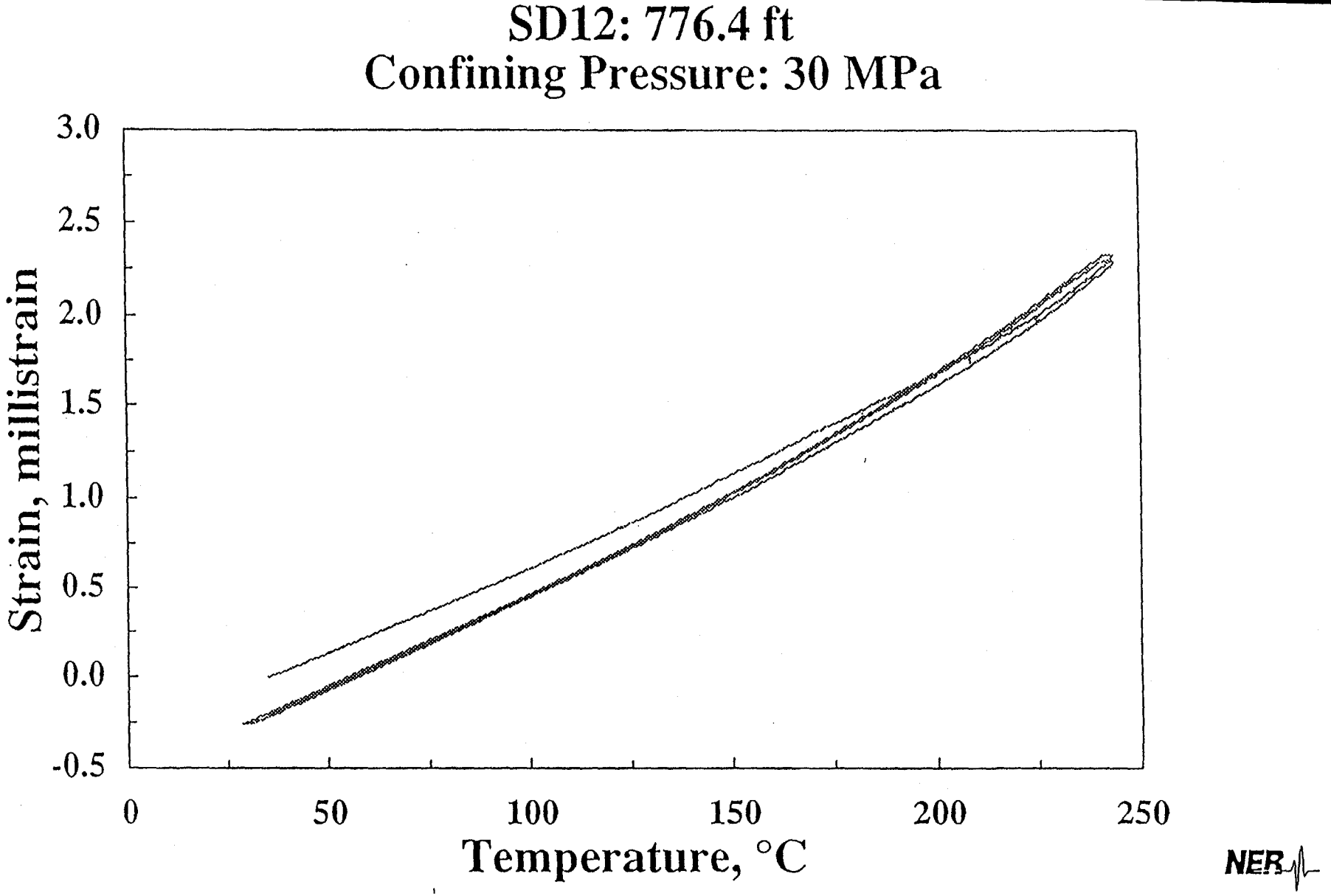

Figure A2-19: Axial strain on the test specimen of TSw2 tuff is plotted as a function of temperature. Two test cycles were performed over a nominal range of 25 to 250 °C. These data were collected at a confining pressure 30 MPa.

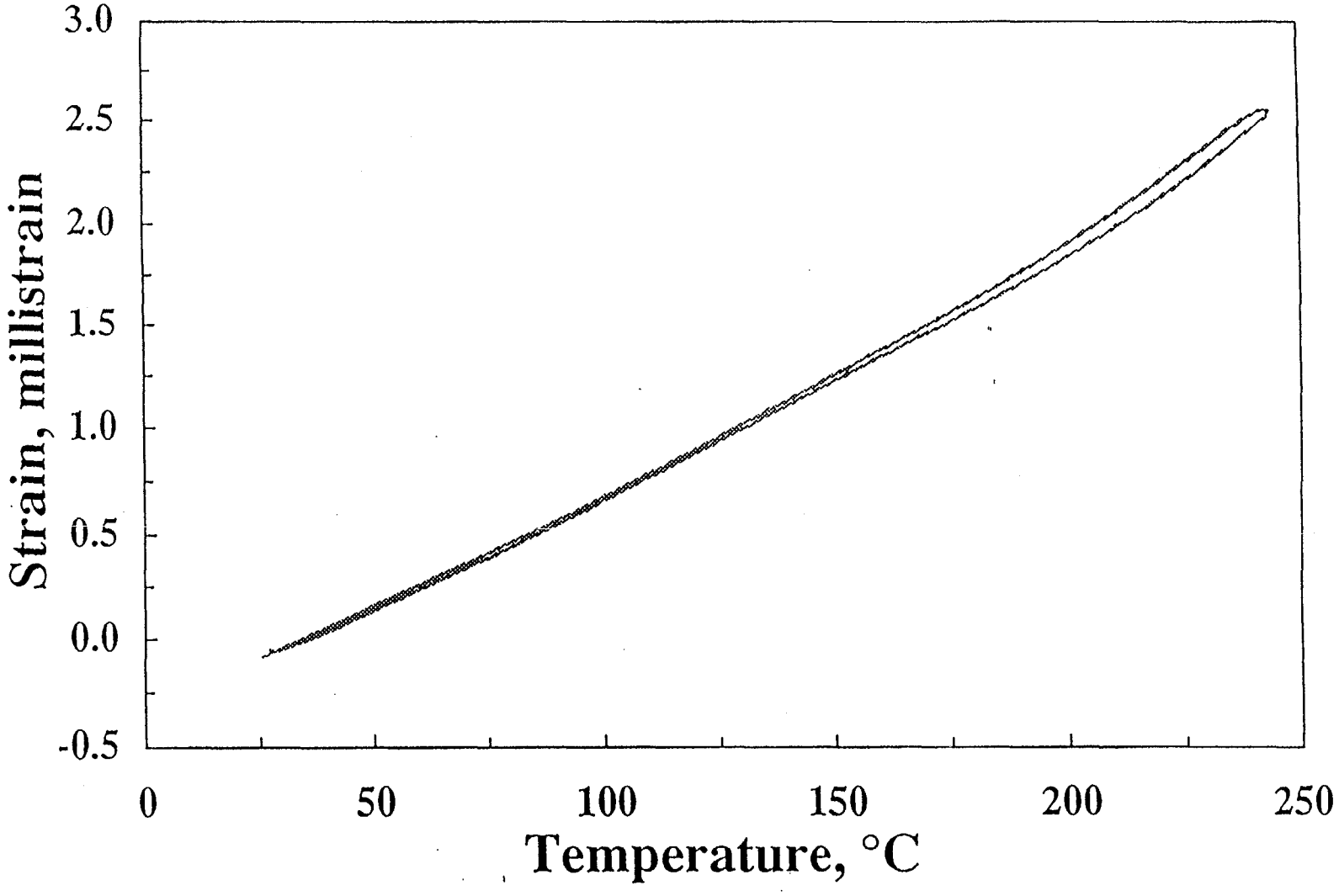

Figure A2-20: Axial strain on the test specimen of TSw2 tuff is plotted as a function of temperature. Two test cycles were performed over a nominal range of 25 to 250 °C. These

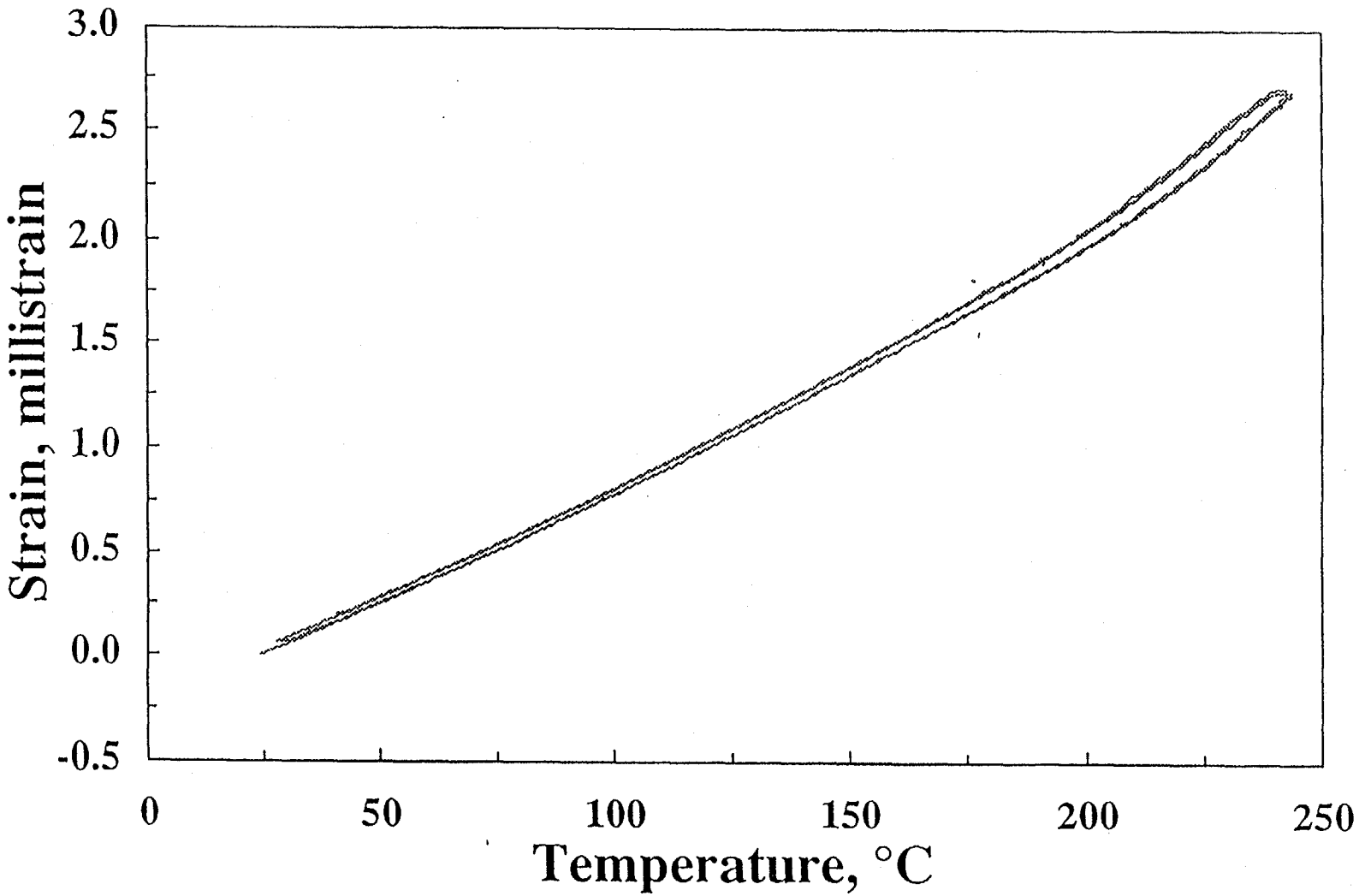

Figure A2-21: Axial strain on the test specimen of TSw2 tuff is plotted as a function of temperature. Two test cycles were performed over a nominal range of 25 to 250 °C. These data were collected at a confining pressure 10 MPa.

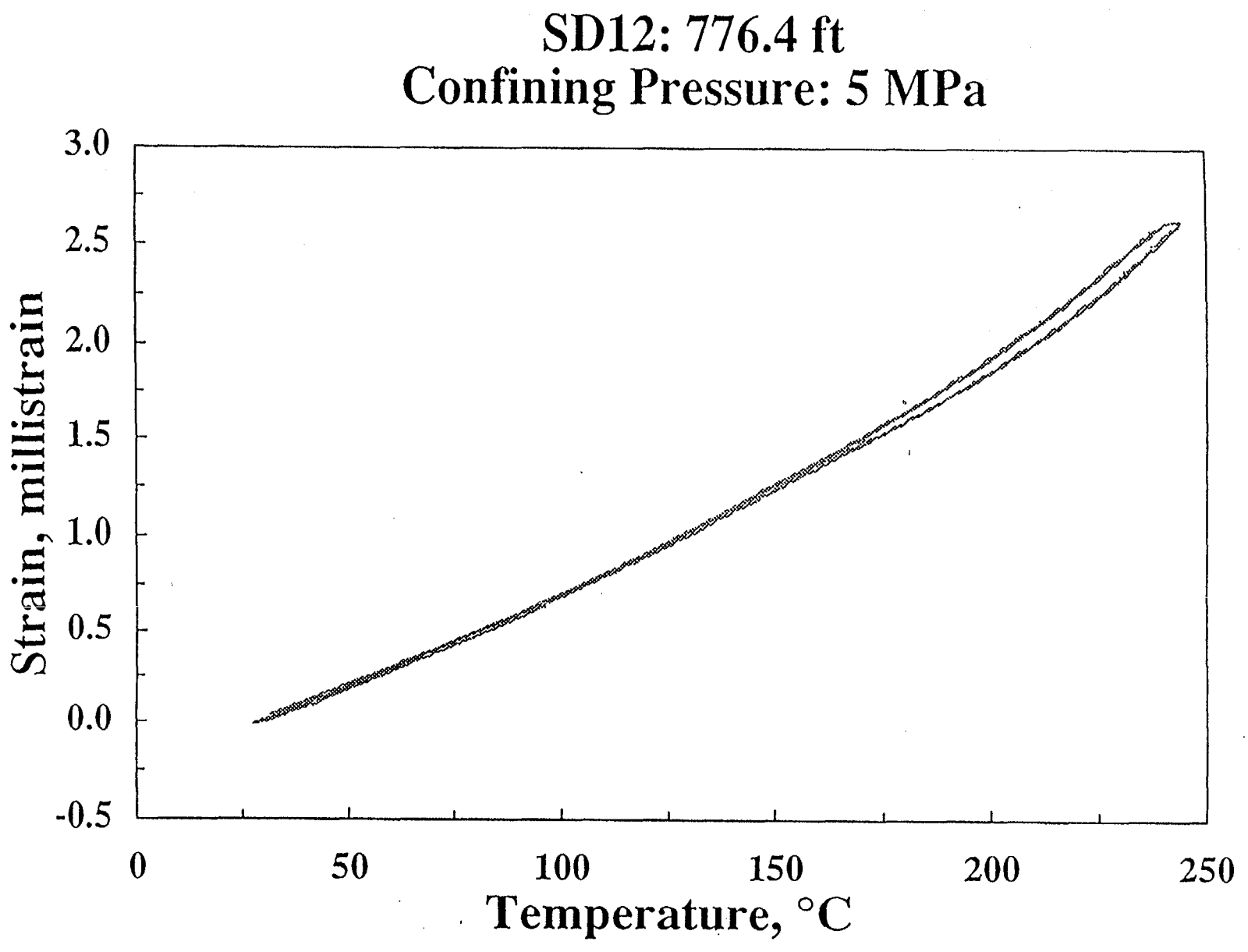

Figure A2-22: Axial strain on the test specimen of TSw2 tuff is plotted as a function of temperature. Two test cycles were performed over a nominal range of 25 to 250 °C. These

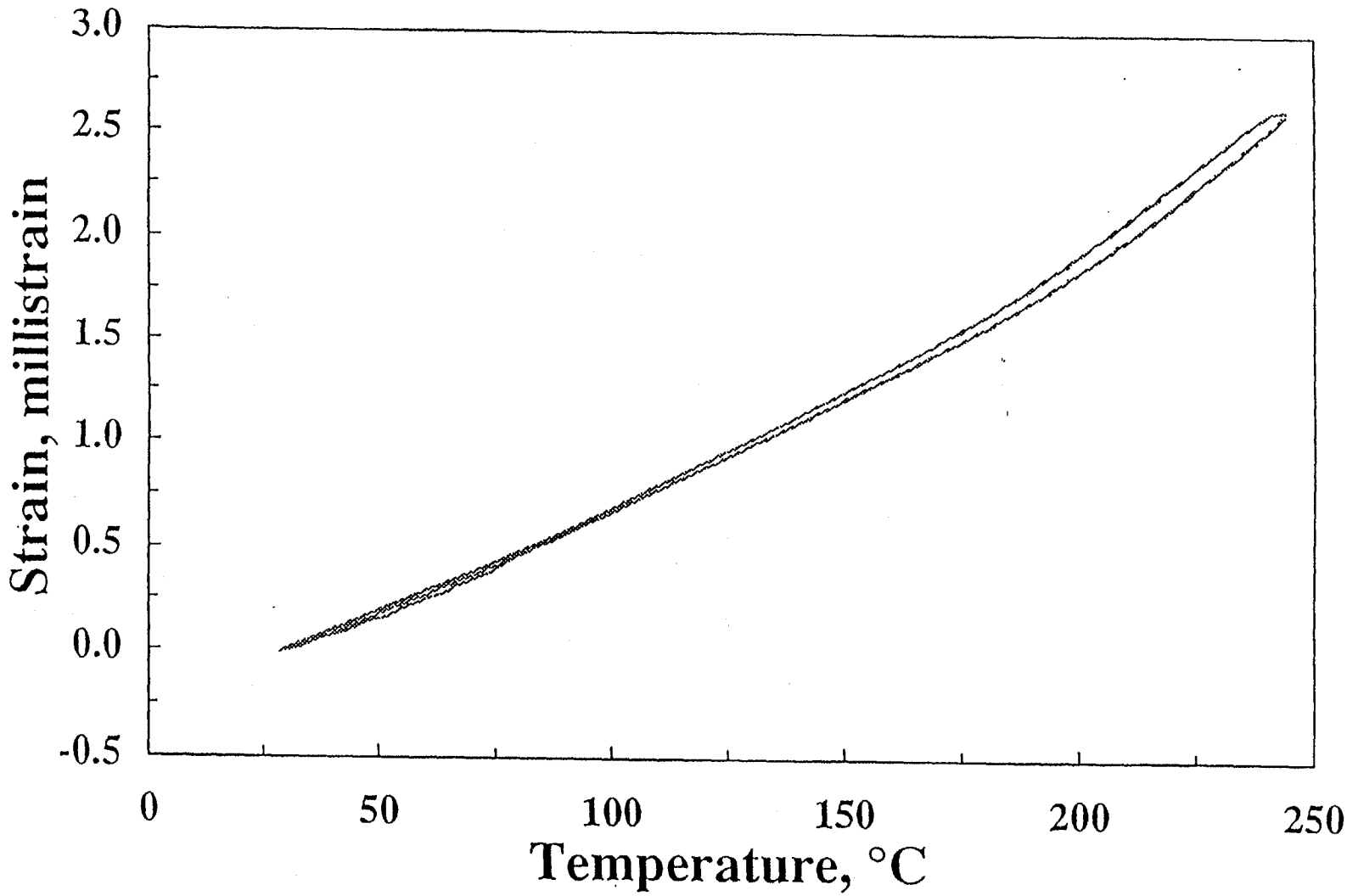

Figure A2-23: Axial strain on the test specimen of TSw2 tuff is plotted as a function of temperature. Two test cycles were performed over a nominal range of 25 to 250 °C. These data were collected at a confining pressure 1.0 MPa.

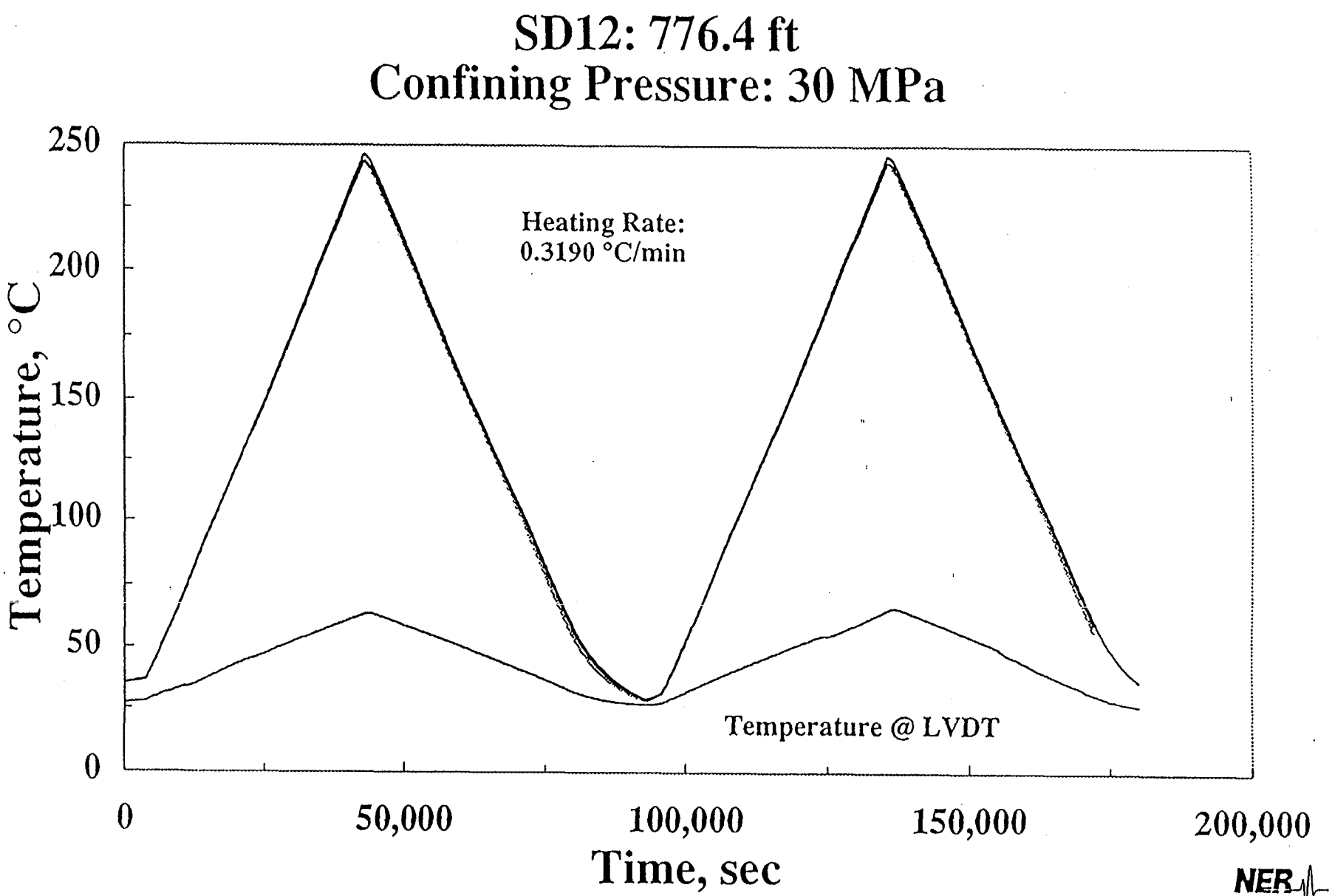

Figure A2-24: Temperature is plotted as a function of time for four locations in the sample assembly. The upper curves represent temperatures at the base, midpoint, and top of the test specimen. The lower curve indicates the temperature at the LVDTs. The experiment was performed at a confining pressure of 30 MPa.

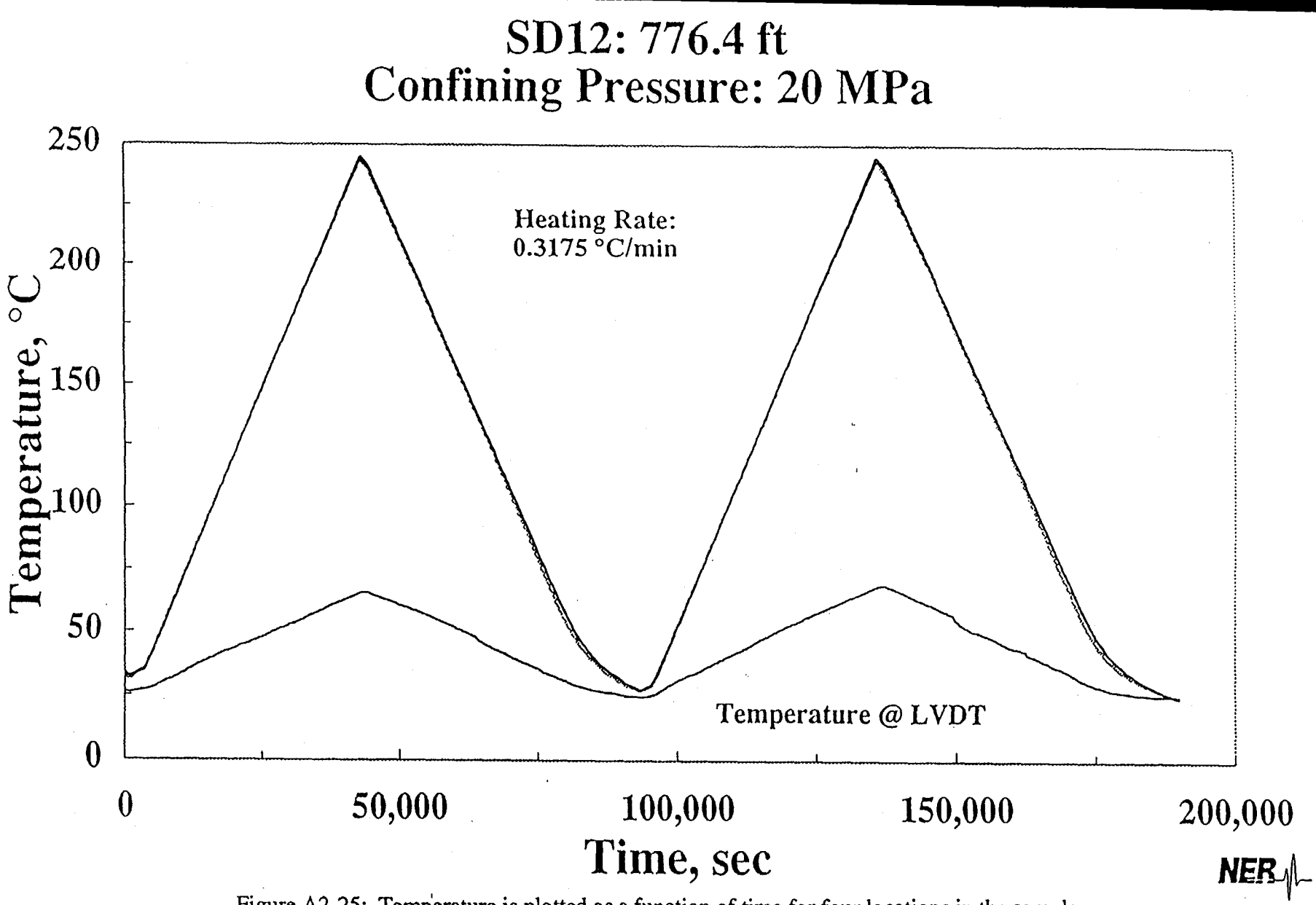

Figure A2-25: Temperature is plotted as a function of time for four locations in the sample assembly. The upper curves represent temperatures at the base, midpoint, and top of the test specimen. The lower curve indicates the temperature at the LVDTs. The experiment was performed at a confining pressure of 20 MPa.

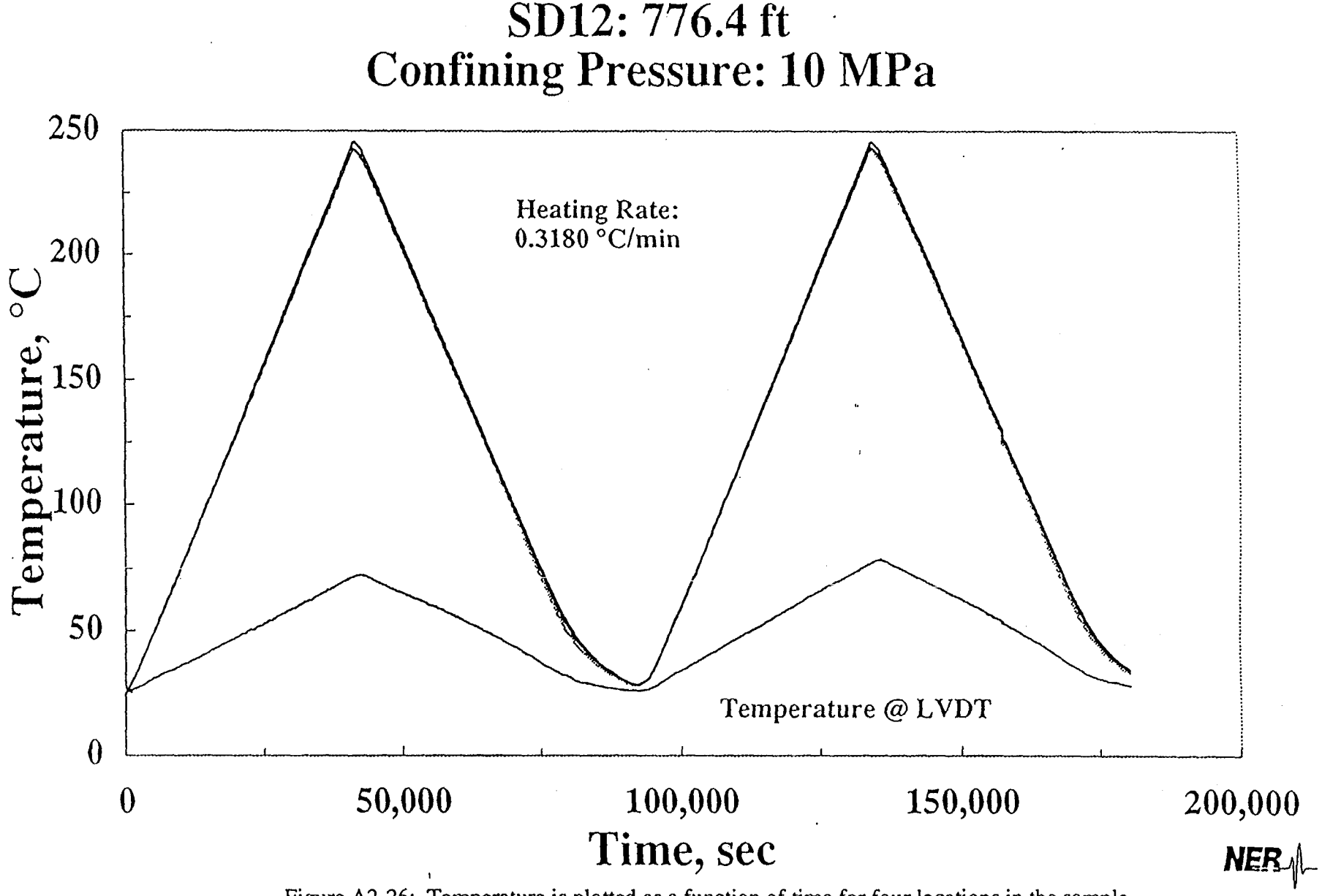

Figure A2-26: Temperature is plotted as a function of time for four locations in the sample assembly. The upper curves represent temperatures at the base, midpoint, and top of the test specimen. The lower curve indicates the temperature at the LVDTs. The experiment

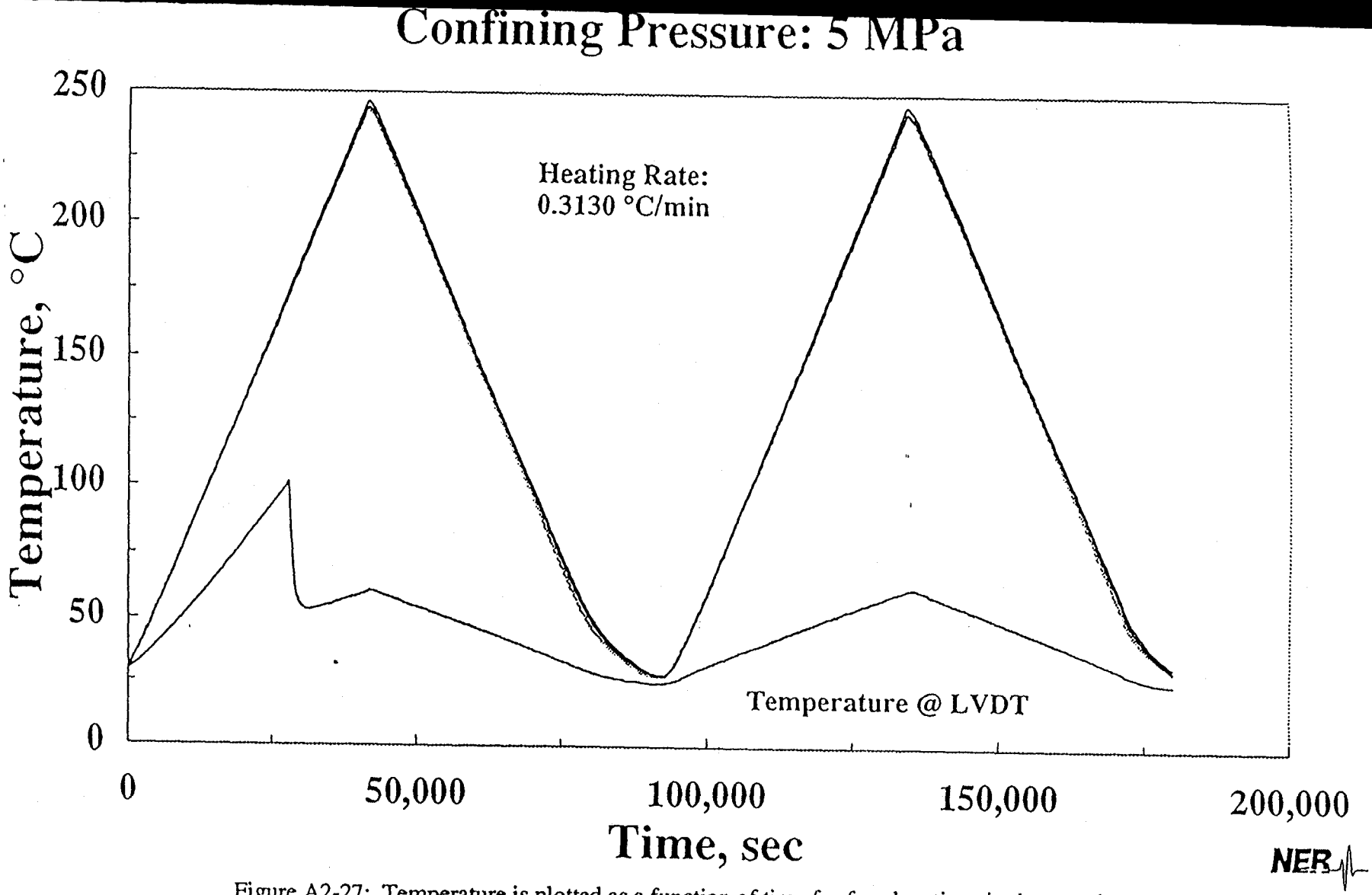

Figure A2-27: Temperature is plotted as a function of time for four locations in the sample assembly. The upper curves represent temperatures at the base, midpoint, and top of the test specimen. The lower curve indicates the temperature at the LVDTs. The experiment was performed at a confining pressure of 5 MPa. Note: The cooling system for the LVDTs failed during the first half of the heating cycle. A temperature increase at the lower portion of the vessel approaching 100 °C was observed. Midway through the cycle the problem was corrected.

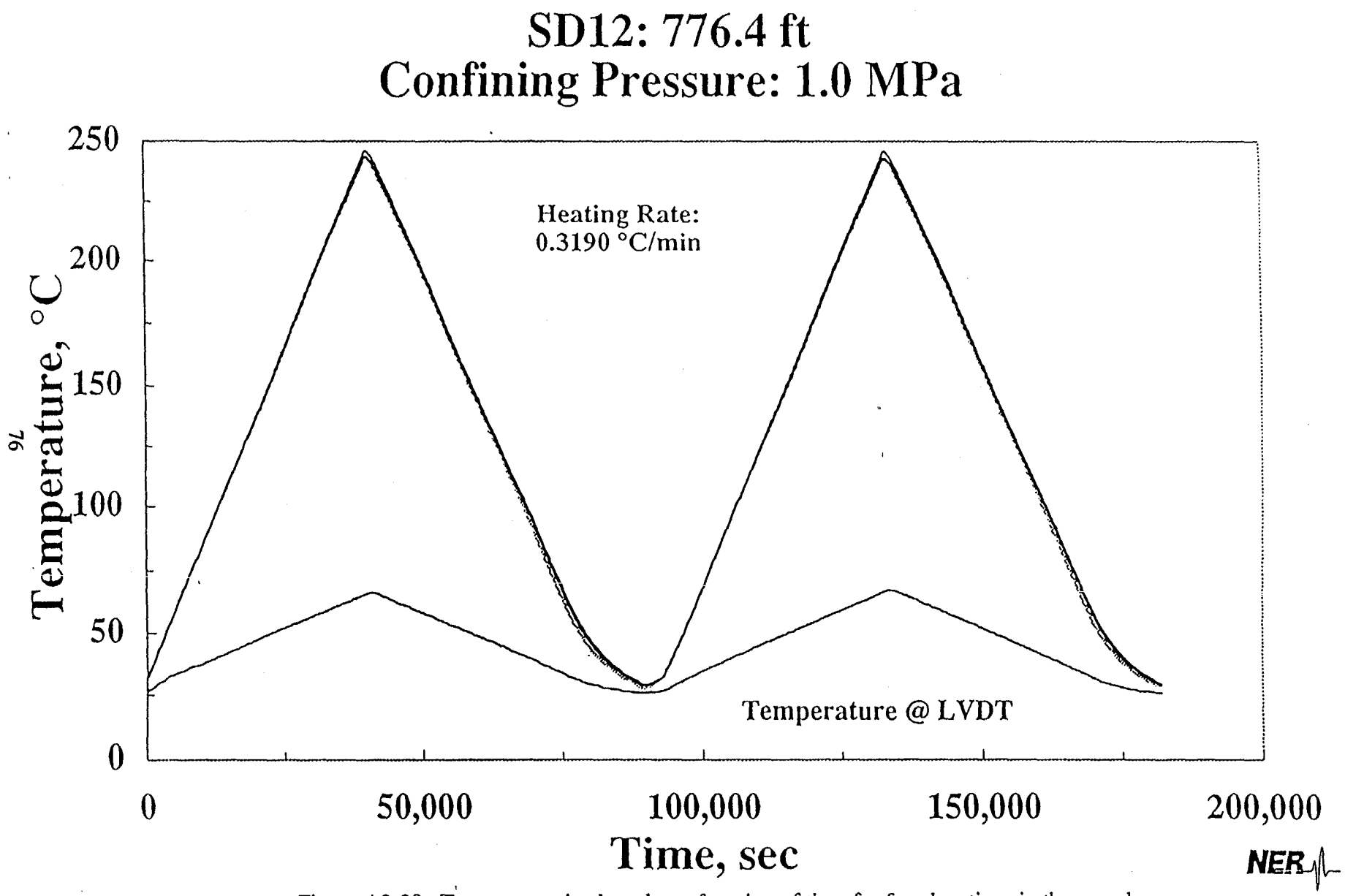

Figure A2-28: Temperature is plotted as a function of time for four locations in the sample assembly. The upper curves represent temperatures at the base, midpoint, and top of the test specimen. The lower curve indicates the temperature at the LVDTs. The experiment

Yucca Mountain Project
Thermal Expansion
Borehole: SD 12
Depth: 883.5 feet

The specimen was thermally cycled to 247 °C at confining pressures of 30, 20, 10, 5 and 1 MPa. Two thermal cycles were performed at each pressure. The heating rate was 0.318 ± 0.010 °C/min.

	Before Testing	After Testing
Length, mm	101.63	101.63
Diameter, mm	50.88	50.85
Mass, g	482.56	479.95
Porosity, %		8.9
Seismic Velocities Parallel to the Specimen Axis		
P-Wave, km/s	4.312	4.490
S(1)-Wave, km/s	2.665	2.823
S(2)-Wave, km/s	2.555	2.805
Seismic Velocities Normal to the Specimen Axis		
P-Wave, km/s	4.483	4.554
S-Wave, km/s	2.780	2.811

NER

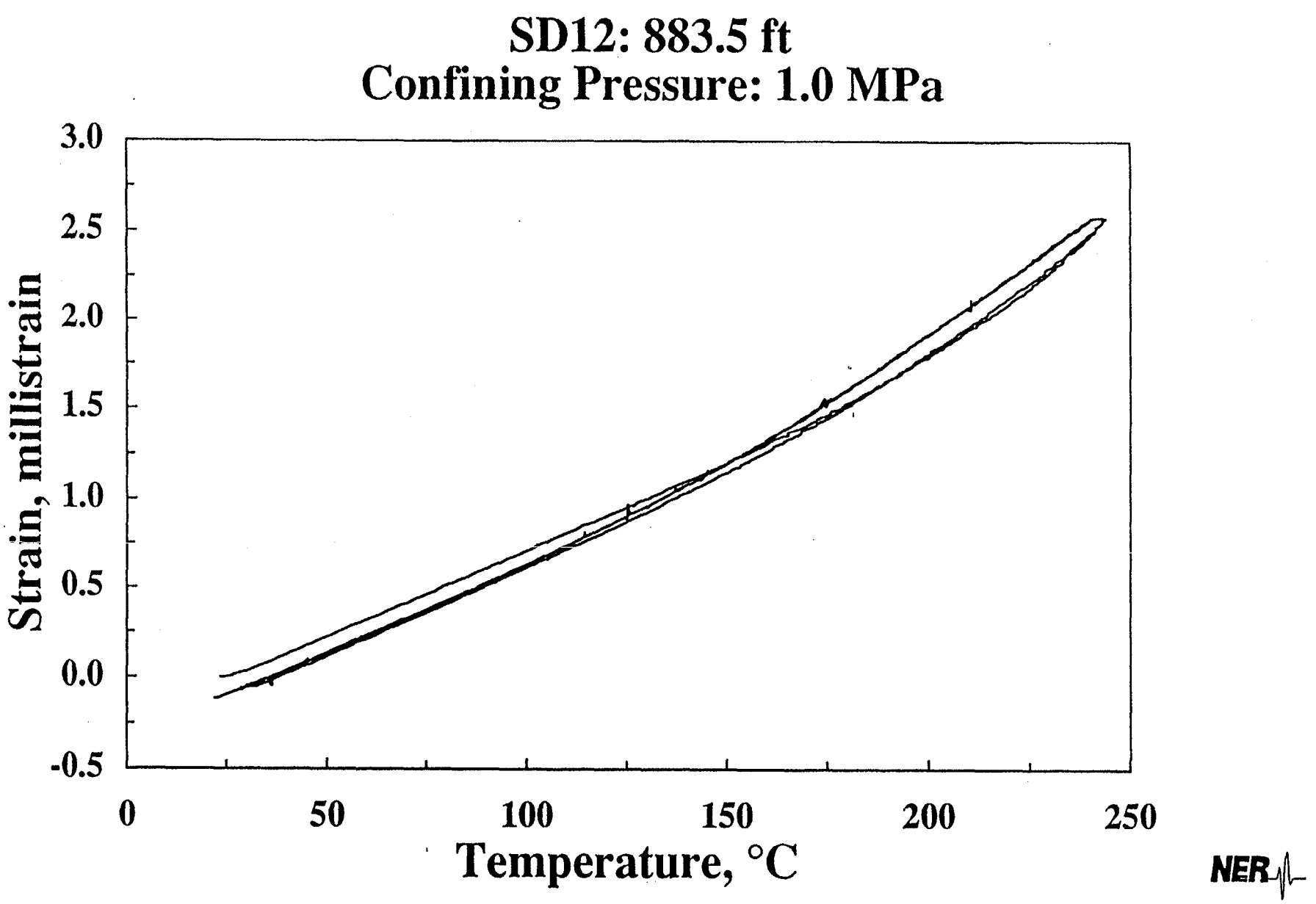

Figure A2-29: Axial strain on the test specimen of TSw2 tuff is plotted as a function of temperature.

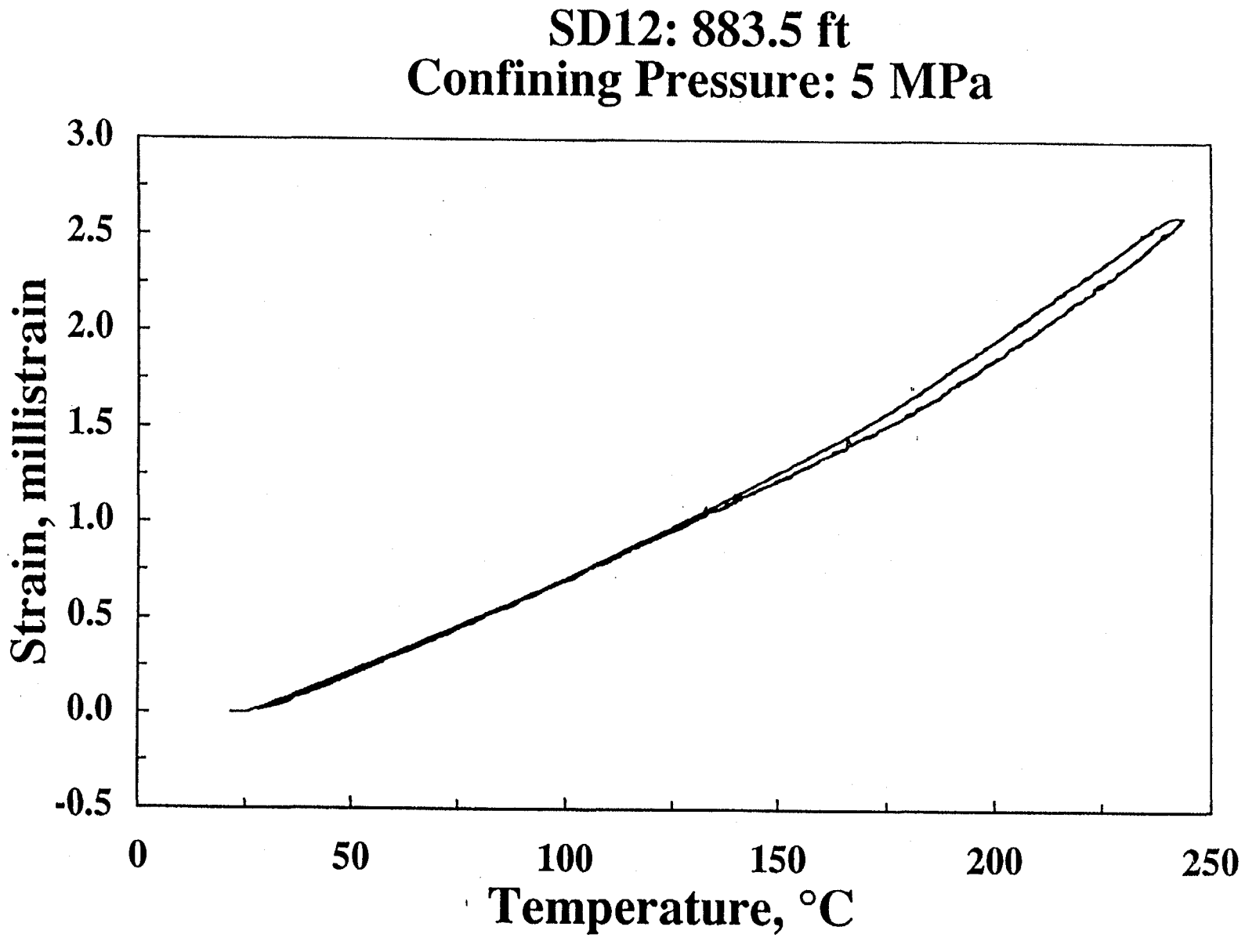

Figure A2-30: Axial strain on the test specimen of TSw2 tuff is plotted as a function of temperature. Two test cycles were performed over a nominal range of 25 to 250 °C. These data were collected at a confining pressure 5 MPa.

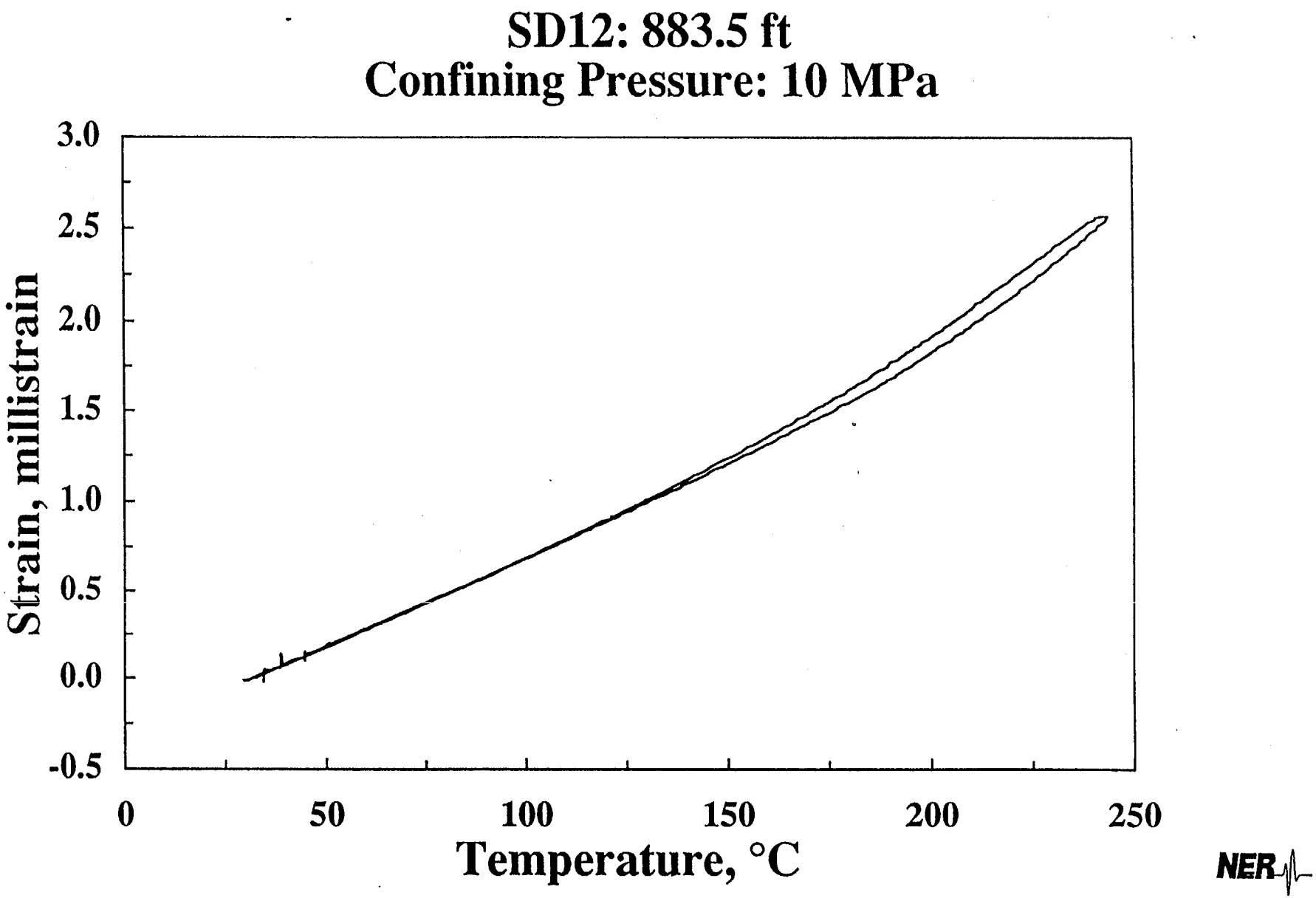

Figure A2-31: Axial strain on the test specimen of TSw2 tuff is plotted as a function of temperature. One test cycle was performed over a nominal range of 25 to 250 °C. These data were collected at a confining pressure 10 MPa. The specimen was removed from the pressure vessel and rejected prior to

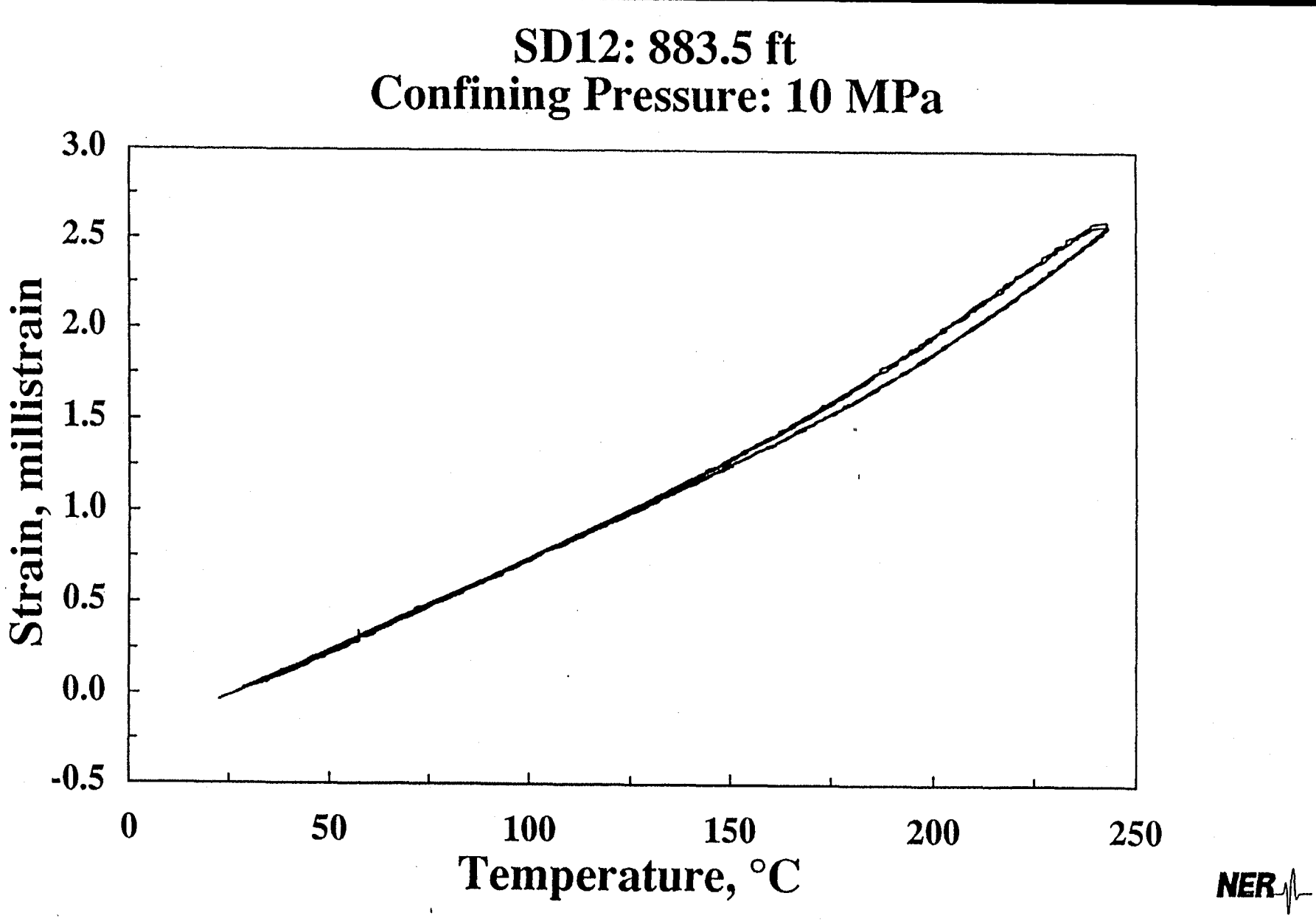

Figure A2-32: Axial strain on the test specimen of TSw2 tuff is plotted as a function of temperature. Two test cycles were performed over a nominal range of 25 to 250 °C. These data were collected at a confining pressure 10 MPa.

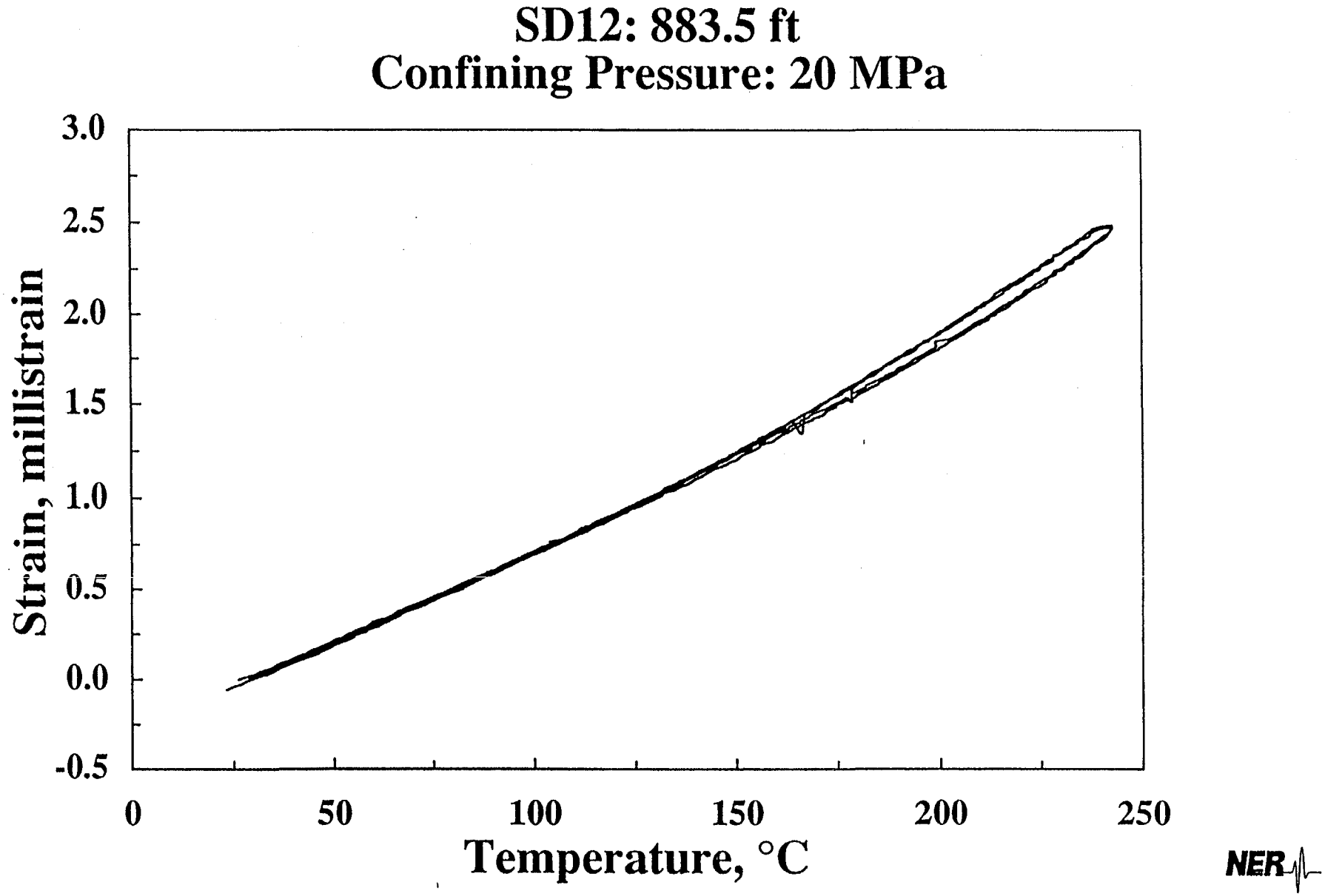

Figure A2-33: Axial strain on the test specimen of TSw2 tuff is plotted as a function of temperature. Two test cycles were performed over a nominal range of 25 to 250 °C. These data were collected at a confining pressure 20 MPa.

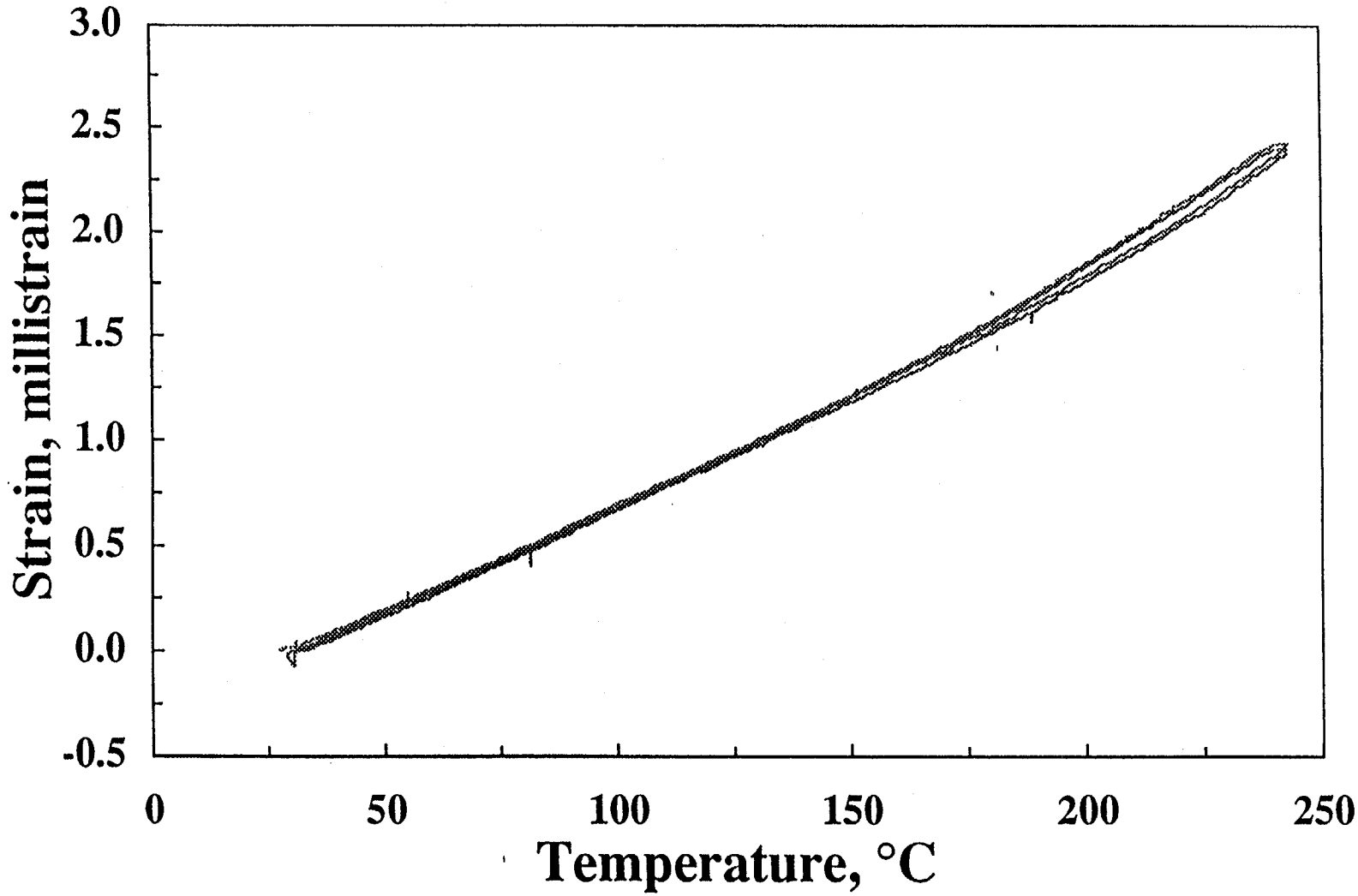

Figure A2-34: Axial strain on the test specimen of TSw2 tuff is plotted as a function of temperature. Two test cycles were performed over a nominal range of 25 to 250 °C. These data were collected at a confining pressure 30 MPa.

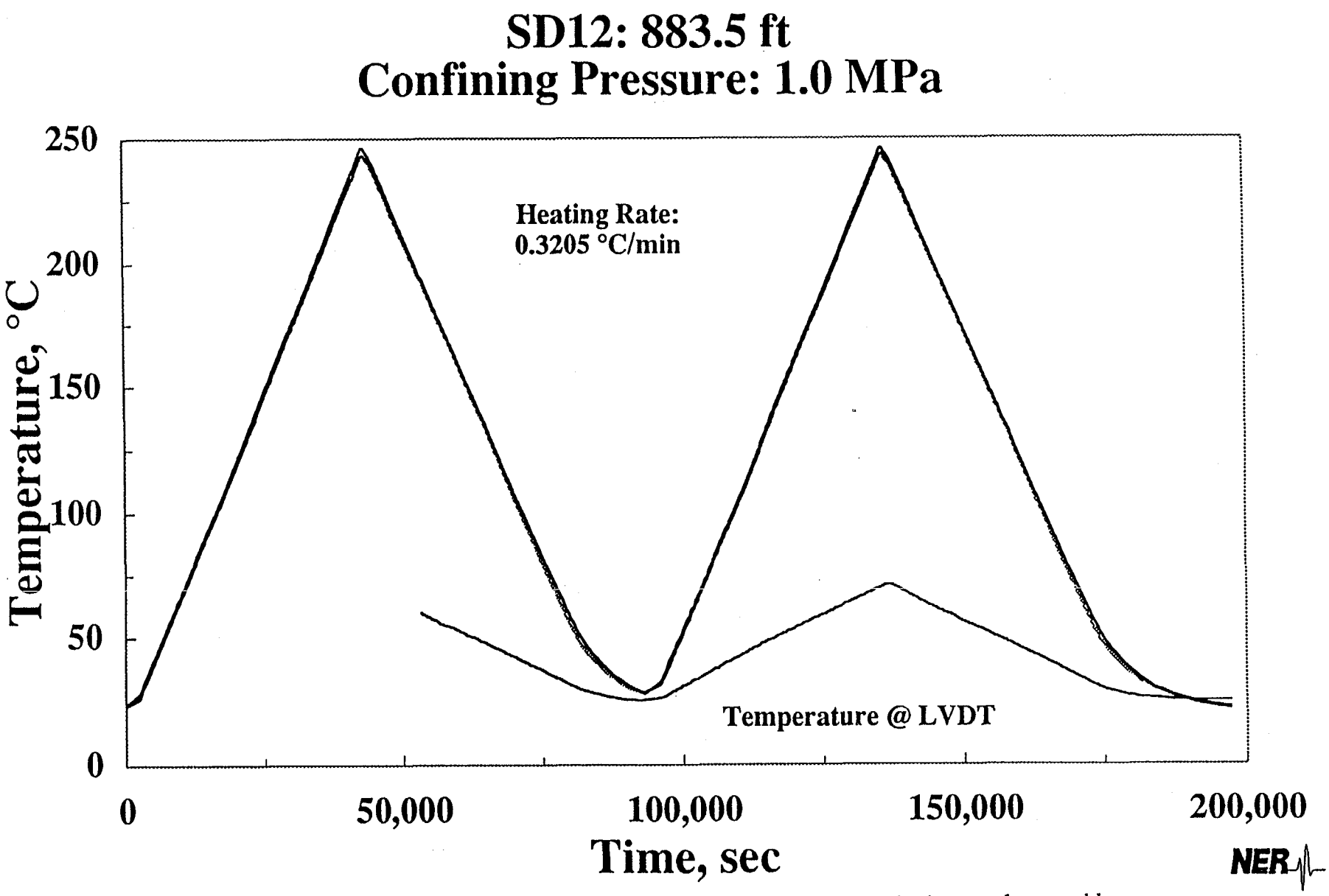

Figure A2-35: Temperature is plotted as a function of time for four locations in the sample assembly. The upper curves represent temperatures at the base, midpoint, and top of the test specimen. The lower curve indicates the temperature at the LVDTs. The experiment was performed at a confining pressure

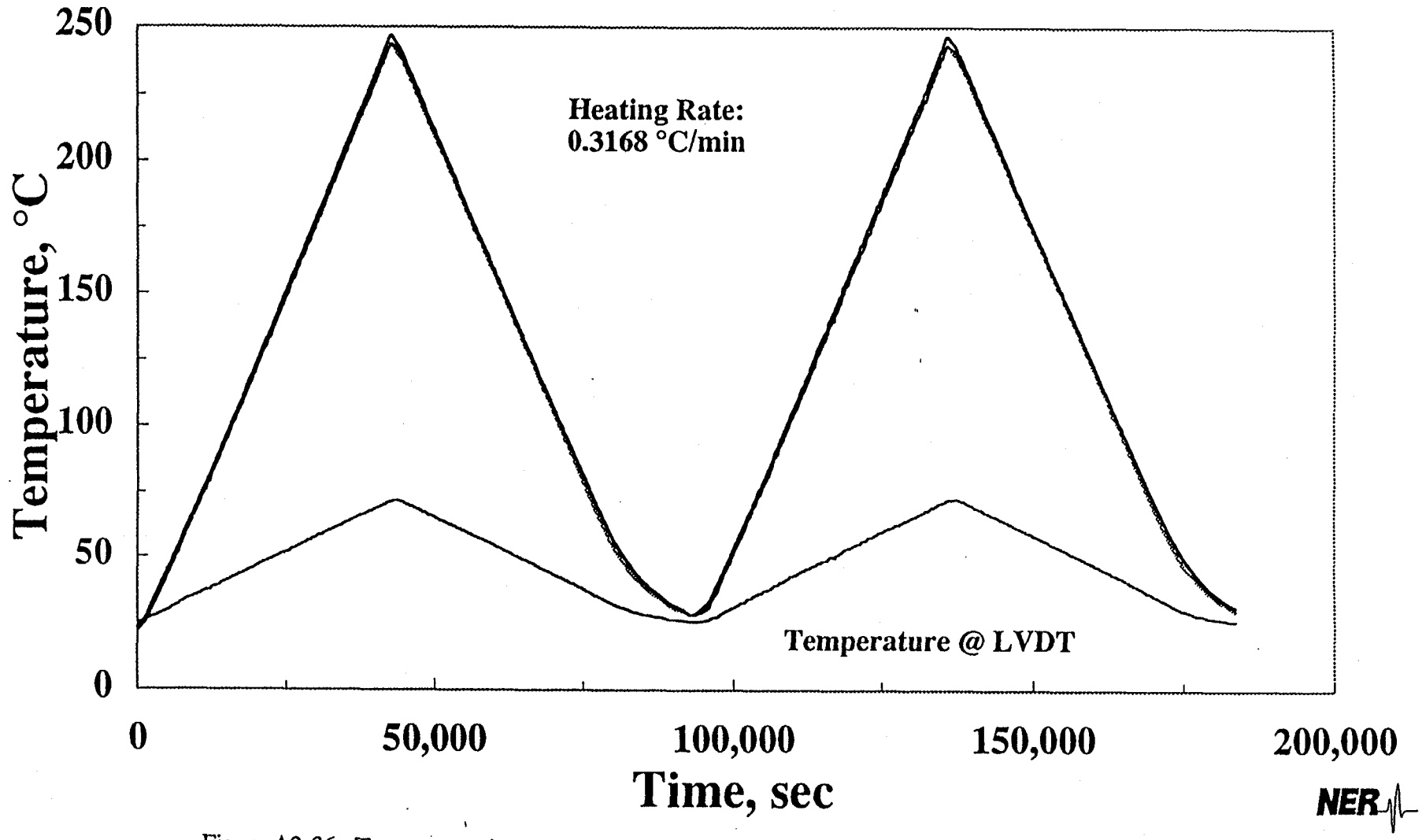

Figure A2-36: Temperature is plotted as a function of time for four locations in the sample assembly. The upper curves represent temperatures at the base, midpoint, and top of the test specimen. The lower curve indicates the temperature at the LVDTs. The experiment was performed at a confining pressure of 5 MPa.

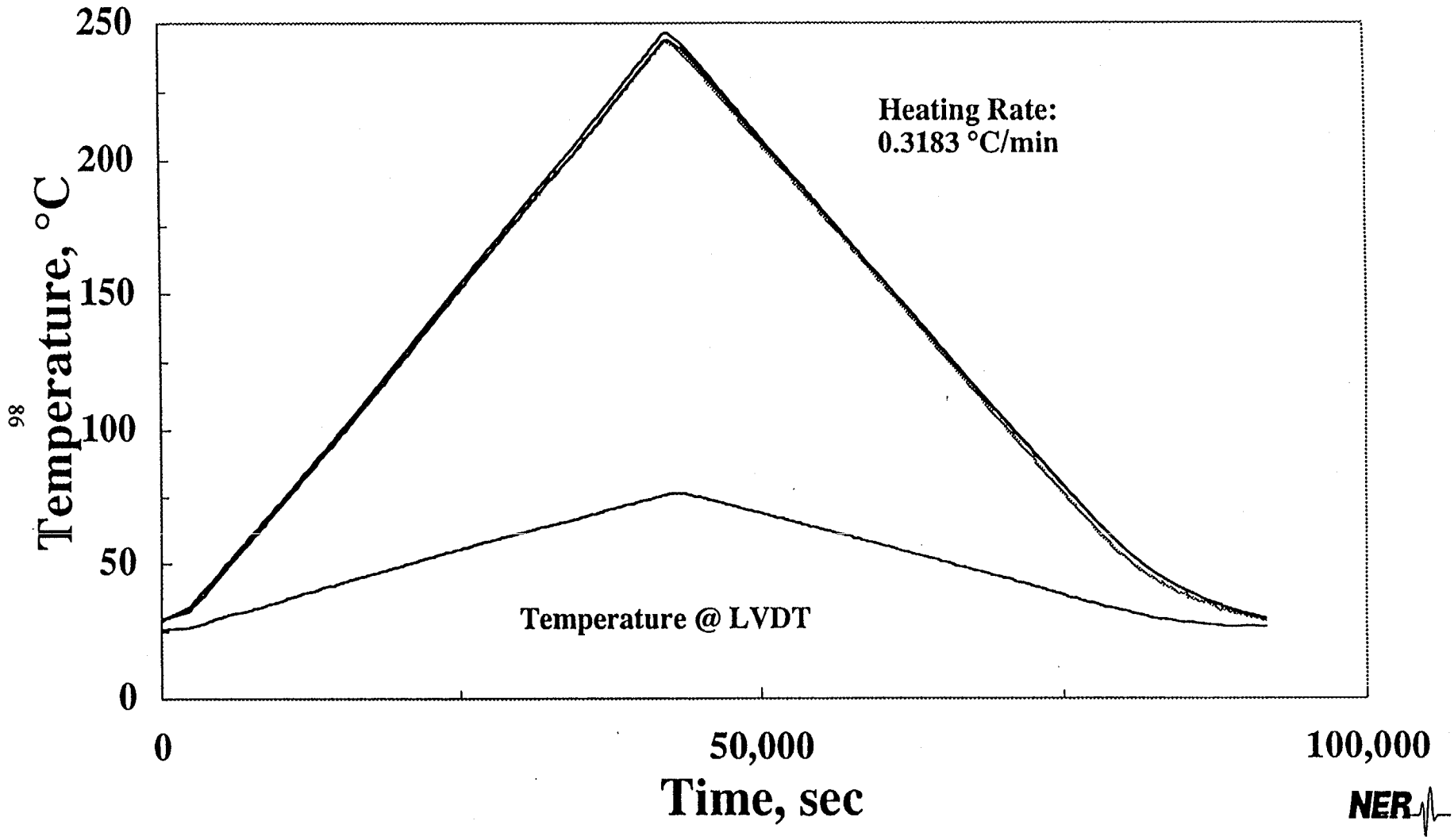

Figure A2-37: Temperature is plotted as a function of time for four locations in the sample assembly. The upper curves represent temperatures at the base, midpoint, and top of the test specimen. The lower curve indicates the temperature at the LVDTs. The experiment was performed at a confining pressure of 10 MPa. Only one thermal cycle was carried out. The specimen was removed from the pressure

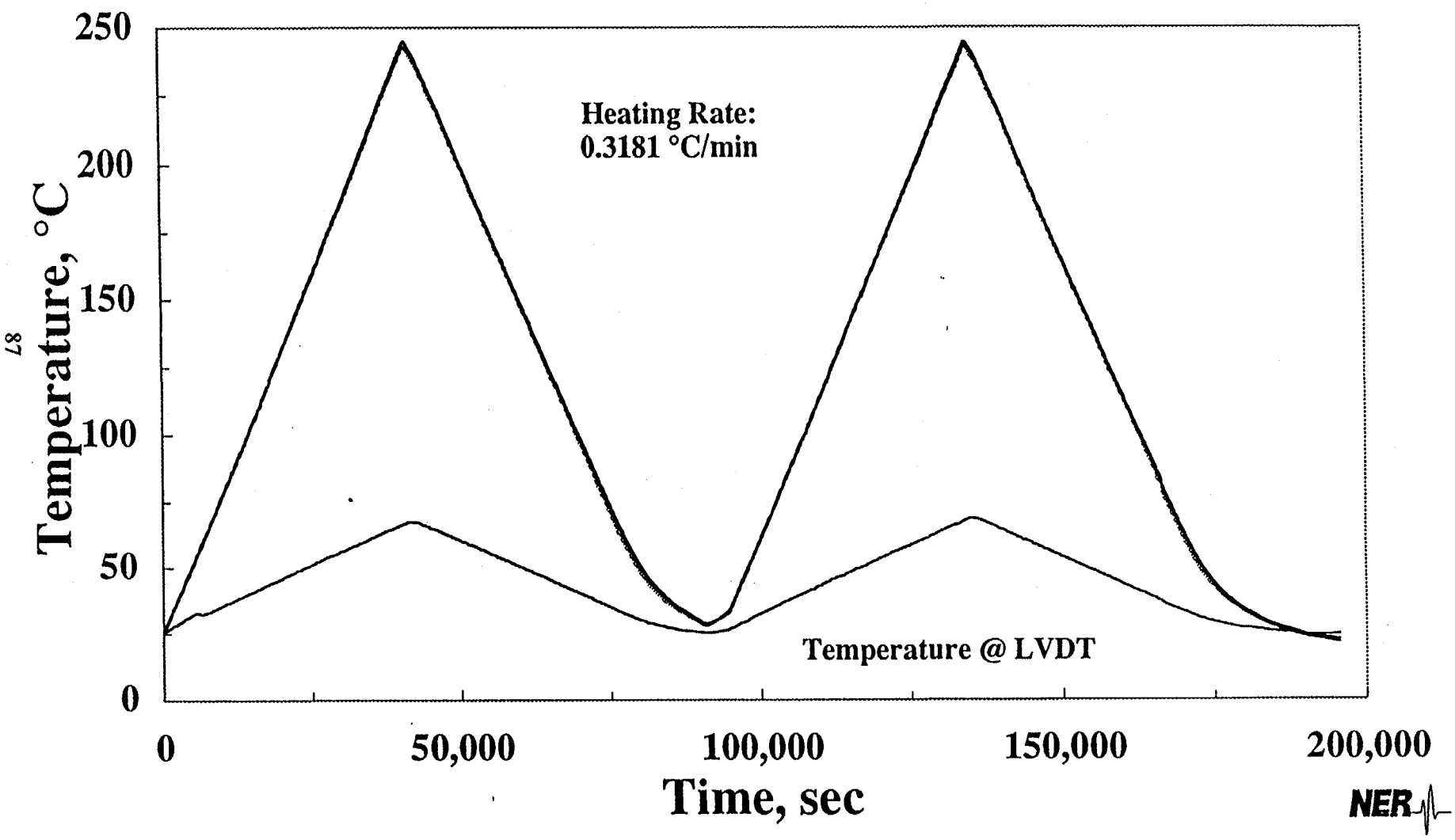

Figure A2-38: Temperature is plotted as a function of time for four locations in the sample assembly. The upper curves represent temperatures at the base; midpoint, and top of the test specimen. The lower curve indicates the temperature at the LVDTs. The experiment was performed at a confining pressure of 10 MPa.

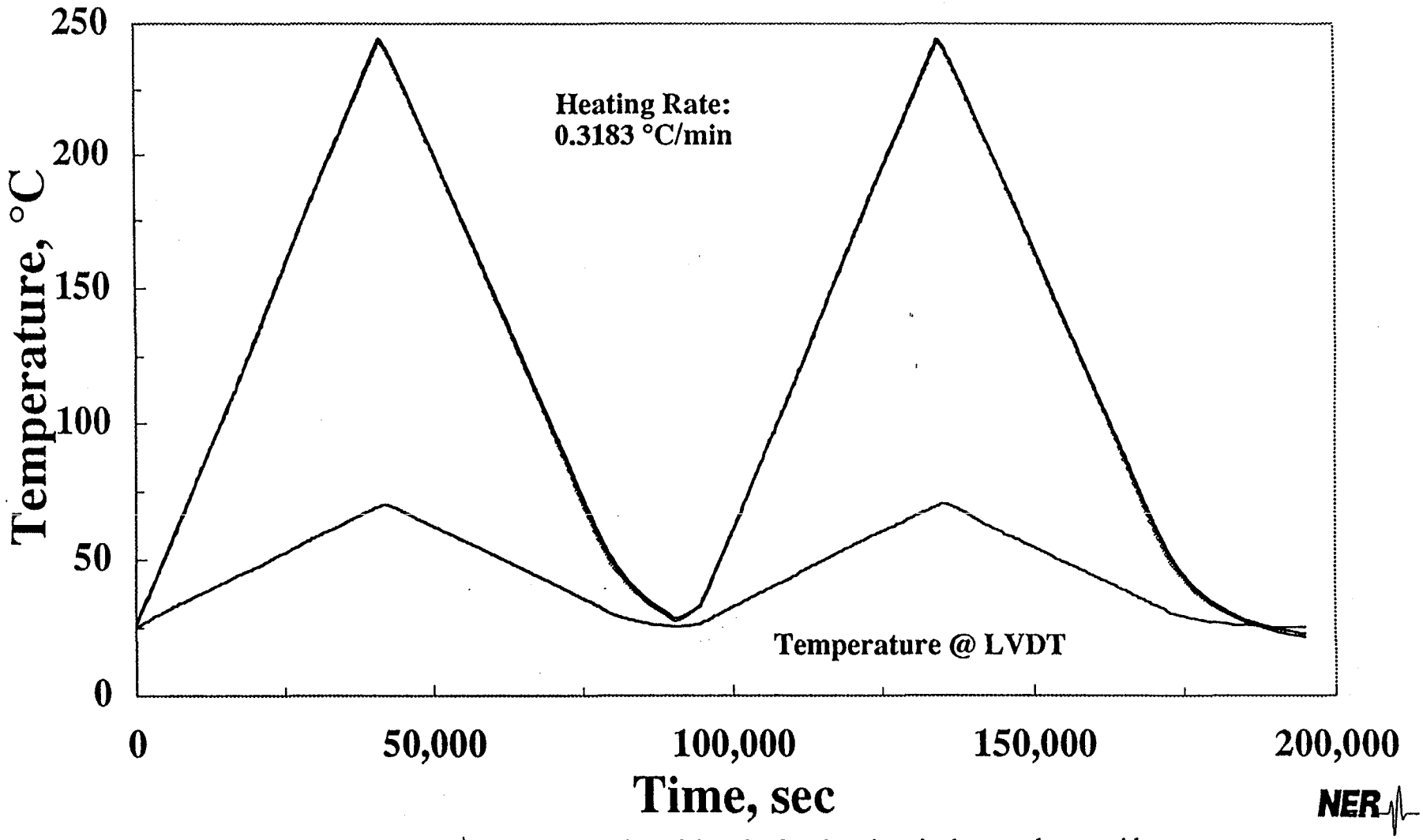

Figure A2-39: Temperature is plotted as a function of time for four locations in the sample assembly. The upper curves represent temperatures at the base, midpoint, and top of the test specimen. The lower curve indicates the temperature at the LVDTs. The experiment was performed at a confining pressure of 20 MPa.

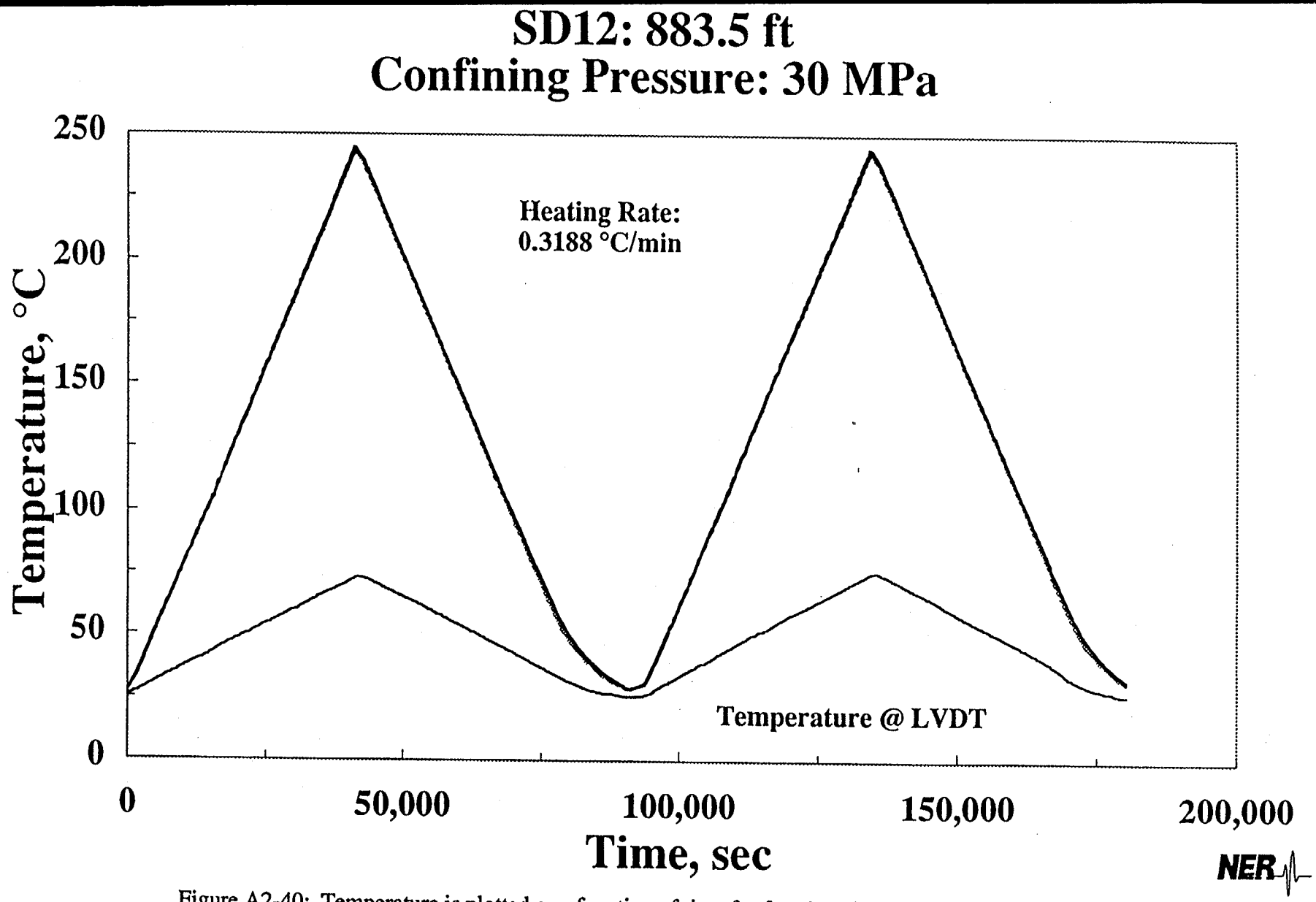

Figure A2-40: Temperature is plotted as a function of time for four locations in the sample assembly. The upper curves represent temperatures at the base, midpoint, and top of the test specimen. The lower curve indicates the temperature at the LVDTs. The experiment was performed at a confining pressure of 30 MPa.

Yucca Mountain Project
Thermal Expansion
Borehole: SD 12
Depth: 1204.8 feet

The specimen was thermally cycled to 247 °C at confining pressures of 1, 5, 10 and 30 MPa. Two thermal cycles were performed at each pressure. The heating rate was 0.314 ± 0.005 °C/min.

	Before Testing	After Testing
Length, mm	101.57	101.57
Diameter, mm	50.80	50.84
Mass, g	479.43	*487.46* *
Porosity, %	7.6	
Seismic Velocities Parallel to the Specimen Axis		
P-Wave, km/s	4.334	4.544
S(1)-Wave, km/s	2.733	2.783
S(2)-Wave, km/s	2.744	2.789
Seismic Velocities Normal to the Specimen Axis		
P-Wave, km/s	4.478	4.618
S-Wave, km/s	2.778	2.870

* *The jacket leaked at a confining pressure of 10 MPa. The specimen was removed, rejacketed, and retested at 10 MPa. The leak wet the base of the specimen; the increase in the post test mass is most likely due to the oil in the test specimen. More than 75% of the specimen was not wetted.*

NER

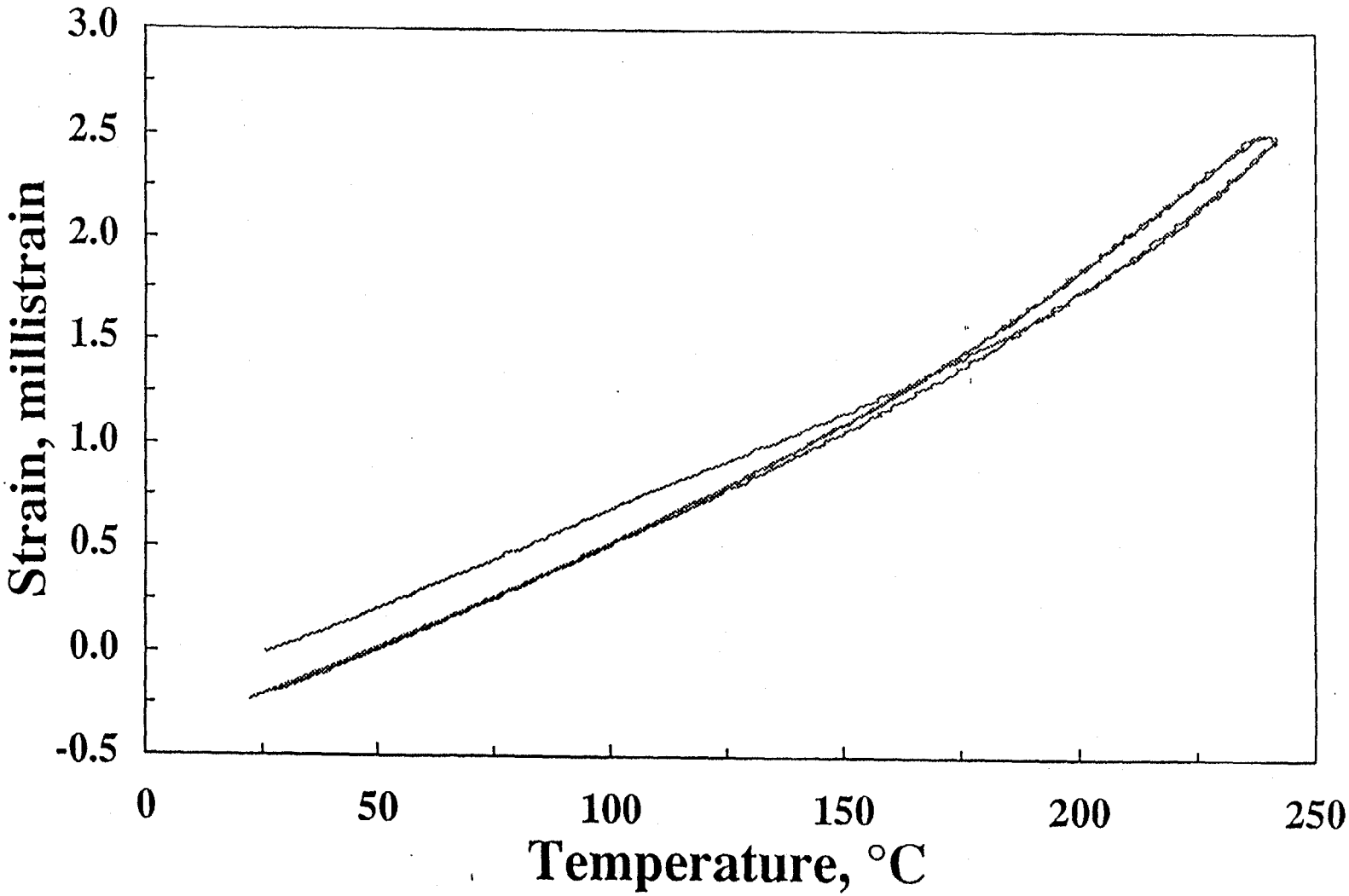

Figure A2-41: Axial strain on the test specimen of TSw2 tuff is plotted as a function of temperature. Two test cycles were performed over a nominal range of 25 to 250 °C. These data were collected at a confining pressure 1.0 MPa.

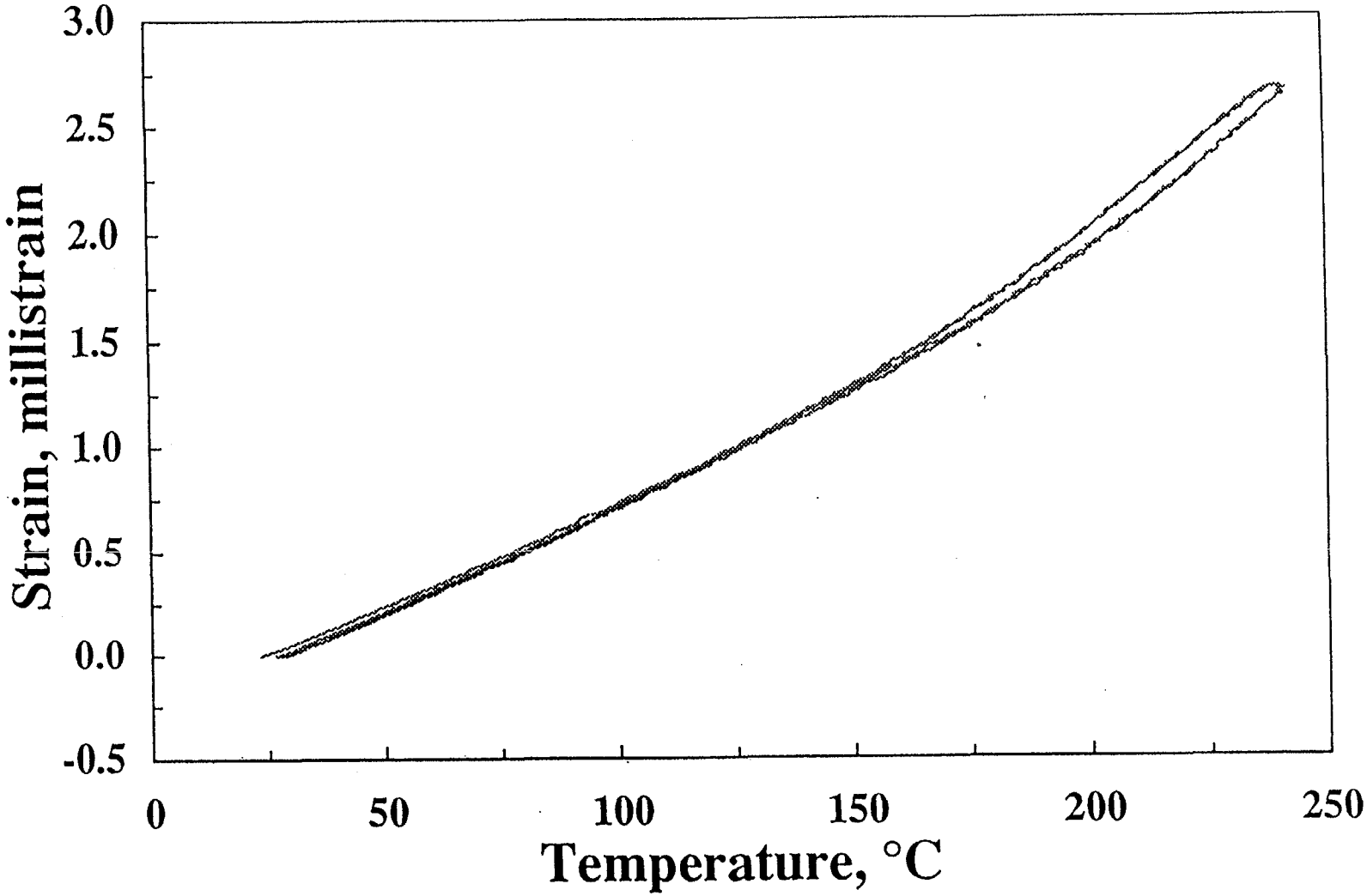

Figure A2-42: Axial strain on the test specimen of TSw2 tuff is plotted as a function of temperature. Two test cycles were performed over a nominal range of 25 to 250 °C. These data were collected at a confining pressure 5 MPa.

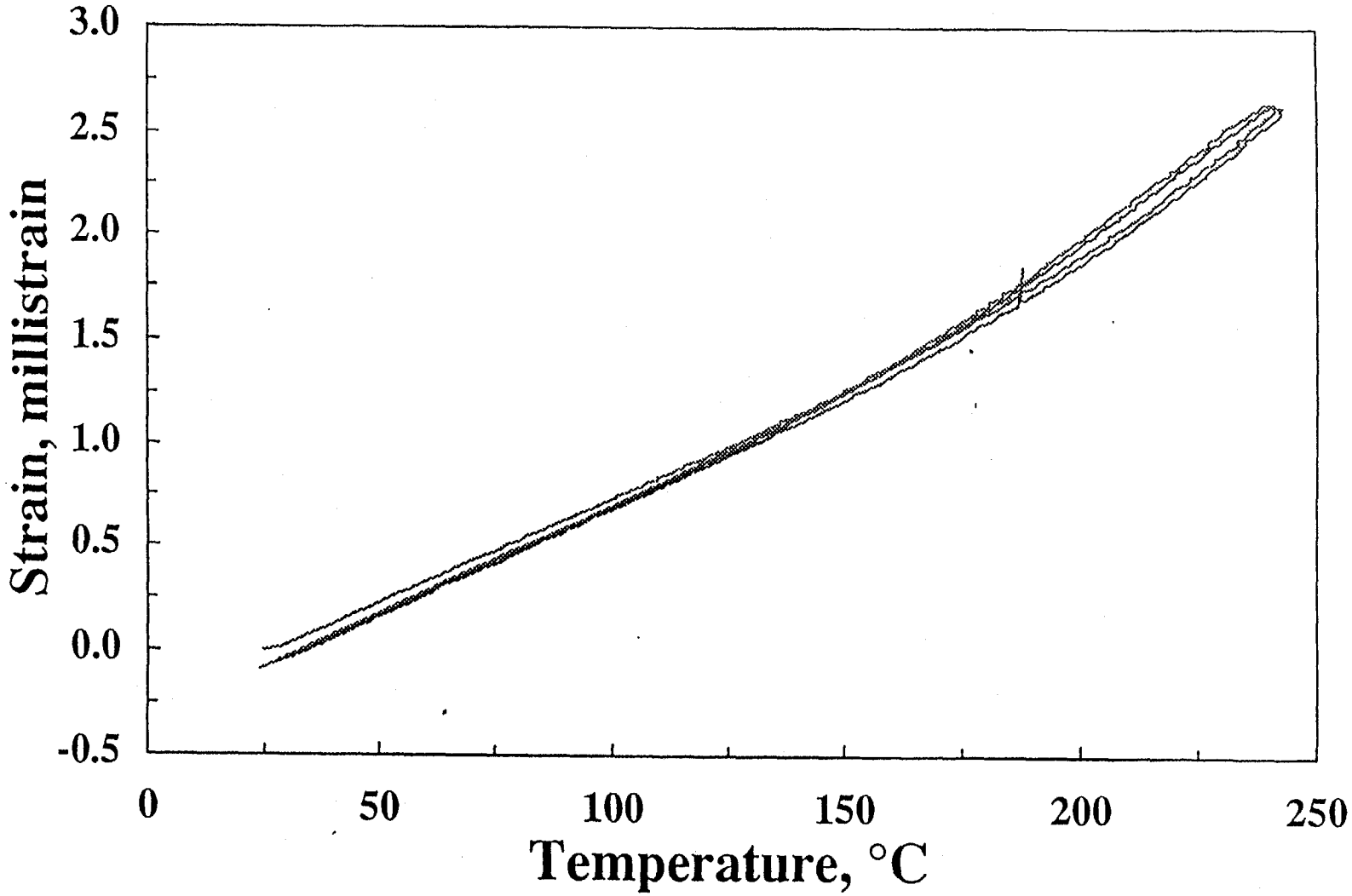

Figure A2-43: Axial strain on the test specimen of TSw2 tuff is plotted as a function of temperature. Two test cycles were performed over a nominal range of 25 to 250 °C. These data were collected at a confining pressure 10 MPa.

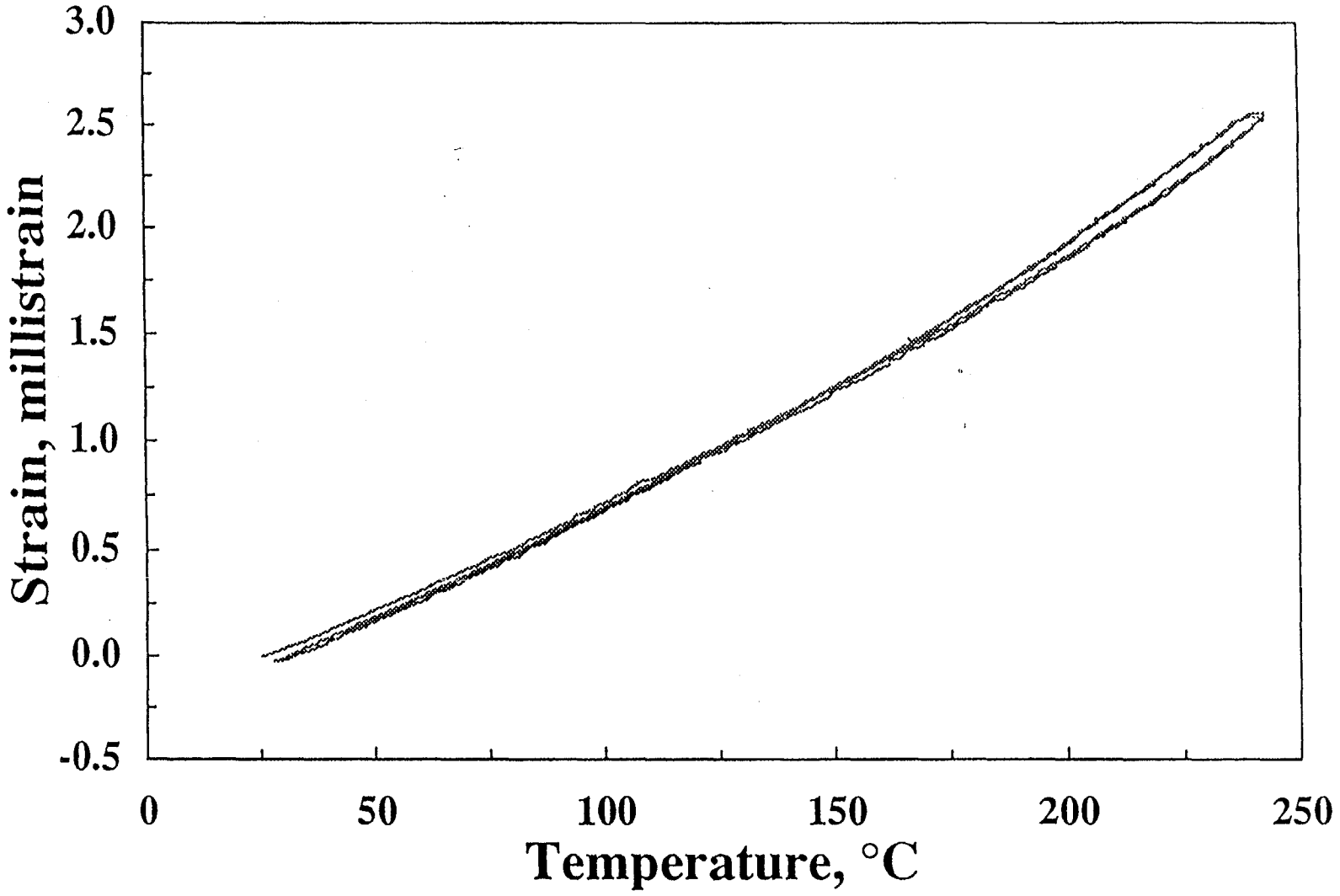

Figure A2-44: Axial strain on the test specimen of TSw2 tuff is plotted as a function of temperature. Two test cycles were performed over a nominal range of 25 to 250 °C. These data were collected at a confining pressure 30 MPa.

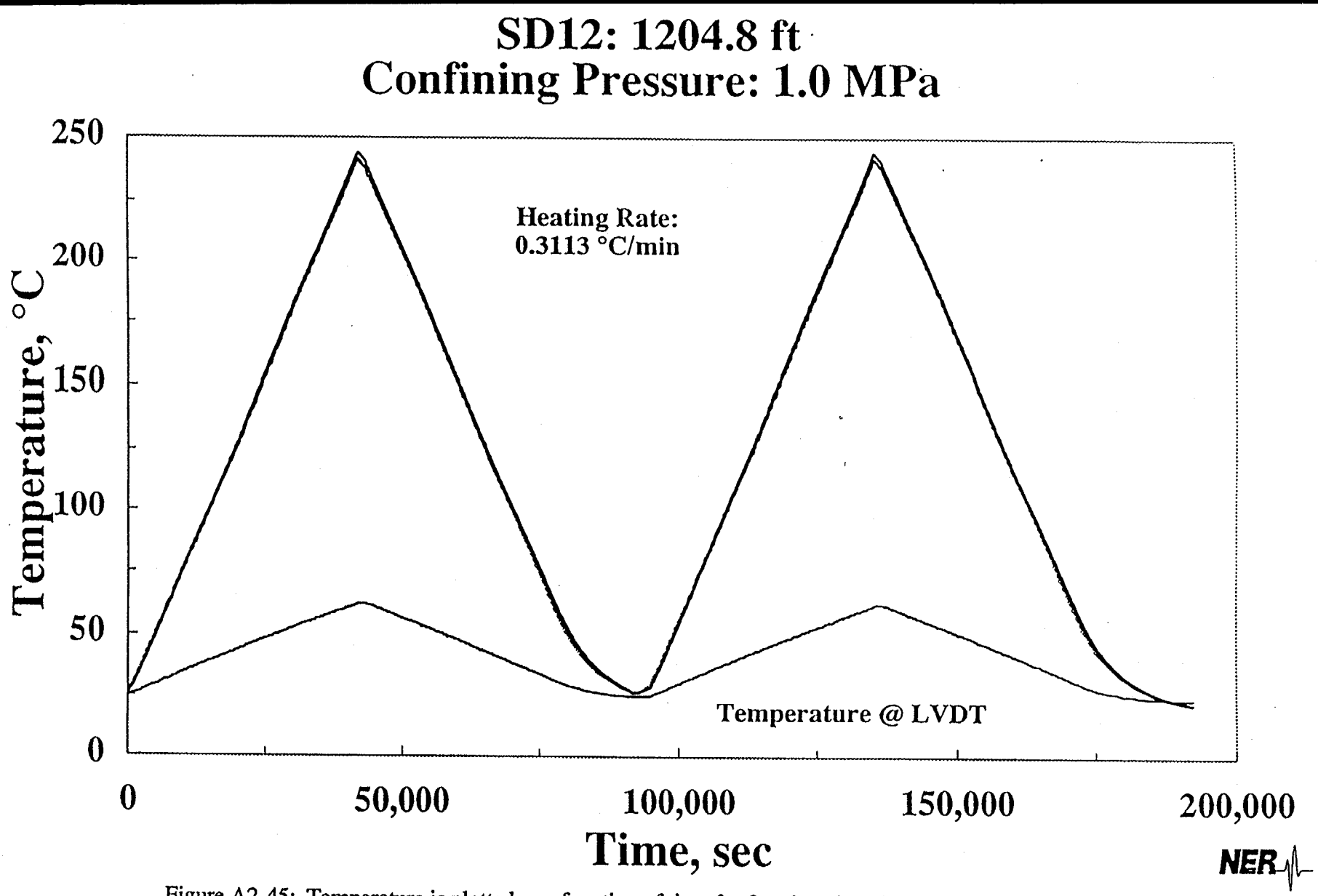

Figure A2-45: Temperature is plotted as a function of time for four locations in the sample assembly. The upper curves represent temperatures at the base, midpoint, and top of the test specimen. The lower curve indicates the temperature at the LVDTs. The experiment was performed at a confining pressure of 1.0 MPa.

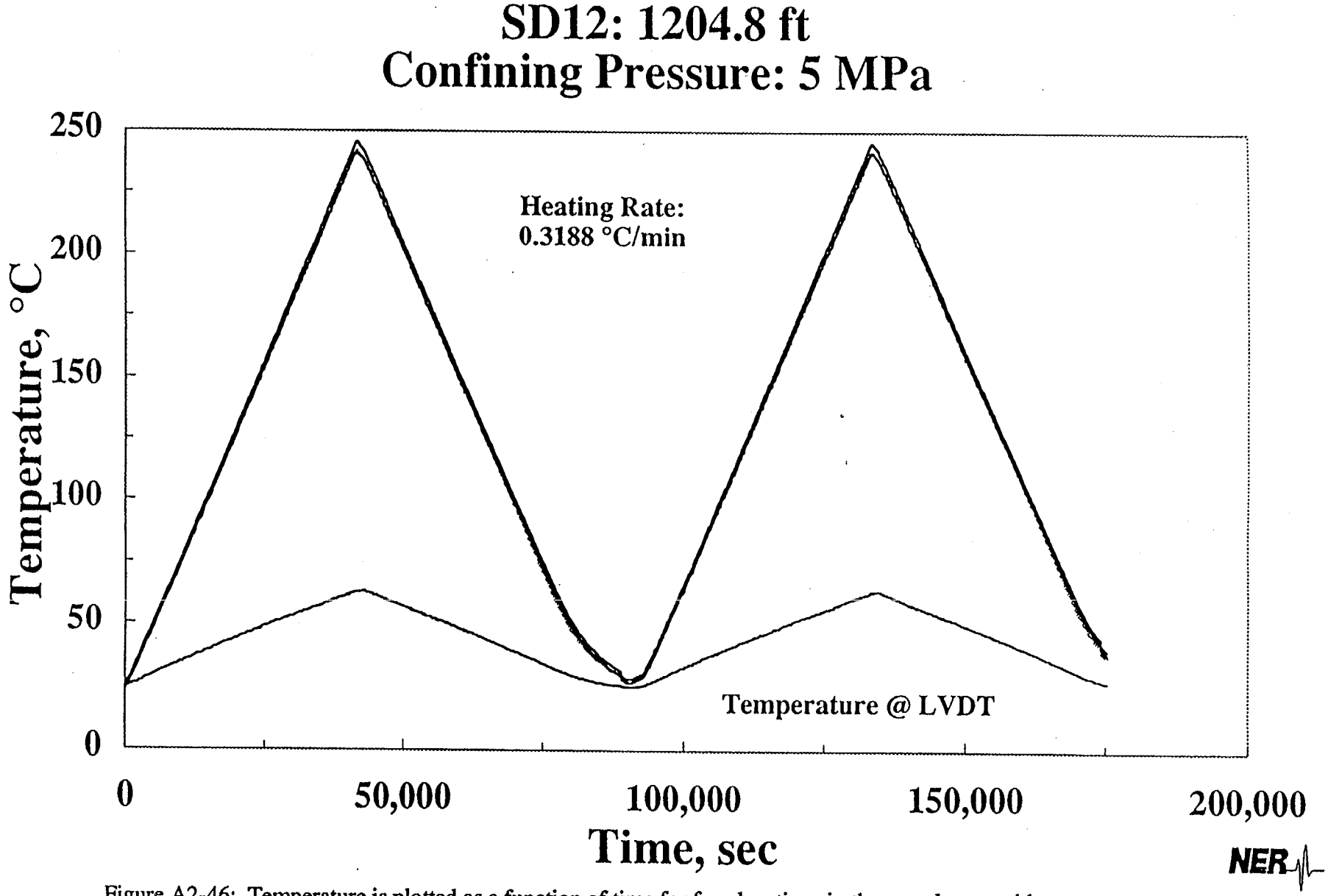

Figure A2-46: Temperature is plotted as a function of time for four locations in the sample assembly. The upper curves represent temperatures at the base, midpoint, and top of the test specimen. The lower curve indicates the temperature at the LVDTs. The experiment was performed at a confining pressure of 5 MPa.

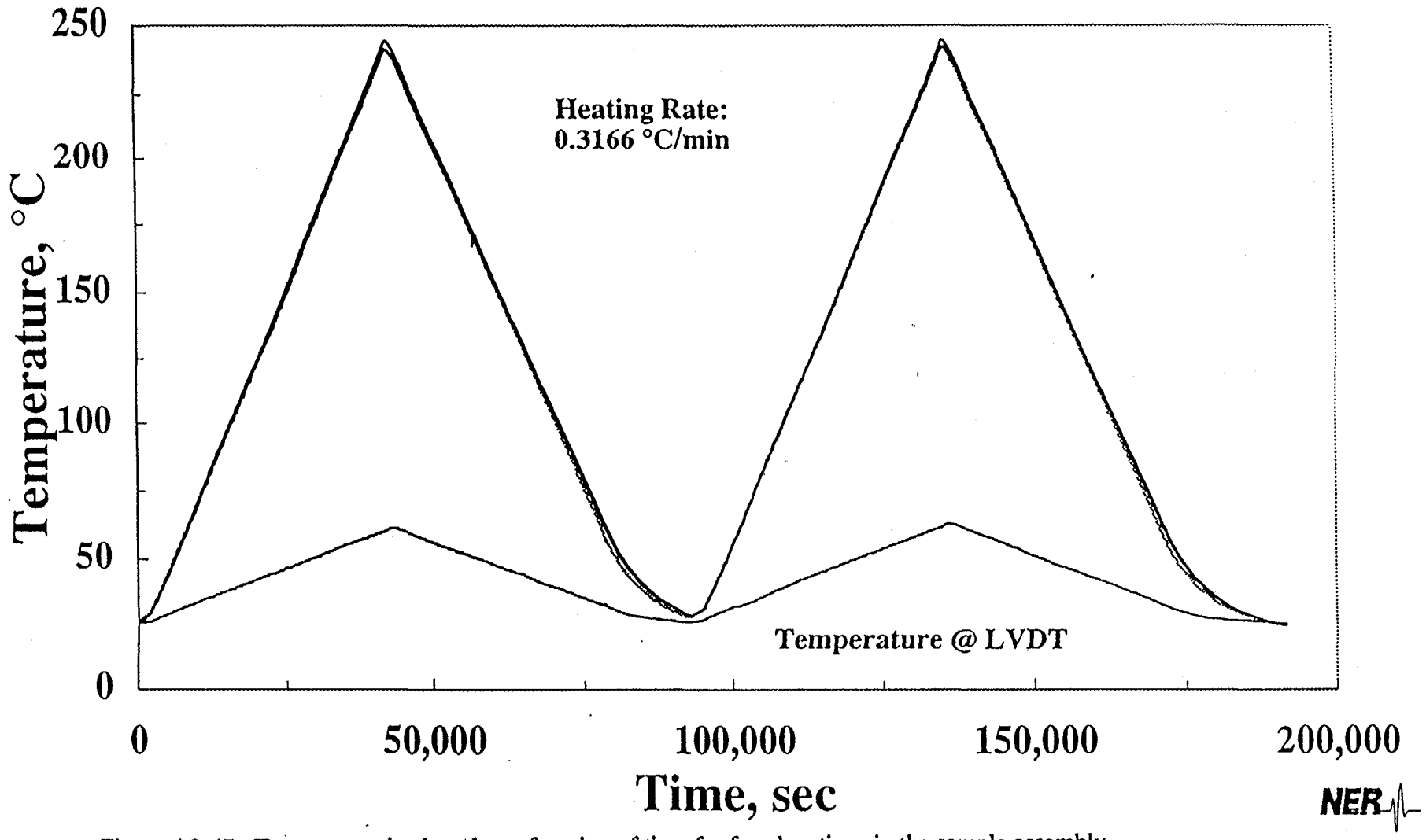

Figure A2-47: Temperature is plotted as a function of time for four locations in the sample assembly. The upper curves represent temperatures at the base, midpoint, and top of the test specimen. The lower curve indicates the temperature at the LVDTs. The experiment was performed at a confining pressure of 10 MPa.

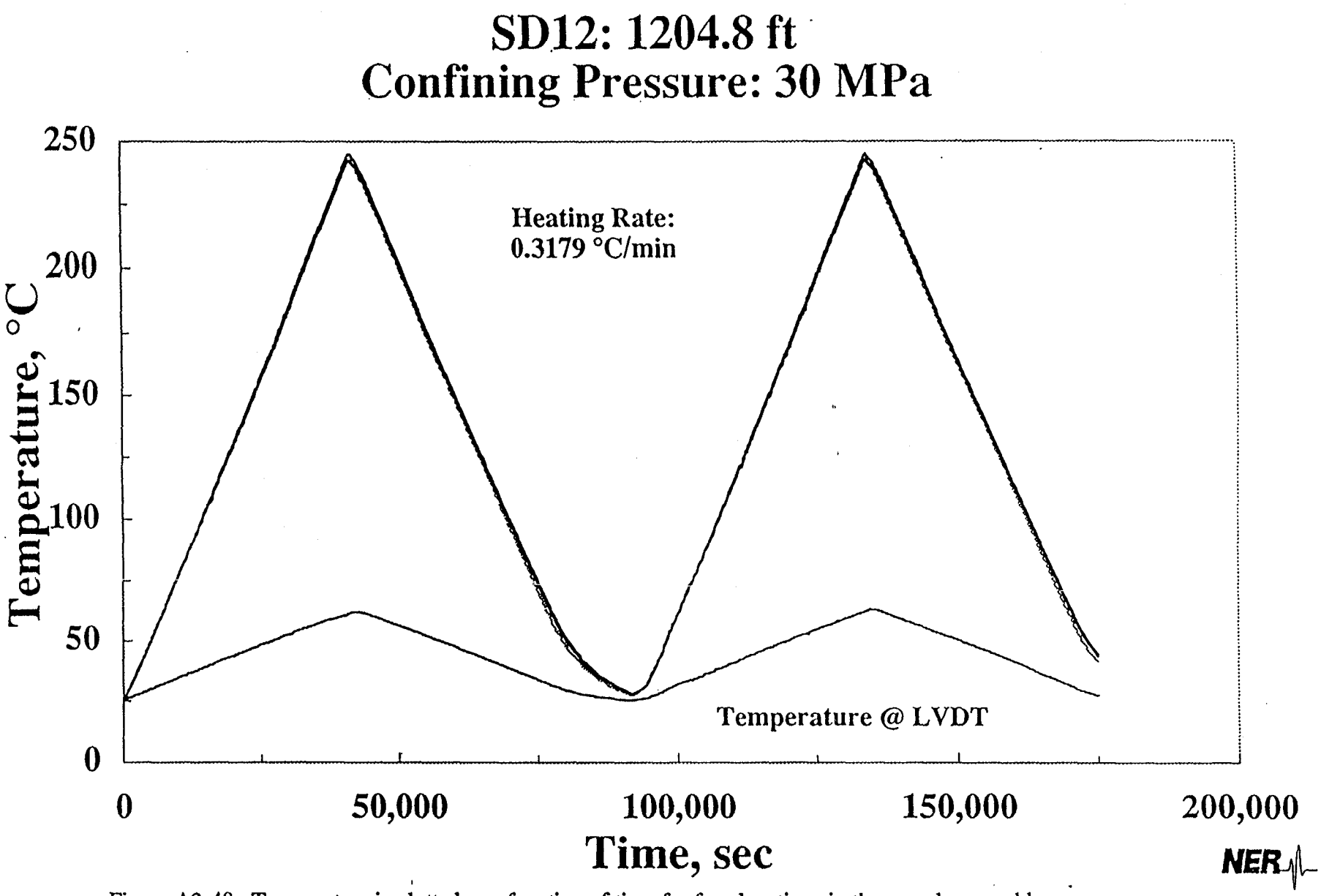

Figure A2-48: Temperature is plotted as a function of time for four locations in the sample assembly. The upper curves represent temperatures at the base, midpoint, and top of the test specimen. The lower curve indicates the temperature at the LVDTs. The experiment was performed at a confining pressure

APPENDIX III

System checks are performed using a specimen of AISI 446 stainless steel. The test specimen has the same nominal dimensions as the tuff specimens used in the thermal expansion measurements. The purpose of these measurements is to verify the performance of the system over the same temperature and displacement range expected for the TSw2 tuff by measuring the thermal expansion on a specimen with known thermal characteristics.

The specimen is jacketed and tested in the same way as the tuff specimens outlined in Section 2.3.3 except that only one thermal cycle was performed. System checks were performed prior to the series of experiments on tuff and after three experiments were completed. Data for the initial and mid sequence system checks are presented.

The following data are presented for each test: (1) the displacement measured with each LVDT, (these data were not corrected for the thermal expansion in the Invar 36 alloy and sample assembly), (2) strain as a function of temperature, (for reference the thermal expansion of AISI 446 stainless steel is shown in the plot,) and (3) temperatures at four locations throughout the sample assembly as a function of time.

In order for a system check to be satisfactory the deviation between the measured coefficient thermal expansion and the reference coefficient thermal expansion for the specimen must be $\pm$ 5%. The coefficient of thermal expansion was computed over five temperature intervals: 25-50, 51-100, 101-150, 151-200, and 201-250 °C. These data are plotted in Figures A3-3, A3-7, and A3-11. Two system checks were performed prior to initiating the measurements on tuff (May 30 and June 14, 1995). The experiments were conducted at confining pressures of 20 and 30 MPa. On August 16, 1995 the second calibration check was conducted at a confining pressure of 30 MPa. An examination of the data in Figures A3-3, A3-7, and A3-11 show that the system was performing satisfactorily to verify the accuracy of the thermal expansion measurements on tuff.

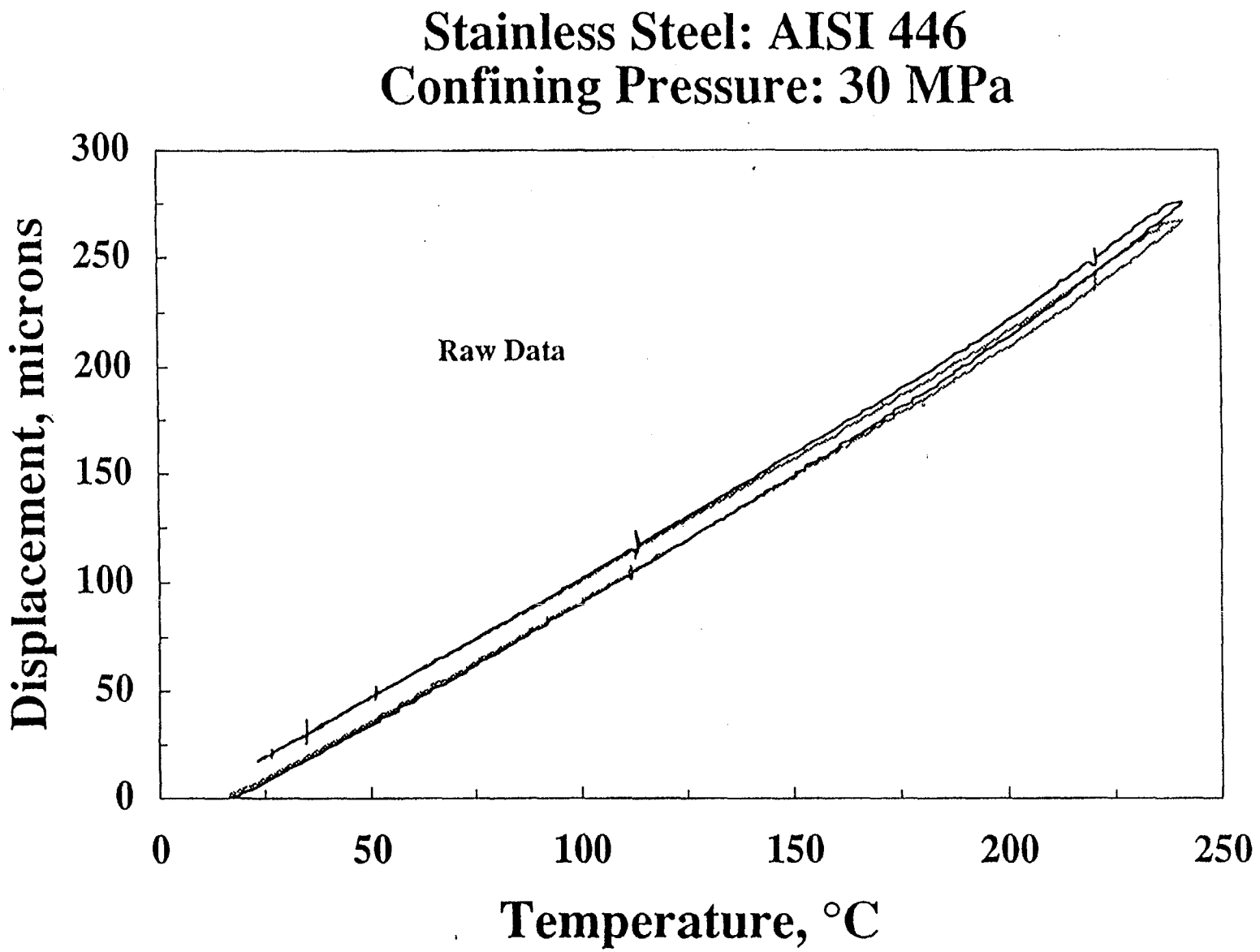

Figure A3-1: The displacement computed from the two LVDTs are plotted as a function of temperature. One thermal cycle was performed on May 30, 1995.

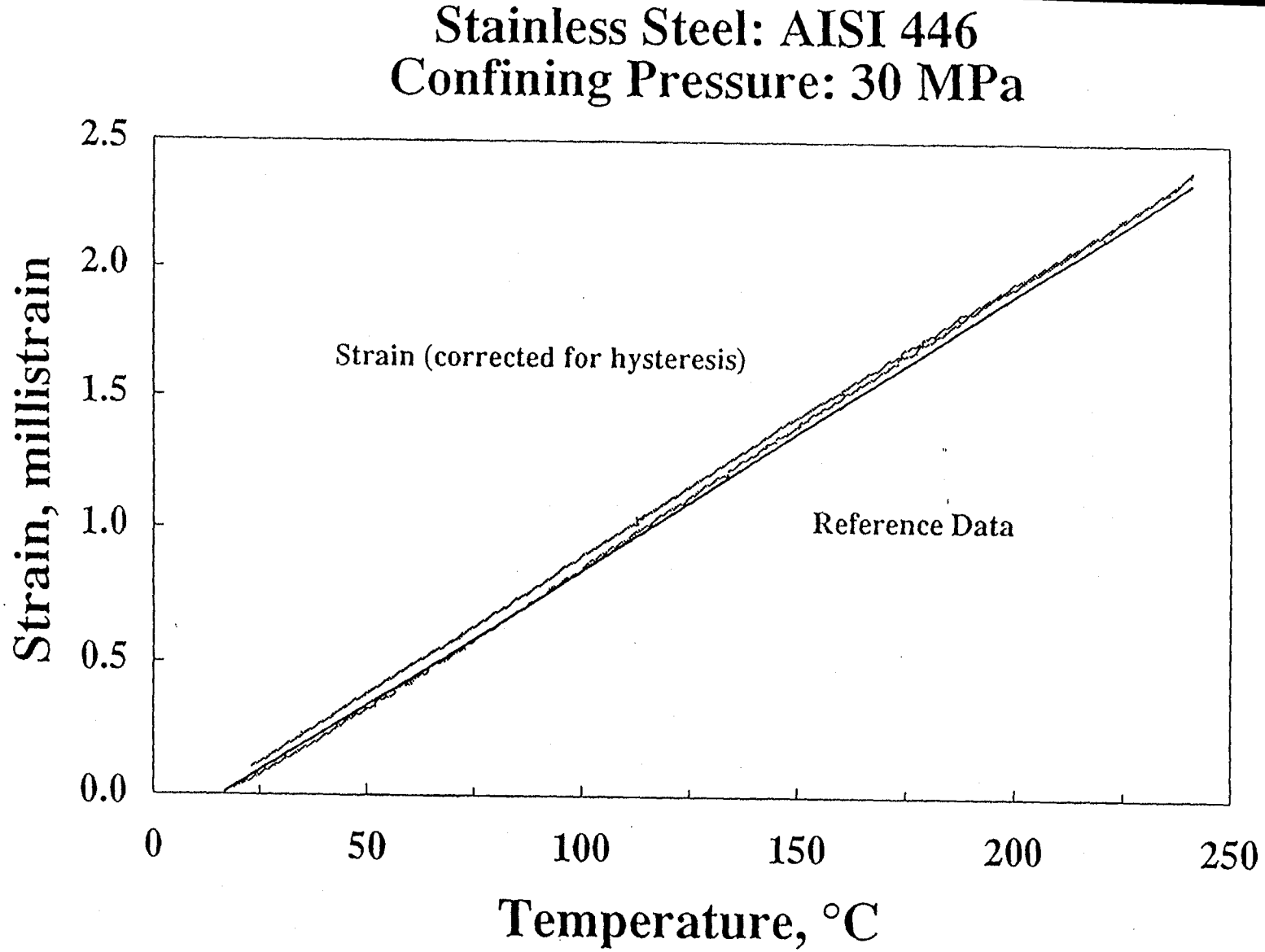

Figure A3-2: The strain is plotted as a function of temperature for the specimen tested on May 30, 1995. The solid line in the figure represents the reference data for AISI 446 stainless steel.

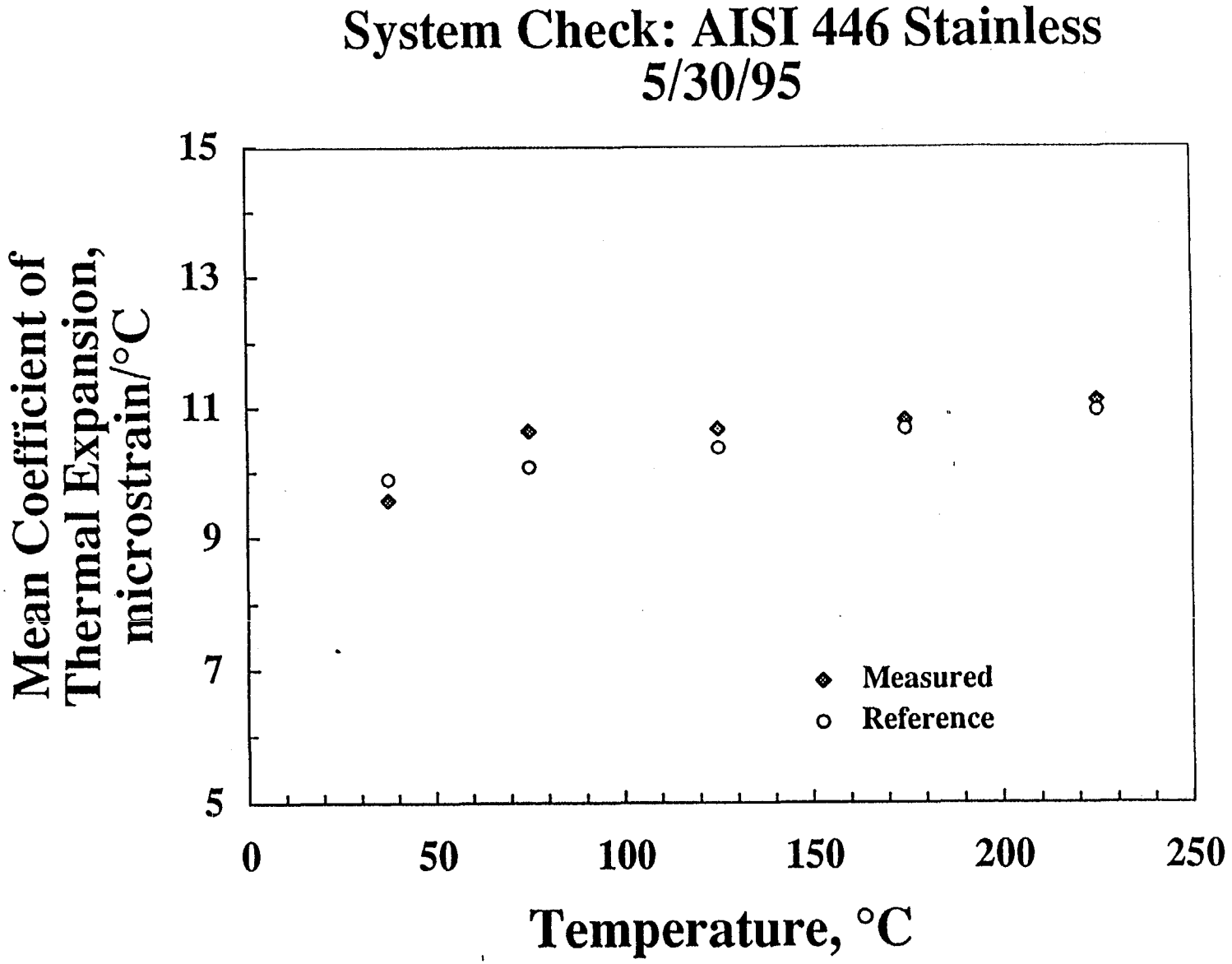

Figure A3-3: The measured and the reference mean coefficients of thermal expansion are plotted as a function of temperature. The coefficients were computed over the following intervals 25-50, 51-100,

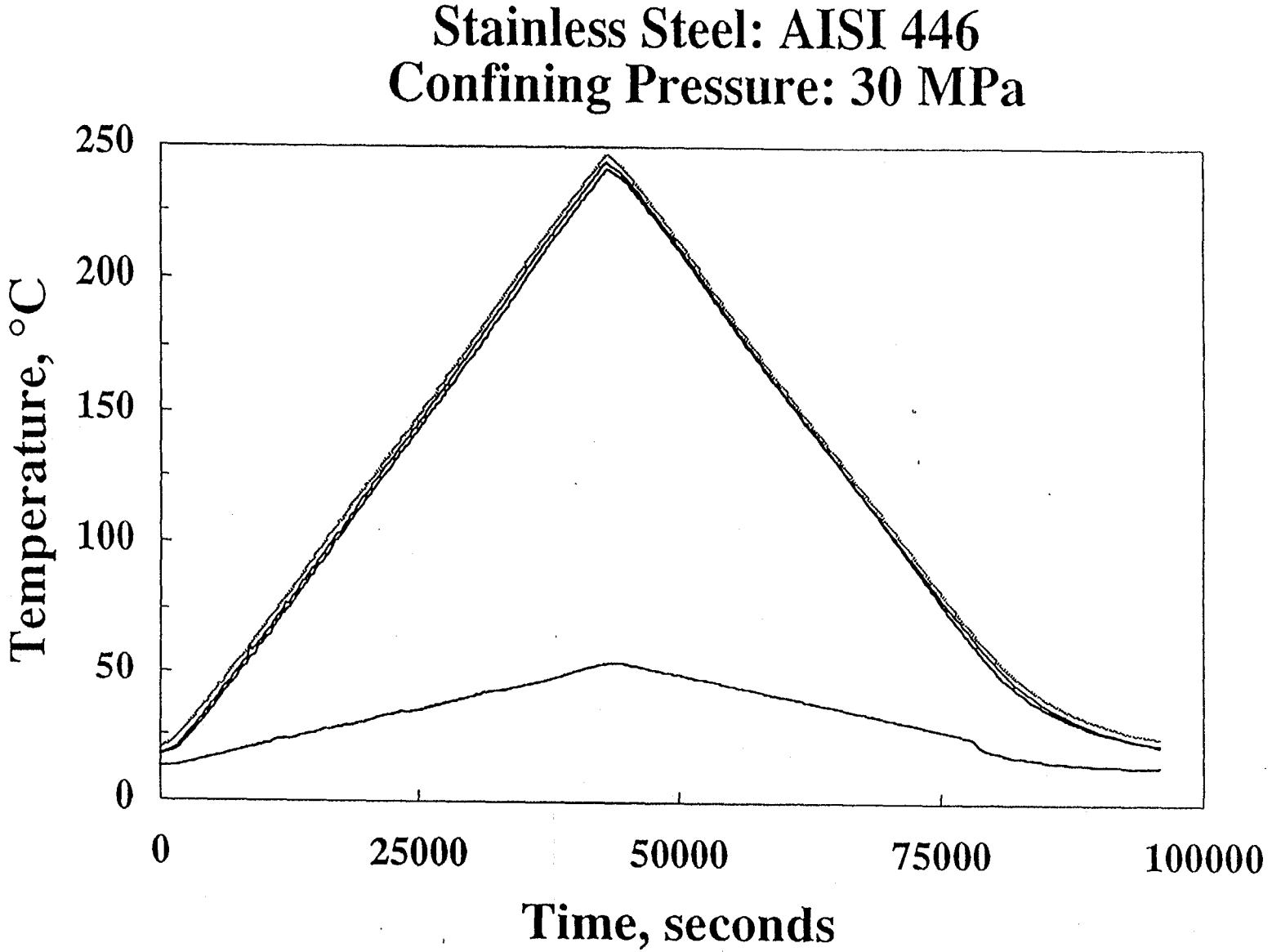

Figure A3-4: Temperature is plotted as a function of time. The upper curve represents data collected at the base, midpoint, and top of the specimen. The lower curve represents data collected at the LVDTs. The experiment was performed on May 30, 1995.

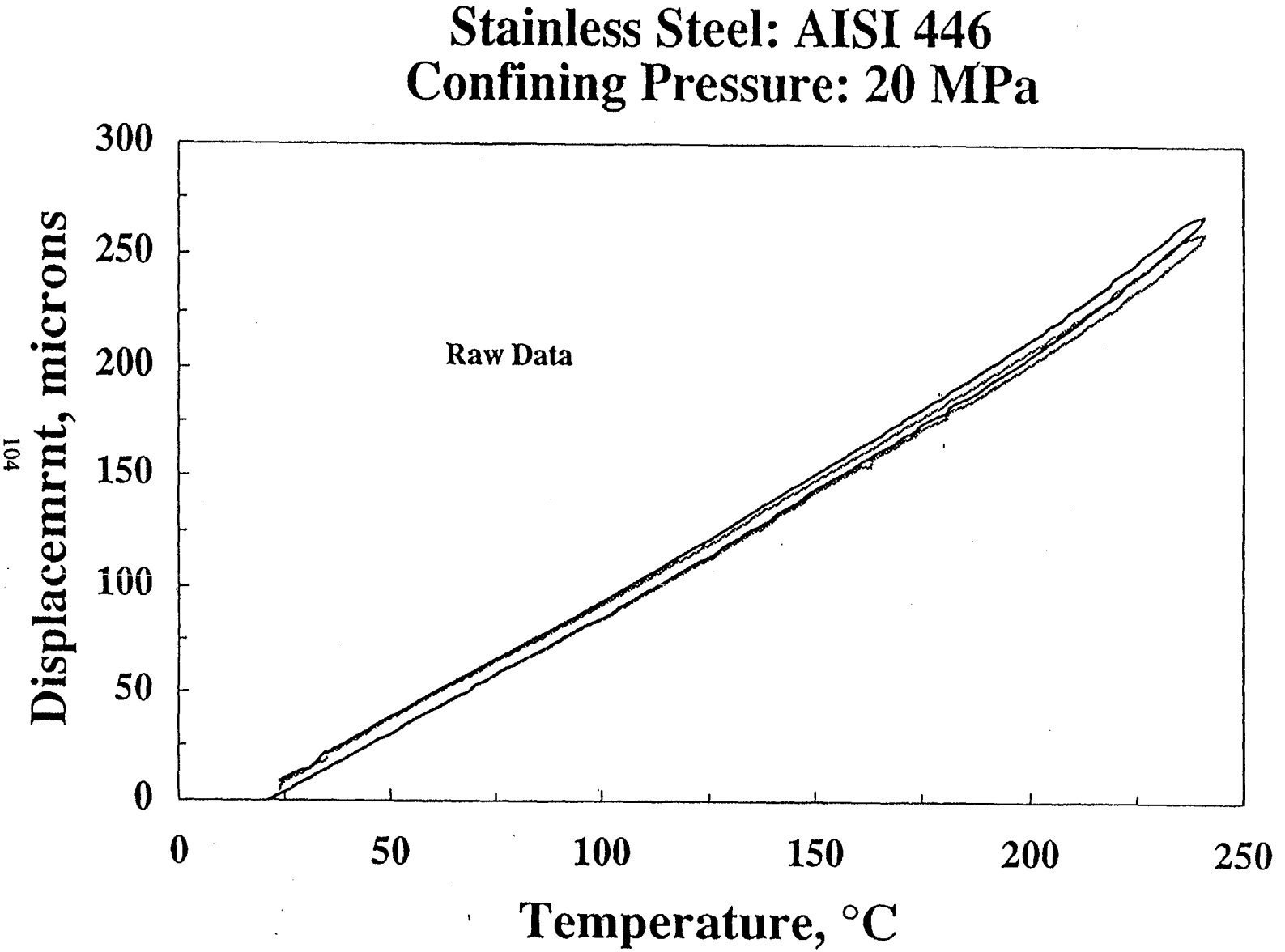

Figure A3-5: The displacement computed from the two LVDTs are plotted as a function of temperature. One thermal cycle was performed on June 14, 1995.

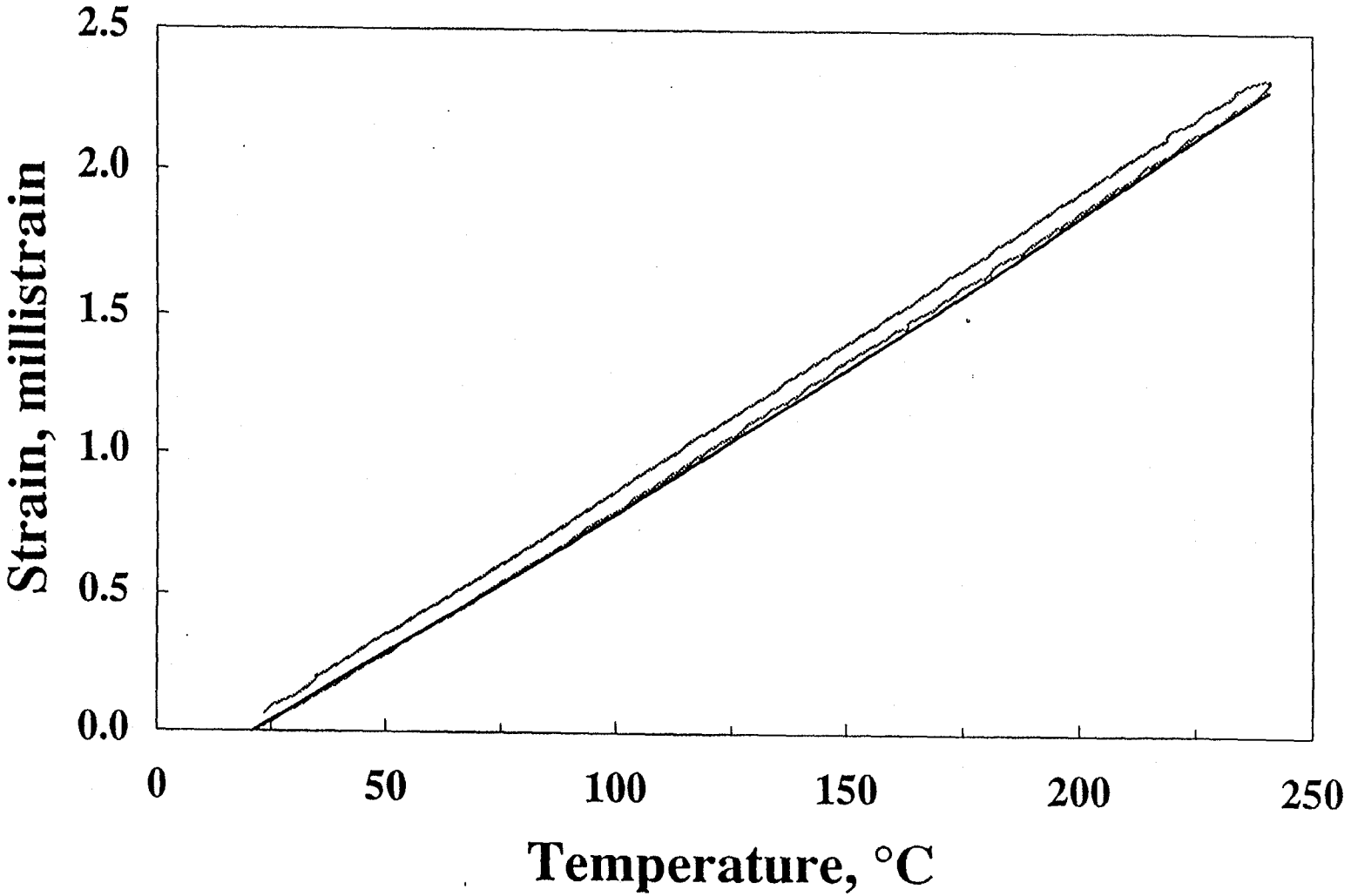

Figure A3-6: The strain is plotted as a function of temperature for the specimen tested on June 14, 1995. The solid line in the figure represents the reference data for AISI 446 stainless steel.

NER

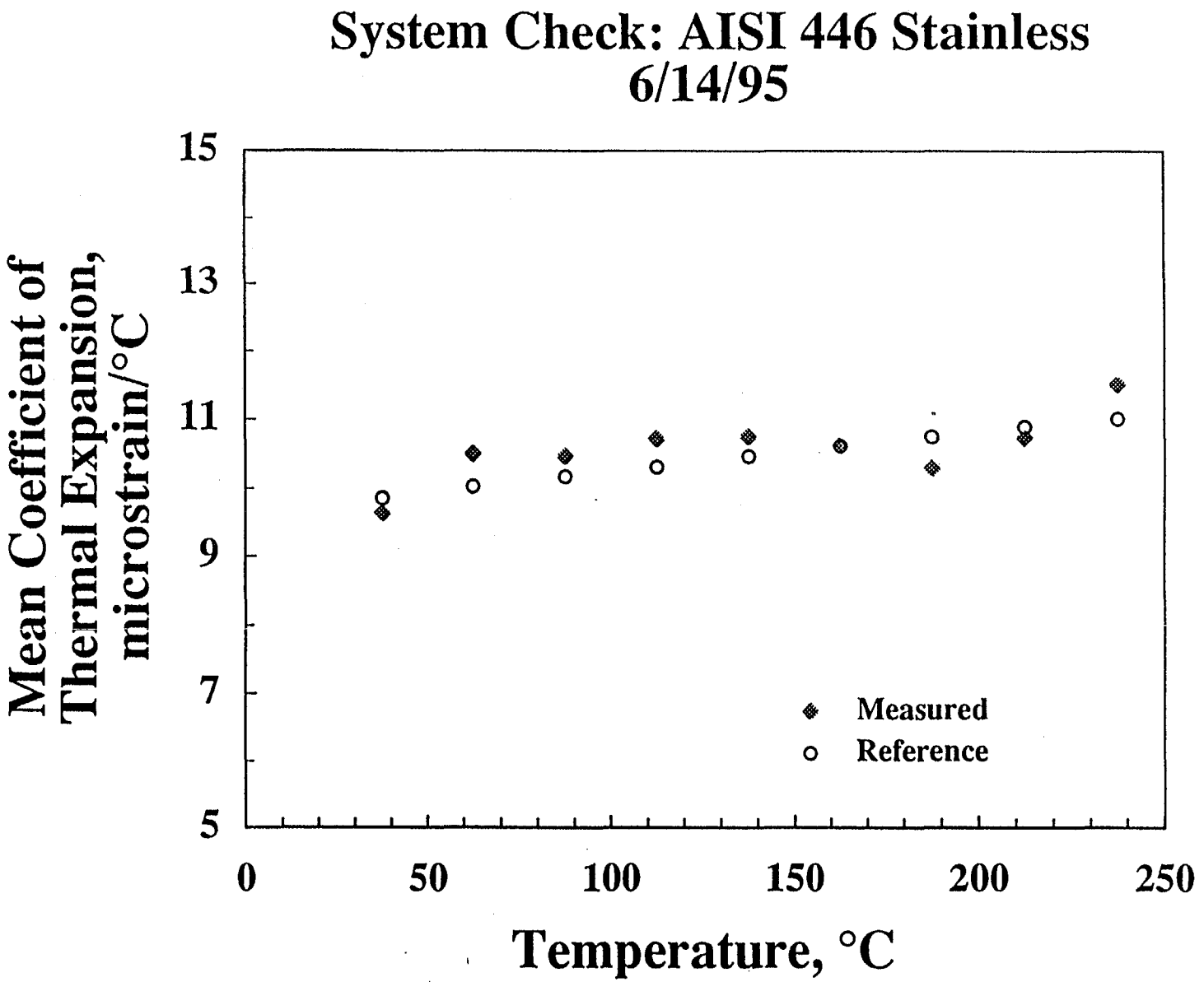

Figure A3-7: The measured and the reference mean coefficients of thermal expansion are plotted as a function of temperature. The coefficients were computed over 25 °C intervals. The data are plotted at

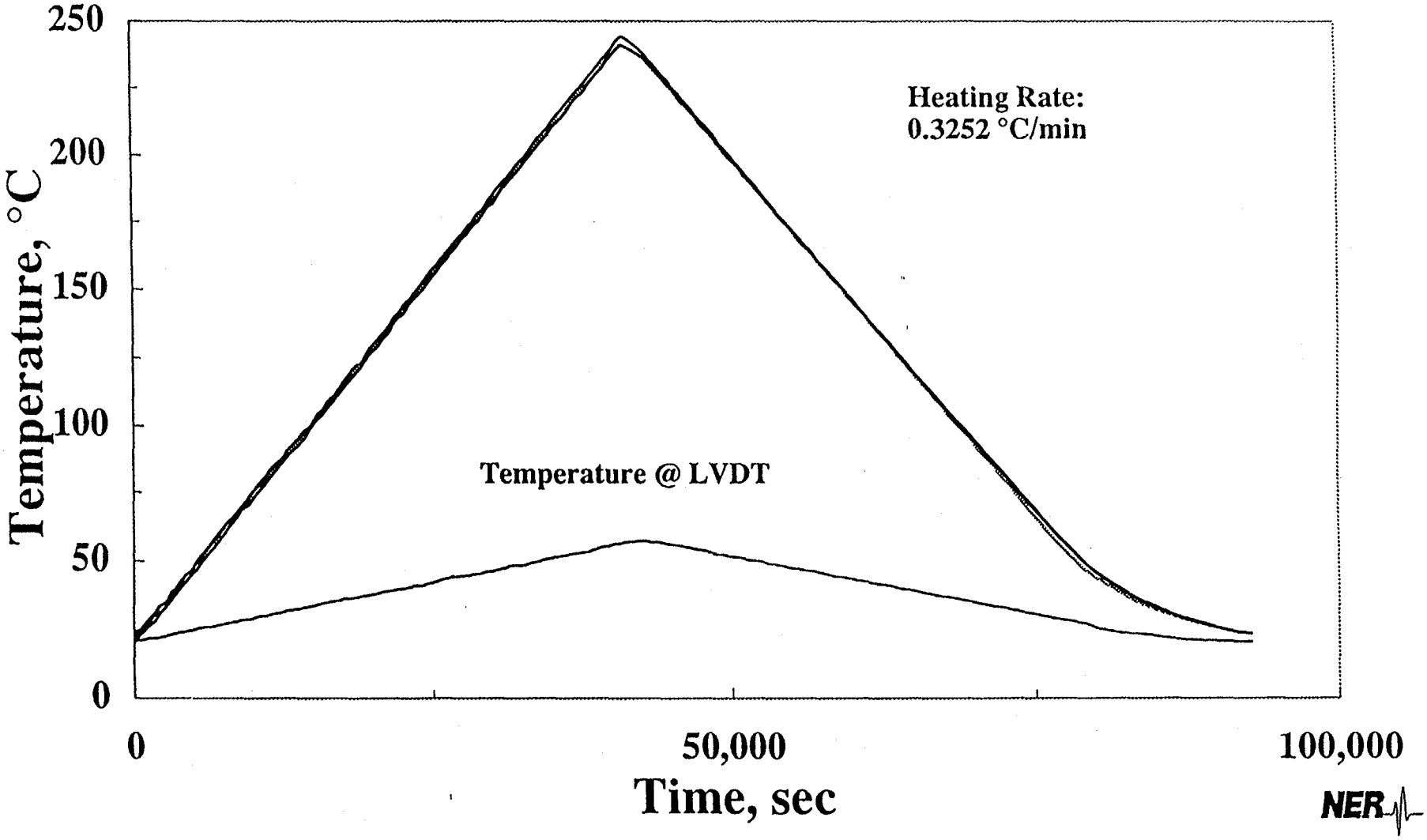

Figure A3-8: Temperature is plotted as a function of time. The upper curve represents data collected at the base, midpoint, and top of the specimen. The lower curve represents data collected at the LVDTs. The experiment was performed on June 14, 1995.

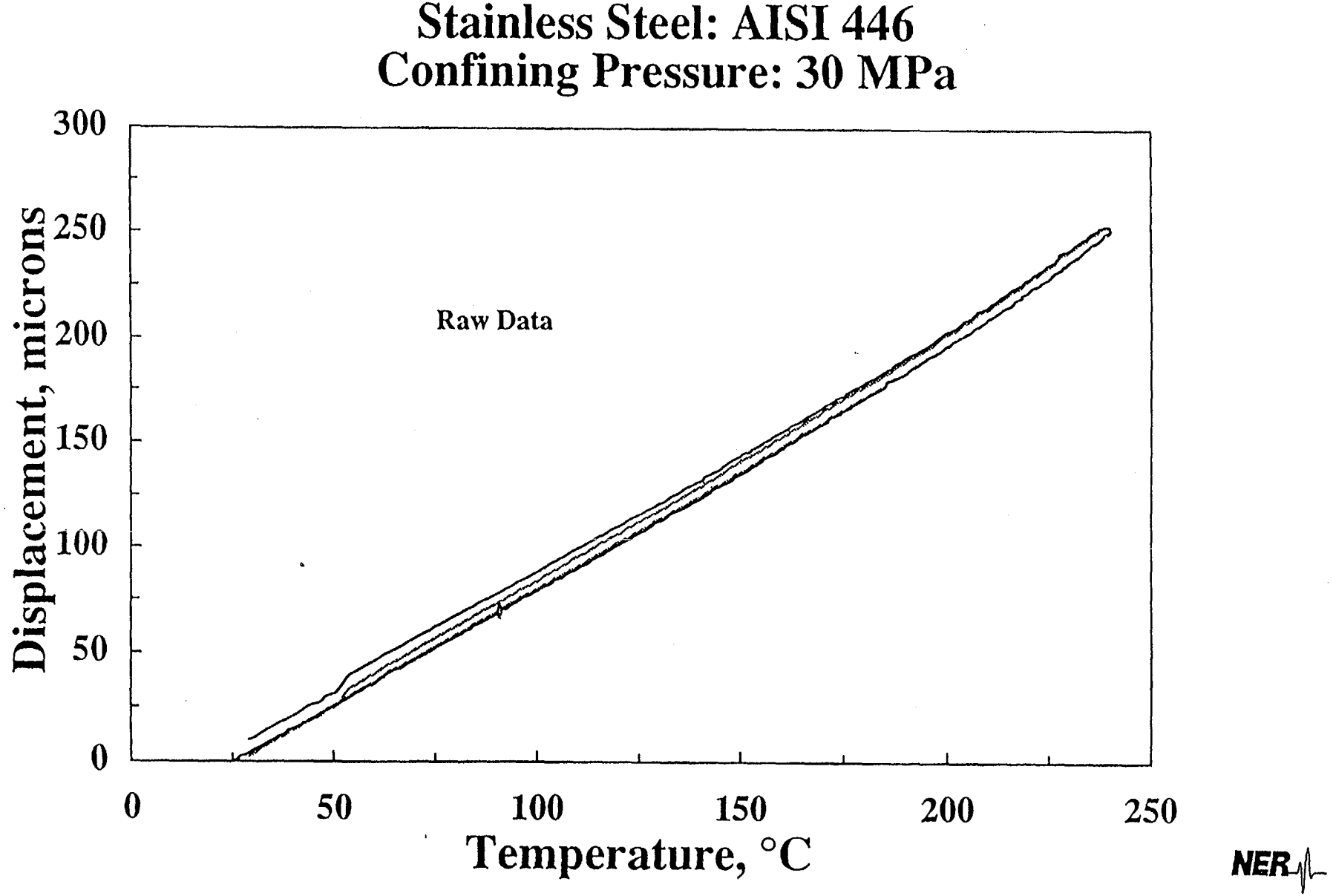

Figure A3-9: The displacement computed from the two LVDTs are plotted as a function of

[illegible] on August 16, 1995

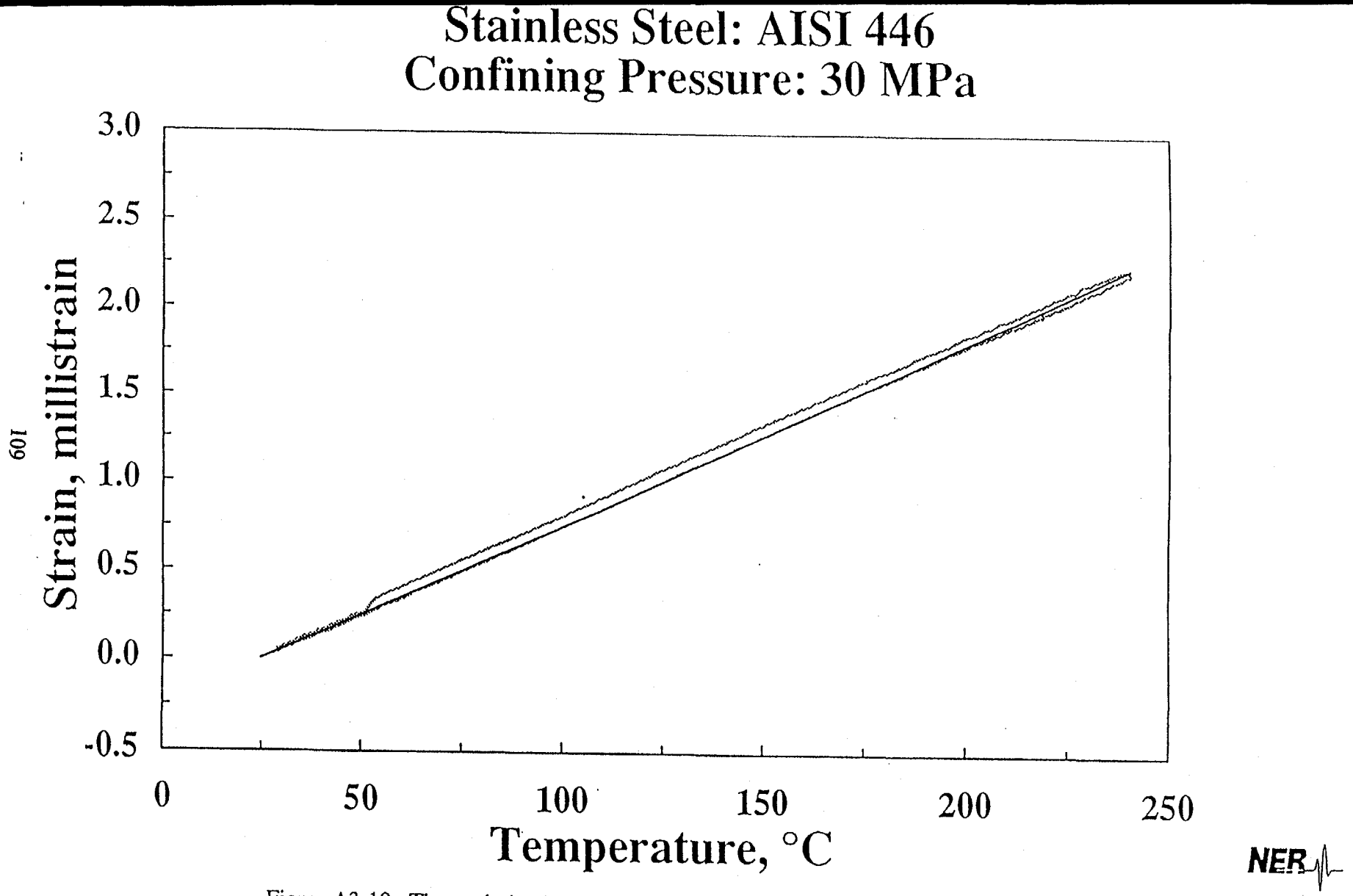

Figure A3-10: The strain is plotted as a function of temperature for the specimen tested on August 16, 1995. The solid line in the figure represents the reference data for AISI 446 stainless steel.

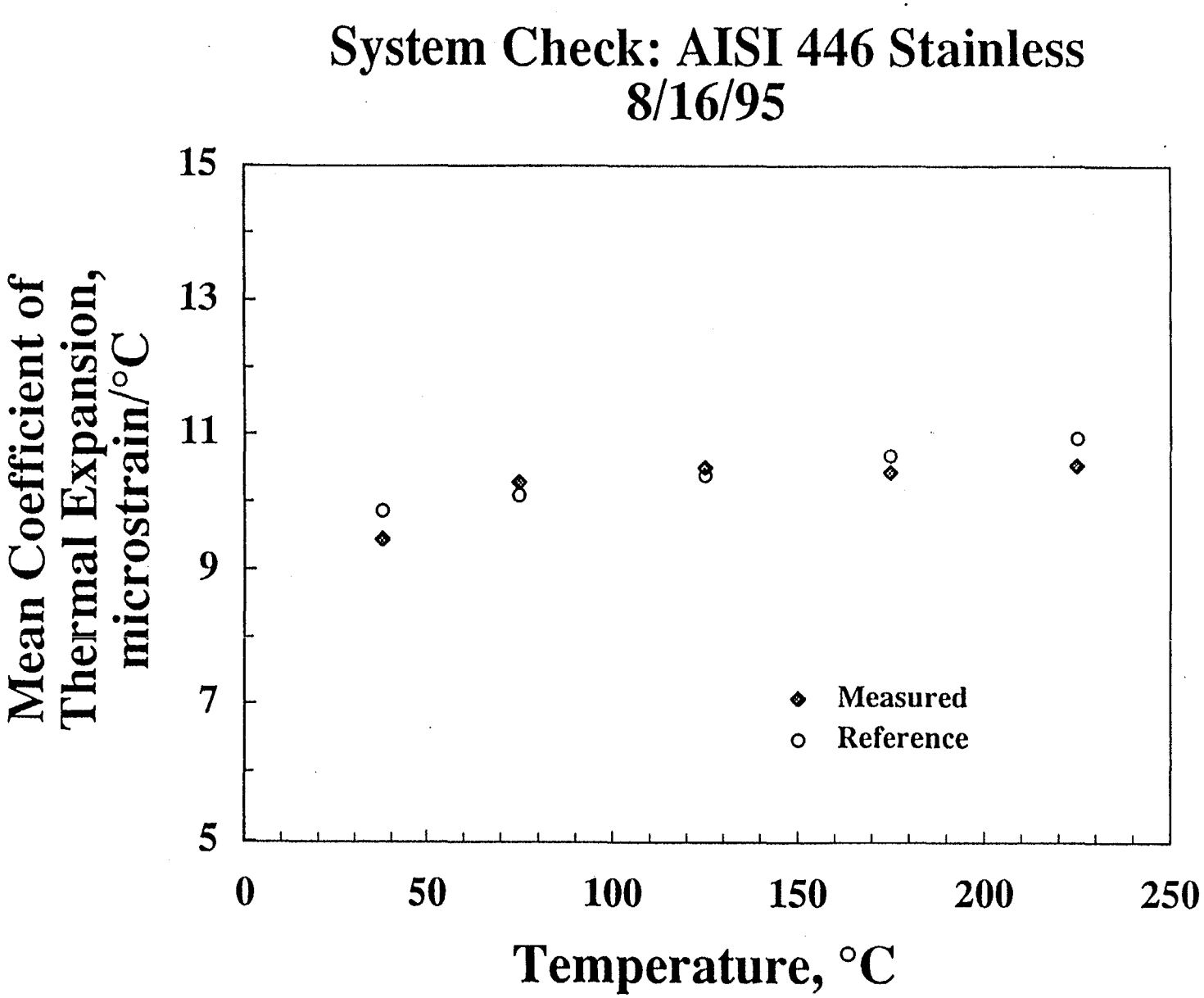

Figure A3-11: The measured and the reference mean coefficients of thermal expansion are plotted as a function of temperature. The coefficients were computed over the following intervals 25-50, 51-100,

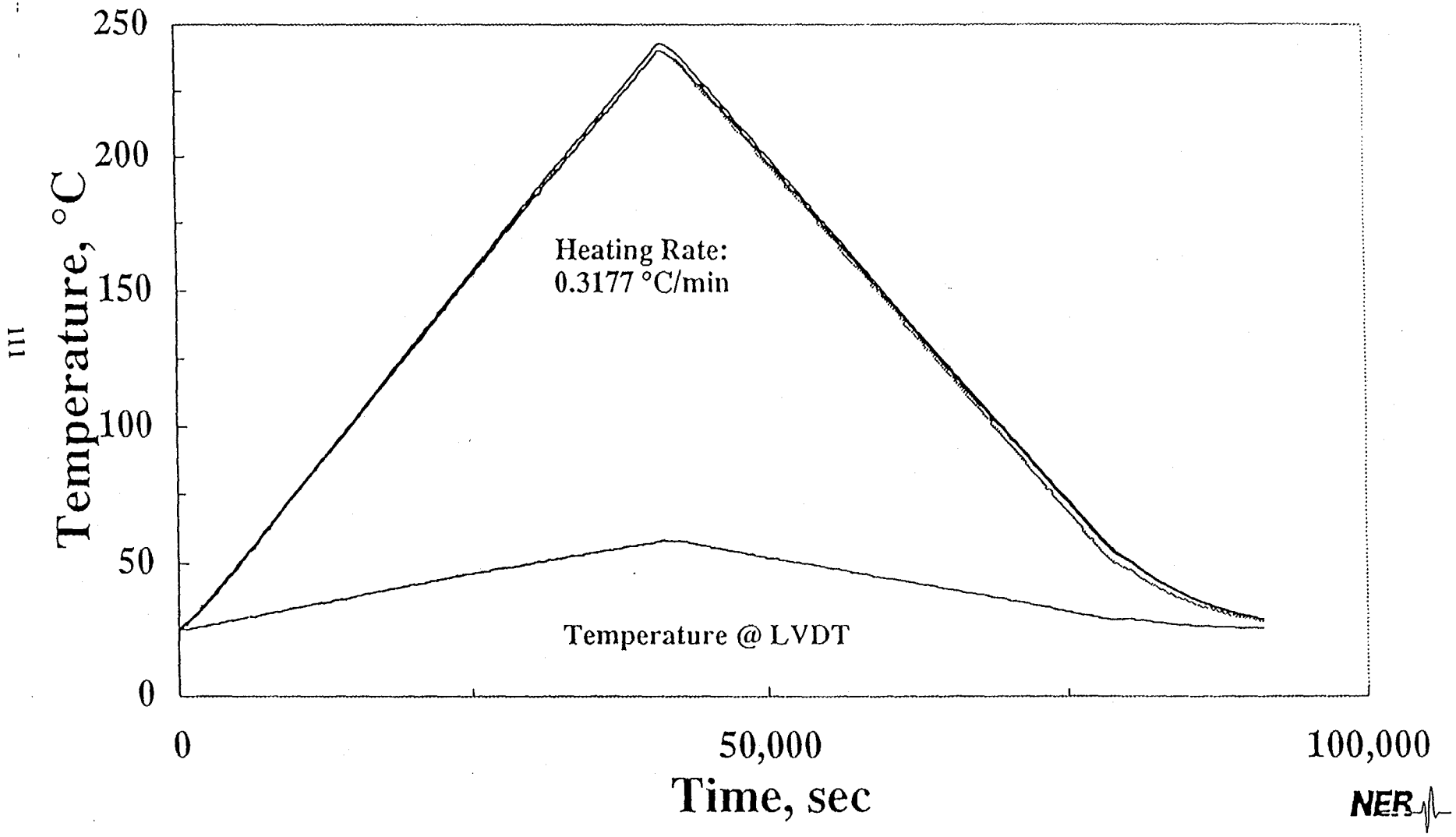

Figure A3-12: Temperature is plotted as a function of time. The upper curve represents data collected at the base, midpoint, and top of the specimen. The lower curve represents data collected at the LVDTs. The experiment was performed on August 16, 1995.

YUCCA MOUNTAIN SITE CHARACTERIZATION PROJECT
SAND95-1904 - DISTRIBUTION LIST

1 D. A. Dreyfus (RW-1)
Director
OCRWM
US Department of Energy
1000 Independence Avenue SW
Washington, DC 20585

1 L. H. Barrett (RW-2)
Acting Deputy Director
OCRWM
US Department of Energy
1000 Independence Avenue SW
Washington, DC 20585

1 S. Rousso (RW-40)
Office of Storage and Transportation
OCRWM
US Department of Energy
1000 Independence Avenue SW
Washington, DC 20585

1 R. A. Milner (RW-30)
Office of Program Management
and Integration
OCRWM
US Department of Energy
1000 Independence Avenue SW
Washington, DC 20585

1 D. R. Elle, Director
Environmental Protection Division
DOE Nevada Field Office
US Department of Energy
P.O. Box 98518
Las Vegas, NV 89193-8518

1 T. Wood (RW-14)
Contract Management Division
OCRWM
US Department of Energy
1000 Independence Avenue SW
Washington, DC 20585

4 Victoria F. Reich, Librarian
Nuclear Waste Technical Review Board
1100 Wilson Blvd., Suite 910
Arlington, VA 22209

1 Wesley Barnes, Project Manager
Yucca Mountain Site Characterization
Office
US Department of Energy
P.O. Box 30307 MS 523
Las Vegas, NV 89036-0307

1 Director, Public Affairs Office
c/o Technical Information Resource Center
DOE Nevada Operations Office
US Department of Energy
P.O. Box 98518
Las Vegas, NV 89193-8518

8 Technical Information Officer
DOE Nevada Operations Office
US Department of Energy
P.O. Box 98518
Las Vegas, NV 89193-8518

1 J. R. Dyer, Deputy Project Manager
Yucca Mountain Site Characterization Office
US Department of Energy
P.O. Box 30307 MS 523
Las Vegas, NV 89036-0307

1 S. A. Orrell
Laboratory Lead for YMP
M&O/Sandia National Laboratories
1180 Town Center Dr.
Las Vegas, NV 89134

1 J. A. Canepa
Laboratory Lead for YMP
EES-13, Mail Stop J521
M&O/Los Alamos National Laboratory
P.O. Box 1663
Los Alamos, NM 87545

1 Repository Licensing & Quality
Assurance
Project Directorate
Division of Waste Management, MS T7J-9
US NRC
Washington, DC 20555

1 Senior Project Manager for Yucca
Mountain
Repository Project Branch
Division of Waste Management, MS T7J-9
US NRC
Washington, DC 20555

1 NRC Document Control Desk
Division of Waste Management, MS T7J-9
US NRC
Washington, DC 20555

1 Chad Glenn
NRC Site Representative
301 E Stewart Avenue, Room 203
Las Vegas, NV 89101

1 Center for Nuclear Waste
Regulatory Analyses
Southwest Research Institute
6220 Culebra Road
Drawer 28510
San Antonio, TX 78284

2 W. L. Clarke
Laboratory Lead for YMP
M&O/ Lawrence Livermore Nat'l Lab
P.O. Box 808 (L-51)
Livermore, CA 94550

1 Robert W. Craig
Technical Project Officer
US Geological Survey
1180 Town Center Dr.
Las Vegas, NV 89134

1 J. S. Stuckless,
Senior Science Advisor
MS 425
Yucca Mountain Project Branch
US Geological Survey
P.O. Box 25046
Denver, CO 80225

1 L. D. Foust, Asst. General Mgr.
Nevada Site
TRW Environmental Safety Systems
1180 Town Center Dr.
Las Vegas, NV 89134

1 A. L. Flint
U. S. Geological Survey
1180 Town Center Dr.
Las Vegas, NV 89134

1 Robert L. Strickler
Vice President & General Manager
TRW Environmental Safety Systems, Inc.
2650 Park Tower Dr.
Vienna, VA 22180

1 Jim Krulik, Technical Program Officer
US Bureau of Reclamation
Code D-8322
P.O. Box 25007
Denver, CO 80225-0007

1 B. T. Brady
Records Specialist
US Geological Survey
MS 421
P.O. Box 25046
Denver, CO 80225

1 M. D. Voegele
Deputy of Technical Operations
M&O/SAIC
1180 Town Center Dr.
Las Vegas, NV 89134

2 A. T. Tamura
Science and Technology Division
OSTI
US Department of Energy
P.O. Box 62
Oak Ridge, TN 37831

1 P. J. Weeden, Acting Director
Nuclear Radiation Assessment Div.
US EPA
Environmental Monitoring Sys. Lab
P.O. Box 93478
Las Vegas, NV 89193-3478

1 John Fordham, Deputy Director
Water Resources Center
Desert Research Institute
P.O. Box 60220
Reno, NV 89506

1 The Honorable Jim Regan
Chairman
Churchill County Board of
Commissioners
10 W. Williams Avenue
Fallon, NV 89406

1 R. R. Loux
Executive Director
Agency for Nuclear Projects
State of Nevada
Evergreen Center, Suite 252
1802 N. Carson Street
Carson City, NV 89710

1 Brad R. Mettam
Inyo County Yucca Mountain
Repository Assessment Office
P. O. Drawer L
Independence, CA 93526

1 Vernon E. Poe
Office of Nuclear Projects
Mineral County
P.O. Box 1600
Hawthorne, NV 89415

1 Les W. Bradshaw
Program Manager
Nye County Nuclear Waste Repository
Project Office
P.O. Box 1767
Tonopah, NV 89049

1 Florindo Mariani
White Pine County Coordinator
P. O. Box 135
Ely, NV 89301

1 Tammy Manzini
Lander County Yucca Mountain
Information Officer
P.O. Box 10
Austin, NV 89310

1 Jason Pitts
Lincoln County Nuclear Waste
Program Manager
P. O. Box 158
Pioche, NV 89043

1 Dennis Bechtel, Coordinator
Nuclear Waste Division
Clark County Dept. of Comprehensive
Planning
P.O. Box 55171
Las Vegas, NV 89155-1751

1 Juanita D. Hoffman
Nuclear Waste Repository
Oversight Program
Esmeralda County
P.O. Box 490
Goldfield, NV 89013

1 Sandy Green
Yucca Mountain Information Office
Eureka County
P.O. Box 714
Eureka, NV 89316

1 Economic Development Dept.
City of Las Vegas
400 E. Stewart Avenue
Las Vegas, NV 89101

1 Community Planning & Development
City of North Las Vegas
P.O. Box 4086
North Las Vegas, NV 89030

2 Librarian
YMP Research & Study Center
1180 Town Center Dr.
Las Vegas, NV 89134

1 Library Acquisitions
Argonne National Laboratory
Building 203, Room CE-111
9700 S. Cass Avenue
Argonne, IL 60439

1 Glenn Van Roekel
Manager, City of Caliente
P.O. Box 158
Caliente, NV 89008

1 G. S. Bodvarsson
Head, Nuclear Waste Department
Lawrence Berkeley National Laboratory
1 Cyclotron Road, MS 50E
Berkeley, CA 94720

1 Steve Hanauer (RW-2)
OCRWM
U. S. Department of Energy
1000 Independence Ave.
Washington, DC 20585

5 Randolph J. Martin III
New England Research
76 Olcott Drive
White River, VT 05001

1 Robert W. Clayton
M&O/WCFS
1180 Town Center Drive
Las Vegas, NV 89134

1 Richard C. Quitmeyer
M&O/WCFS
1180 Town Center Drive
Las Vegas, NV 89134

1 Mark C. Tynan
DOE/YMPSCO
1180 Town Center Drive MS 523/HL
Las Vegas, NV 89134

2 James R. Connolly
Dept. of Earth and Planetary Science
Northrop Hall
Albuquerque, NM 87131-11126

	MS	
15	1325	R. H. Price, 6811
5	0751	N. Brodsky, 6117
1	0751	L. S. Costin, 6117
5	1399	D. S. Kessel, 6850
2	1399	M. Riggins, 6850
2	1330	K. Hart, 6811 100/1.2.3.2.7.1.2/SAND95-1904/QA
20	1330	WMT Library, 6752

1	9018	Central Technical Files, 8940-2
5	0899	Technical Library, 4414
2	0619	Review and Approval Desk, 12690, For DOE/OSTI